



This is a repository copy of *The VLT-FLAMES Tarantula Survey I. Introduction and observational overview*.

White Rose Research Online URL for this paper:

<http://eprints.whiterose.ac.uk/120562/>

Version: Accepted Version

---

**Article:**

Evans, C.J., Taylor, W.D., Henault-Brunet, V. et al. (39 more authors) (2011) The VLT-FLAMES Tarantula Survey I. Introduction and observational overview. *Astronomy and Astrophysics*, 530. A108. ISSN 0004-6361

<https://doi.org/10.1051/0004-6361/201116782>

---

**Reuse**

Unless indicated otherwise, fulltext items are protected by copyright with all rights reserved. The copyright exception in section 29 of the Copyright, Designs and Patents Act 1988 allows the making of a single copy solely for the purpose of non-commercial research or private study within the limits of fair dealing. The publisher or other rights-holder may allow further reproduction and re-use of this version - refer to the White Rose Research Online record for this item. Where records identify the publisher as the copyright holder, users can verify any specific terms of use on the publisher's website.

**Takedown**

If you consider content in White Rose Research Online to be in breach of UK law, please notify us by emailing [eprints@whiterose.ac.uk](mailto:eprints@whiterose.ac.uk) including the URL of the record and the reason for the withdrawal request.

# The VLT-FLAMES Tarantula Survey

## I: Introduction and observational overview

C. J. Evans<sup>1</sup>, W. D. Taylor<sup>2</sup>, V. Hénault-Brunet<sup>2</sup>, H. Sana<sup>3</sup>, A. de Koter<sup>3,4</sup>, S. Simón-Díaz<sup>5,6</sup>, G. Carraro<sup>7</sup>, T. Bagnoli<sup>3</sup>, N. Bastian<sup>8,9</sup>, J. M. Bestenlehner<sup>10</sup>, A. Z. Bonanos<sup>11</sup>, E. Bressert<sup>9,12,13</sup>, I. Brott<sup>4,14</sup>, M. A. Campbell<sup>2</sup>, M. Cantiello<sup>15</sup>, J. S. Clark<sup>16</sup>, E. Costa<sup>17</sup>, P. A. Crowther<sup>18</sup>, S. E. de Mink<sup>19\*</sup>, E. Doran<sup>18</sup>, P. L. Dufton<sup>20</sup>, P. R. Dunstall<sup>20</sup>, K. Friedrich<sup>15</sup>, M. Garcia<sup>5,6</sup>, M. Gieles<sup>21</sup>, G. Gräfener<sup>10</sup>, A. Herrero<sup>5,6</sup>, I. D. Howarth<sup>22</sup>, R. G. Izzard<sup>15</sup>, N. Langer<sup>15</sup>, D. J. Lennon<sup>23</sup>, J. Maíz Apellániz<sup>24\*\*</sup>, N. Markova<sup>25</sup>, F. Najarro<sup>26</sup>, J. Puls<sup>27</sup>, O. H. Ramirez<sup>3</sup>, C. Sabín-Sanjulián<sup>5,6</sup>, S. J. Smartt<sup>20</sup>, V. E. Stroud<sup>16,28</sup>, J. Th. van Loon<sup>29</sup>, J. S. Vink<sup>10</sup> and N. R. Walborn<sup>19</sup>

<sup>1</sup> UK Astronomy Technology Centre, Royal Observatory Edinburgh, Blackford Hill, Edinburgh, EH9 3HJ, UK

<sup>2</sup> Scottish Universities Physics Alliance (SUPA), Institute for Astronomy, University of Edinburgh, Royal Observatory Edinburgh, Blackford Hill, Edinburgh, EH9 3HJ, UK

<sup>3</sup> Astronomical Institute Anton Pannekoek, University of Amsterdam, Kruislaan 403, 1098 SJ, Amsterdam, The Netherlands

<sup>4</sup> Astronomical Institute, Utrecht University, Princetonplein 5, 3584CC, Utrecht, The Netherlands

<sup>5</sup> Instituto de Astrofísica de Canarias, E-38200 La Laguna, Tenerife, Spain

<sup>6</sup> Departamento de Astrofísica, Universidad de La Laguna, E-38205 La Laguna, Tenerife, Spain

<sup>7</sup> European Southern Observatory, Alonso de Cordova 1307, Casilla, 19001, Santiago 19, Chile

<sup>8</sup> Excellence Cluster Universe, Boltzmannstr. 2, 85748 Garching, Germany

<sup>9</sup> School of Physics, University of Exeter, Stocker Road, Exeter EX4 4QL, UK

<sup>10</sup> Armagh Observatory, College Hill, Armagh, BT61 9DG, Northern Ireland, UK

<sup>11</sup> Institute of Astronomy & Astrophysics, National Observatory of Athens, I. Metaxa & Vas. Pavlou Street, P. Penteli 15236, Greece

<sup>12</sup> European Southern Observatory, Karl-Schwarzschild-Strasse 2, D87548, Garching bei München, Germany

<sup>13</sup> Harvard-Smithsonian CfA, 60 Garden Street, Cambridge, MA 02138, USA

<sup>14</sup> University of Vienna, Department of Astronomy, Türkenschanzstr. 17, 1180, Vienna, Austria

<sup>15</sup> Argelander-Institut für Astronomie der Universität Bonn, Auf dem Hügel 71, 53121 Bonn, Germany

<sup>16</sup> Department of Physics and Astronomy, The Open University, Walton Hall, Milton Keynes, MK7 6AA, UK

<sup>17</sup> Departamento de Astronomía, Universidad de Chile, Camino el Observatorio 1515, Las Condes, Santiago, Chile

<sup>18</sup> Dept. of Physics & Astronomy, Hounsfeld Road, University of Sheffield, S3 7RH, UK

<sup>19</sup> Space Telescope Science Institute, 3700 San Martin Drive, Baltimore, MD 21218, USA

<sup>20</sup> Department of Physics & Astronomy, Queen's University Belfast, Belfast BT7 1NN, Northern Ireland, UK

<sup>21</sup> Institute of Astronomy, University of Cambridge, Madingley Road, Cambridge, CB3 0HA, UK

<sup>22</sup> Dept. of Physics & Astronomy, University College London, Gower Street, London, WC1E 6BT, UK

<sup>23</sup> ESA/STScI, 3700 San Martin Drive, Baltimore, MD 21218, USA

<sup>24</sup> Instituto de Astrofísica de Andalucía-CSIC, Glorieta de la Astronomía s/n, E-18008 Granada, Spain

<sup>25</sup> Institute of Astronomy with NAO, Bulgarian Academy of Sciences, PO Box 136, 4700 Smoljan, Bulgaria

<sup>26</sup> Centro de Astrobiología (CSIC-INTA), Ctra. de Torrejón a Ajalvir km-4, E-28850 Torrejón de Ardoz, Madrid, Spain

<sup>27</sup> Universitäts-Sternwarte, Scheinerstrasse 1, 81679 München, Germany

<sup>28</sup> Faulkes Telescope Project, University of Glamorgan, Pontypridd, CF37 1DL, Wales, UK

<sup>29</sup> Astrophysics Group, School of Physical & Geographical Sciences, Keele University, Staffordshire, ST5 5BG, UK

## ABSTRACT

The VLT-FLAMES Tarantula Survey (VFTS) is an ESO Large Programme that has obtained multi-epoch optical spectroscopy of over 800 massive stars in the 30 Doradus region of the Large Magellanic Cloud (LMC). Here we introduce our scientific motivations and give an overview of the survey targets, including optical and near-infrared photometry and comprehensive details of the data reduction. One of the principal objectives was to detect massive binary systems via variations in their radial velocities, thus shaping the multi-epoch observing strategy. Spectral classifications are given for the massive emission-line stars observed by the survey, including the discovery of a new Wolf-Rayet star (VFTS 682, classified as WN5h), 2' to the northeast of R136. To illustrate the diversity of objects encompassed by the survey, we investigate the spectral properties of sixteen targets identified by Gruendl & Chu from *Spitzer* photometry as candidate young stellar objects or stars with notable mid-infrared excesses. Detailed spectral classification and quantitative analysis of the O- and B-type stars in the VFTS sample, paying particular attention to the effects of rotational mixing and binarity, will be presented in a series of future articles to address fundamental questions in both stellar and cluster evolution.

**Key words.** open clusters and associations: individual: 30 Doradus – stars: early-type – stars: fundamental parameters – binaries: spectroscopic – stars: Wolf-Rayet

## 1. Introduction

Massive stars have played an important role in galaxy evolution throughout cosmological time via their intense winds, ultraviolet radiation fields, chemical processing, and explosions. For instance, they dominate the rest-frame ultraviolet spectra of star-forming, Lyman-break galaxies, in which multiple ‘starburst’ components (or mergers) are seen out to redshifts of at least  $z \sim 5$  (Douglas et al. 2010). Indeed, they are thought to have been a major factor in the reionization of the early universe (Haiman & Loeb 1997), comprising the dominant component in the earliest galaxies, in which the star-formation rate appears to increase by a factor of ten over a period of just 200 Myr (Bouwens et al. 2011).

Population synthesis codes such as Starburst99 (Leitherer et al. 1999, 2010) form the bridge between our understanding of the physics and evolution of individual stars, and efforts to analyse entire populations on galaxy scales via interpretation of their integrated light. The sensitivity of the 8–10 m class telescopes has enabled spectroscopy of individual massive stars in galaxies at Mpc distances (e.g., Gieren et al. 2005; Kudritzki et al. 2008), including some in low-metallicity dwarf galaxies, in which the local conditions are close to those found in the early universe (e.g., Bresolin et al. 2006, 2007; Evans et al. 2007).

Unfortunately, we are currently limited to observations of the brightest stars in such galaxies. Only in the Galaxy and Magellanic Clouds can we potentially assemble large observational samples of massive stars that span a wide range of metallicity and intrinsic luminosities. Ultraviolet satellites have enabled substantial surveys of terminal wind velocities (e.g., Howarth & Prinja 1989; Prinja et al. 1990) and rotational velocities (Penny 1996; Howarth et al. 1997; Penny & Gies 2009). However, both observational and computational challenges have precluded the atmospheric analysis of a large, coherent sample of O-type stars from optical spectroscopy, with studies limited to several tens of objects at most (e.g. Herrero et al. 2000, 2002; Repolust et al. 2004; Mokiem et al. 2005, 2006, 2007; Massey et al. 2009). At lower masses, while large observational samples of early B-type stars are available, recent results have highlighted some serious problems regarding our understanding of massive-star evolution (Hunter et al. 2008, 2009; Brott et al. 2011). This leaves us in a situation where fundamental questions concerning the formation, evolution, and eventual fate of massive stars remain unanswered, particularly in the context of results that point to the majority of high-mass stars being in binary/multiple systems (e.g. Sana & Evans 2011).

The Tarantula Nebula (NGC 2070, 30 Doradus – hereafter ‘30 Dor’) in the Large Magellanic Cloud (LMC) is the brightest H II region in the Local Group. It is comprised of multiple generations of star formation, with at least five distinct populations (Walborn & Blades 1997), similar to cluster complexes seen well beyond the Local Group (e.g., Bastian et al. 2006). At the heart of 30 Dor is Radcliffe 136 (R136, Feast et al. 1960), a massive, young stellar cluster (1–2 Myr; e.g., de Koter et al. 1998; Massey & Hunter 1998) dominated by early O-type and hydrogen-rich WN-type stars, some of which are thought to have current masses in excess of  $150 M_{\odot}$  (Crowther et al. 2010). To the north and west of R136 there is significant molecular gas (Werner et al. 1978; Johansson et al. 1998) with embedded massive stars, which has been suggested as a second generation

of (perhaps triggered) star formation around R136 (Walborn & Blades 1997; Walborn et al. 1999a, 2002).

By virtue of its location in the LMC, the distance to 30 Dor is well constrained (we adopt a distance modulus to the LMC of 18.5, e.g., Gibson 2000) and the foreground extinction is relatively low compared to some of the most massive Galactic clusters. Moreover, the metallicity of the LMC ( $\sim 50\%$  solar) is well matched to typical results for high-redshift galaxies (e.g. Erb et al. 2006; Nesvadba et al. 2008).

Thus, 30 Dor provides an excellent opportunity to study a broad age range of massive stars within a single complex of star formation. In addition to the rich populations of O- and early B-type stars, there are over twenty Wolf-Rayet (W-R) stars, (including examples of both WN and WC subclasses, e.g., Breysacher et al. 1999), several transition Of/WN stars (Crowther & Walborn, in preparation), and candidates for high-mass young stellar objects (YSOs) identified from mid-infrared observations with the *Spitzer Space Telescope* (see Section 5). With its rich stellar populations, 30 Dor is the ideal laboratory in which to investigate important outstanding questions regarding the physical properties, binary fraction, chemical enrichment, and evolution of the most massive stars, as well as the relation of massive stars to the formation and evolution of stellar clusters (e.g., de Koter et al. 2008; Portegies Zwart et al. 2010).

Building on experience from the VLT-FLAMES Survey of Massive Stars (Evans et al. 2005, 2006), we introduce the VLT-FLAMES Tarantula Survey (VFTS), a multi-epoch spectral survey of over 800 massive stars in the 30 Dor region, including  $\sim 300$  O-type stars. In a series of articles, the VFTS data will be used to investigate the properties of stellar winds and rotational mixing in O-type stars, and to extend studies of rotational mixing in B-type stars. In particular, the surface abundances of O-type stars are expected to be modified via the effects of rotational mixing but, to date, nitrogen abundances have not been determined for a large observational sample. The inclusion of new models of N III in the FASTWIND model atmosphere code (Puls et al. 2005, 2011), combined with analytical methods such as those developed by Mokiem et al. (2005) or the use of a large model grid, means that such a critical test of evolutionary predictions is now feasible.

30 Dor is known to have a rich binary population (Bosch et al. 2009) – a key feature of the VFTS is a multi-epoch observational strategy to obtain clear indications of binarity<sup>1</sup> in the large majority of the targets. This will add a valuable component to quantitative analysis of the spectra and interpretation of the results, enabling tests of the predictions of evolutionary models that include all of the relevant physical processes for both single stars and binary systems (e.g. Langer et al. 2008). The survey also includes multi-epoch spectroscopy in the inner part of 30 Dor with the FLAMES–ARGUS integral-field unit (IFU) to obtain an improved estimate of the velocity dispersion of single stars in R136, which will be used to determine the dynamical mass of the cluster.

This introductory article presents the significant observational material in one resource, comprising details of target selection, observational strategy and data reduction (Section 2), optical and infrared photometry of the targets (Section 3), spectral classifications for the observed massive emission-line and cooler-type stars (Section 4), and a discussion of the spectral properties of stars with published mid-infrared excesses (Section 5); concluding remarks are given in Section 6.

Send offprint requests to: C. J. Evans at chris.evans@stfc.ac.uk

\* Hubble Fellow

\*\* Ramón y Cajal Fellow

<sup>1</sup> Hereafter we use ‘binary’ as shorthand for both true binaries and multiple systems.

## 2. Spectroscopy

The Tarantula Survey employs three modes of the Fibre Large Array Multi-Element Spectrograph (FLAMES; Pasquini et al. 2002) instrument on the VLT:

- *Medusa–Giraffe*: The majority of the spectra were obtained using the Medusa fibre-feed to the Giraffe spectrograph. There are a total of 132 Medusa fibres available for science (or sky) observations, deployable within a 25' diameter field-of-view and with a diameter of 1''.2 on the sky.
- *ARGUS–Giraffe*: The ARGUS IFU was used to observe five pointings of R136 and its environs in the central part of 30 Dor. The IFU was used in the 0''.52 per spatial pixel (spaxel) mode, such that its  $22 \times 14$  microlenses provide a total field-of-view for a single pointing of  $12'' \times 7''$  on the sky.
- *UVES*: In parallel to the ARGUS observations, the fibre feed to the red arm of the Ultraviolet and Visual Echelle Spectrograph (UVES) was used to observe a small sample of stars in the inner part of 30 Dor at greater spectral resolving power than that delivered by Giraffe.

The target selection is discussed in Section 2.1, followed by a description of the reductions of the three spectroscopic components of the survey (Sections 2.2, 2.3, and 2.4).

### 2.1. Target selection

The Medusa fibre configurations were prepared using two sources. Within a radius of  $\sim 60''$  of the core, targets were (with a couple of exceptions) taken from Brian Skiff's reworking of the astrometry from the *UBV* catalogue of Selman et al. (1999)<sup>2</sup>. Targets beyond this region were selected from preliminary reductions of *B*- and *V*-band observations (with the B/123 and V/89 filters, respectively) with the Wide-Field Imager (WFI) at the 2.2 m Max-Planck-Gesellschaft (MPG)/ESO telescope at La Silla (from observations by J. Alves, B. Vandame & Y. Beletsky; programme 076.C-0888). Four overlapping WFI fields were observed that cover approximately one square degree – our FLAMES observations primarily include sources from the first (northeast) WFI pointing, supplemented to the west by targets from the second. The median seeing in the reduced images is  $\sim 0''.8$ , although the conditions were non-photometric and stars brighter than approximately 14th magnitude were saturated.

Source detections in the WFI frames were performed using the DAOPHOT package (Stetson 1987) within IRAF. The astrometry was calibrated using stars from the UCAC-2 catalogue (Zacharias et al. 2004), which has an astrometric precision to better than 0''.1 (sufficient for the diameter of the Medusa fibres).

In a bid to avoid significant selection biases we did not employ any colour cuts on our input target lists. The only constraint imposed was a magnitude cut (before final photometric calibration) of  $V \leq 17$  mag, to ensure adequate signal-to-noise (S/N) in the resulting spectra. The Fibre Positioner Observation Support Software (FPOSS) was used with our combined ‘Selman–Skiff’ and WFI catalogue to create nine Medusa configurations, hereafter referred to as fields ‘A’ through to ‘I’. Exactly 1000 targets were observed with the Medusa–Giraffe mode in these nine configurations. The reductions and characteristics of these data are discussed below. After rejection of foreground stars (and a small number of others due to issues relating to data quality, see

Section 2.2.4), we have Medusa (or UVES) observations of 893 unique targets.

A full catalogue of the survey targets is given in Table 5 (published online) in which they are RA-sorted and given a running number, which hereafter serves as an identifier of the form VFTS ##. Given its importance and rich stellar populations, 30 Dor has been the subject of numerous studies over the past decades – the final column of Table 5 provides a thorough (but not exhaustive) list of previous aliases/identifications for our targets.

FLAMES has a corrected field-of-view of 25'. This means that with one central telescope pointing we were able to observe stars in some of the local environs of 30 Dor as well as in the main body of the H II region. The distribution of the Medusa (and UVES) targets is shown in Figure 1, overlaid on a section of the *V*-band WFI mosaic. The targets are primarily located in the main 30 Dor nebula (NGC 2070), but also include at least three separate associations: 1) Hodge 301, approximately 3' to the northwest of R136 (Hodge 1988), which is somewhat older than the rest of 30 Dor (20 to 25 Myr, Grebel & Chu 2000); 2) NGC 2060 (*aka* 30 Dor B and LHA 120-N 157B), 6.5' to the southwest of R136, which is associated with a supernova remnant (e.g. Chu et al. 1992); 3) SL 639 (Shapley & Lindsay 1963), 7.5' to the southeast. The survey targets span a total diameter just in excess of 20', with over 500 of them within a 5' ( $\approx 75$  pc) radius from the centre of R136. Distances to each target from R136 (specifically, R136-a1:  $\alpha = 5^{\text{h}} 38^{\text{m}} 42\overset{\text{s}}{.}39$ ,  $\delta = -69^{\circ} 06' 02\overset{\text{s}}{.}91$ , J2000.0) are given in the fifth and sixth columns of Table 5, in arcmin and pc, respectively.

### 2.2. VLT Medusa–Giraffe spectroscopy

#### 2.2.1. Observational strategy

The nine Medusa fibre configurations (‘A’–‘I’) were observed using three of the standard Medusa–Giraffe settings (LR02, LR03, and HR15N). These provide intermediate-resolution spectroscopy of the lines commonly used in quantitative analysis of massive stars in the 3960–5070 Å region, combined with higher-resolution observations of the H $\alpha$  line to provide a diagnostic of the stellar wind intensity.

The wavelength coverage and spectral resolution ( $\Delta\lambda$ , as determined by the mean full-width at half-maximum of arc lines in the wavelength calibration exposures) is summarised in Table 1. We also give the effective resolving power,  $R$  (i.e.,  $\lambda/\Delta\lambda$ ), for the central wavelength of each setting.

Most of the Medusa observations were obtained over the period 2008 October to 2009 February, with a seeing constraint of  $\leq 1''.2$ . Pairs of exposures were taken in each observing block (OB). To obtain sufficient S/N for quantitative analysis of each target, three OBs at both the LR02 and LR03 settings were observed, and two at HR15N. No explicit time constraints were placed on the execution of these OBs and, in the majority of cases, the sequences at a given wavelength setting were observed consecutively (but not in all, e.g., the LR03 observations of Field D). The modified Julian Dates (MJD) for each OB are given in Tables A.1 and A.2 in the appendix (published online).

The key observational feature of the survey is three repeat OBs at the LR02 setting to detect radial velocity variables (epochs 4, 5, and 6 in the appendix). These were scheduled in the service queue such that a minimum of 28 days had passed between execution of the third and fourth epochs, similarly between the fourth and fifth. The sixth epoch was obtained in 2009 October. The inclusion of the extra epoch a year later signifi-

<sup>2</sup> [ftp://cdsarc.u-strasbg.fr/pub/cats/J/A+A/341/98](http://cdsarc.u-strasbg.fr/pub/cats/J/A+A/341/98)

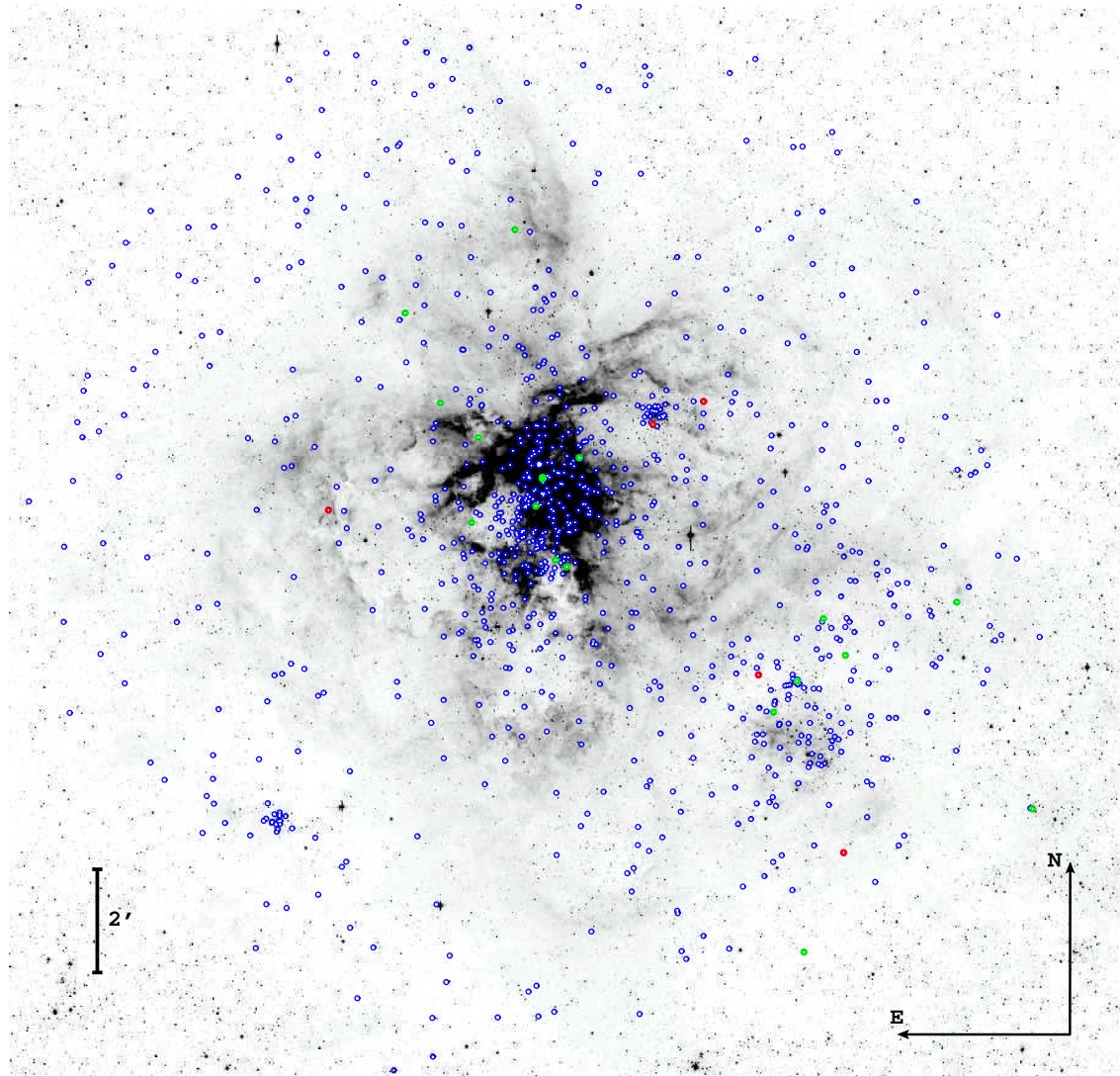


**Fig. 1.** FLAMES–Medusa targets overlaid on the  $V$ -band WFI image. The targets (blue circles) are primarily in the central part of 30 Dor, but also span the broader region including Hodge 301 ( $\sim 3'$  NW of R136), NGC 2060 ( $\sim 6.5'$  SW), and SL 639 ( $\sim 7.5'$  SE). To highlight their locations, the emission-line stars discussed in Section 4.1 are encircled in green, and the five luminous red supergiants from Section 4.3 are encircled in red.

cantly helps with the detection of both intermediate- and long-period binaries. An important part of the interpretation of these multi-epoch spectra will be modelling of the detection sensitivities to put firm limits on the observed binary fraction (Sana et al. in preparation).

Owing to the nature of service-mode observations, a small number of the OBs at the LR02 wavelength setting were repeated for operational reasons, e.g., deterioration of the seeing beyond the required constraints during the exposure, failure of the tracking on the guide star, etc. In cases where full exposures (i.e. 1815 s) were completed, these observations were retained – even if the S/N is lower than in other frames, there will be useful radial velocity information for some targets. This leads to the ‘extra’ frames for Fields A, B, E, and I in Tables A.1 and A.2. There is also an extra LR03 exposure of Field F (‘LR03 01 [c]’), included out-of-sequence of its execution. This OB was aborted mid-execution because the telescope was being used for interferometric observations – the one completed exposure was retained

**Table 1.** Summary of the wavelength coverage, exposure time per observing block (OB), and measured spectral resolution ( $\Delta\lambda$ ) of the different FLAMES modes and settings used in the survey.

Mode	Setting	Exp. time/OB [s]	$\lambda$ -coverage [Å]	$\Delta\lambda$ [Å]	$R$
Medusa	LR02	$2 \times 1815$	3960–4564	0.61	7 000
Medusa	LR03	$2 \times 1815$	4499–5071	0.56	8 500
Medusa	HR15N	$2 \times 2265$	6442–6817	0.41	16 000
ARGUS	LR02	$2 \times 1815$	3960–4570	0.40	10 500
UVES	520	$2 \times 1815$	4175–6200	0.10	53 000

**Notes.** The UVES data do not include the 5155 to 5240 Å region because of the gap between the two detectors.

because it provides additional radial velocity information, for example, in the case of R139 (Taylor et al. 2011).

### 2.2.2. Reductions

The ESO Common Pipeline Library (CPL) FLAMES reduction routines (v2.8.7) were used for all of the initial data processing, i.e. bias subtraction, fibre location and (summed) extractions, division by a normalised flat-field, and wavelength calibration. The subsequent reduction stages were:

- *Heliocentric correction*: All spectra were corrected to the heliocentric frame, using the IRAF packages RVCORRECT and DOPCOR.
- *Sky subtraction*: Each sky fibre was inspected for signs of an on-sky source or cross-contamination from bright spectra/emission lines from adjacent fibres on the detector (see Section 2.2.4). Any contaminated sky fibres were rejected (typically one or two per frame) before creating a median sky spectrum, which was then subtracted from all fibres in that observation.
- *Error spectrum*: An error spectrum was produced by the pipeline for each fibre as part of the reduction process. For each wavelength bin it recorded the statistical error arising from the different stages in the reduction, e.g., bias level, detector gain, read-out noise. These data were combined with the errors on the median sky spectrum to obtain an estimate of the overall error for each spectrum.
- *Cosmic-ray rejection*: Our Medusa–Giraffe exposures were taken in consecutive pairs within the OBs. To clean the extracted spectra of cosmic rays we employed a technique developed (by I.D.H.) for the 2dF survey of the Small Magellanic Cloud (SMC) by Evans et al. (2004). For each spectrum, the ratio of the two exposures was calculated. A boxcar 4-sigma clip over 100 wavelength bins was then performed on this ratio value. Any unexpected and significant deviations in the ratio are indicative of a feature in only one of the observations. Because the exposures were consecutive, it is safe to assume that a transient feature was a cosmic ray. The pixels identified as suspect were rejected, then replaced with the value from the sister exposure, appropriately scaled by the ratio of the surrounding region. This approach results in good removal of cosmics, but is not perfect (which would require inter-comparison between three exposures).
- *Rejection of foreground stars*: Preliminary inspection of the LR02 data for each target was used to identify foreground cool-type stars to exclude them from our final catalogue (employing a velocity threshold of  $v_r < 100 \text{ km s}^{-1}$  for rejection). A total of 102 stars were excluded at this stage, which also included a small number of cool stars with LMC-like radial velocities but with very poor S/N.

As an example of the final S/N of the spectra we consider VFTS 553, one of the faintest Medusa targets ( $V = 17.0 \text{ mag}$ , for which the data reveals an early B-type spectrum). The mean S/N ratio in the individual exposures *per resolution element* were  $\sim 50$  for all three wavelength settings (determined using line-free regions of the stellar continuum). In contrast, the S/N for VFTS 527 (R139, one of the brightest targets) exceeds 400 per resolution element in the best spectra (Taylor et al. 2011).

### 2.2.3. Nebular contamination

Related to the sky subtraction, one of the principal limitations of fibre spectroscopy is the subtraction of local nebular

emission. Indeed, at the distance of the Magellanic Clouds, even (seeing-limited) long-slit spectroscopy can suffer difficulties from spatially-varying nebular emission (cf. the *HST* spectroscopy from, e.g. Walborn et al. 2002). Given the significant nebular emission in 30 Dor, the majority of the Giraffe spectra have some degree of nebular contamination.

The combination of extended nebular emission with the stellar flux from a point-source means that, because the seeing conditions vary for different epochs, the relative intensity of the nebular contamination can vary. Apart from a minority of spectra with particularly strong emission, this is not a big problem for the hydrogen Balmer lines, where the core nebular profile can (effectively) be ignored in quantitative analysis (e.g. Mokiem et al. 2006). However, care is required when selecting He I lines for analysis (most notably  $\lambda 4471$ ) because small changes in the nebulosity could be interpreted as evidence for binarity if unchecked with other lines.

### 2.2.4. Cross-contamination of spectra

To keep the observing as simple and homogeneous as possible, a constant exposure time was used for each fibre configuration. A consequence was that bright stars can cross-contaminate adjacent spectra of fainter stars on the detector after dispersion. This cross-contamination between fibres was generally minimal, but inspection of the reduced spectra revealed a small number of fibres that were contaminated by bright emission lines in W–R or ‘slash’ stars and, in a couple of cases, by luminous supergiants with large continuum fluxes.

Thus, for the observation obtained in the best seeing, we inspected the spectra adjacent to all ‘bright’ stars (with counts greater than 10 000) for each Medusa field and wavelength setting. In some instances the contaminated spectra were sky fibres (rejected as described above), but five stellar targets were omitted because they were pathologically contaminated by very strong emission lines. A further 22 stars have some element of cross-contamination – typically an artificial broad emission ‘bump’ at  $\lambda 4686$  from strong He II in emission-line stars in adjacent fibres. These are noted in the final column of Table 5 – quantitative spectral analysis of these stars may not be possible, but the radial velocities from other regions/lines will still be useful to investigate binarity, gas dynamics, etc.

### 2.3. VLT ARGUS–Giraffe spectroscopy

The Medusa data were complemented by five pointings within the central arcminute of 30 Dor with the ARGUS IFU, as shown in the main panel of Figure 2. The coarser ARGUS sampling was used ( $0''.52/\text{microlens}$ , giving a field-of-view of  $11''.5 \times 7''.3$ ), with a seeing constraint of  $\leq 0''.8$ .

These regions are densely populated with stars, particularly in the core of R136. The first IFU pointing (‘A1’ in the figure) was located on the core, with three pointings immediately adjacent. The fifth pointing was located to the NNE of R136 to target a reasonable number of stars at a slightly larger radius from the core.

Full spectral coverage for quantitative analysis is best obtained with AO-corrected or *HST* spectroscopy – our intention here was to probe the dynamics of these inner regions, again with follow-up observations to identify binary systems. Thus, only the LR02 Giraffe setting was used. The resulting wavelength coverage was comparable to that from the Medusa ob-

servations, but at greater resolving power because of the smaller aperture (see Table 1).

Two OBs were observed without time restrictions and, similar to our strategy for the Medusa data, follow-up epochs (third and fourth) were observed with a minimum interval of 28 days. All these data were obtained over the period 2008 October to 2009 March, with a final (fifth) epoch observed in 2009 December/2010 January.

As with the Medusa observations, a number of the ARGUS OBs were re-observed owing to changes in conditions and other operational issues. The full list of completed exposures for the ARGUS frames is given in Table A.3. These epochs also apply to the UVES observations (Section 2.4), which were taken in parallel to the ARGUS data.

The seeing conditions are more critical to these IFU observations than for the Medusa frames, so the adopted nomenclature is slightly different for repeated OBs. The exposures obtained under the best conditions (ascertained from the seeing value recorded in the file headers at the time of observation) are identified as the ‘a+b’ pair, with other exposures following in order of execution (as ‘c+d’ etc.), e.g., epoch four for the fourth pointing (‘A4’).

### 2.3.1. Reduction

The ARGUS frames were reduced using the same methods as for the Medusa data apart from the sky subtraction and the combination of spectra from adjacent spaxels on the sky (individual stars typically extend over several spaxels). The extracted (cosmic-clipped) spectra were corrected to the heliocentric frame, then combined as follows.

Sources were selected if they appeared isolated in the reduced IFU datacube and if they could be matched to a star (or multiple, densely-packed stars) in an archival *HST F555W* image (from the early release science observations of 30 Dor taken with the Wide-Field Camera Three, WFC3). Less isolated sources were also extracted if their spectra could be distinguished from those of their surroundings, and if they had a matching bright source in the WFC3 image. (Some sources are obviously multiple in the WFC3 image but their spectra were retained because they might still prove useful in the analysis of the velocity dispersion of R136.) The spaxels combined for a given source were selected on the basis that they showed the same spectral features (and relative strengths) as the brightest/central spaxel of that source. There are small positional shifts of approximately one spaxel between the different epochs of a given pointing. These shifts were taken into account when defining (for each frame) the spaxels that contribute to each source.

Spectra were extracted for a total of 41 sources from the ARGUS frames. The 37 unique ARGUS sources are appended to the end of Table 5, with coordinates from centroids of matching sources in the WFC3 image (transformed to the same astrometric system as the Selman–Skiff catalogue for consistency). To distinguish from targets observed with Medusa and/or UVES, these sources are given a separate series of RA-sorted identifiers, starting with VFTS 1001. Photometry is available for all but three from Selman et al. (1999), as listed in Table 5. Note that four Medusa/UVES sources were also observed with ARGUS (VFTS 542, 545, 570, and 585), as noted in the final column of Table 5. The five ARGUS pointings and the location of the extracted sources are shown in Figure 2.

The four or five spaxels with the lowest counts in each pointing were used for local sky spectra. Even so, for most sources the nebular subtraction is still far from perfect given the small-scale variations discussed earlier. Before combining the sky spectra, a  $5\sigma$ -clip (compared to the noise of the median spectrum) was employed to remove remaining cosmic rays or artefacts. A weighted-average sky spectrum was created, then subtracted from the spectra from each of the source spaxels.

Differential atmospheric refraction means that the apparent slope of the continuum of a given source varies from spaxel to spaxel. Thus, each spectrum was normalised individually before combining the contribution of different spaxels. This normalisation was done by a spline-fit across carefully selected continuum regions, then division of the spectrum by the resulting smooth curve. This method generally gave an excellent fit to the continuum, but is less certain for spectra with broad emission lines, for which the continuum is hard to define. The final spectrum of each source is a weighted average of the normalised spectra from the individual spaxels, again employing a  $5\sigma$ -clip around the median to remove spurious pixels.

## 2.4. VLT FLAMES–UVES spectroscopy

The fibre feed to the red arm of UVES was used to observe 25 stars in parallel to the ARGUS observations. Twenty of these were also observed with Giraffe – our aim was to exploit the availability of UVES to obtain broader spectral coverage and additional epochs for radial velocity measurements (at even greater precision). The UVES targets are indicated by ‘U’ in the second column of Table 5, and are all from the Selman et al. (1999) catalogue, i.e., in the inner part of 30 Dor near R136.

### 2.4.1. Reduction

The two CCDs in the red arm of UVES were processed separately. With the  $\lambda 5200$  central wavelength setting, the short-wavelength CCD provided coverage of 4175 to 5155 Å, with the long-wavelength CCD spanning 5240 to 6200 Å. The UVES CPL routines (v4.3.0) from ESO were used for the preliminary reduction stages: bias correction, fibre extraction, wavelength calibration, and division by a normalised flat-field frame. Our own IDL routines were then used for merging of the orders and velocity correction to the heliocentric frame. For these bright targets and at this resolving power, the sky background was relatively low – given the problems relating to merging of the echelle orders, subtraction of the sky spectra resulted in a poorer final data product, so they were not used. From analysis of the reduced arc calibration frames, the delivered resolving power was  $R \sim 53\,000$ .

## 3. Photometry

The approximate photometric calibration of the WFI imaging was sufficient for target selection (Section 2.1), but quantitative spectroscopic analysis requires precise photometry. Given the complexity of 30 Dor (in terms of source detection in regions of bright nebulosity) and the non-photometric conditions/saturation of bright stars in the WFI observations, we revisited the data with a more refined photometric analysis.

From combining the Selman–Skiff catalogue and our analysis of the WFI frames we obtained  $B$ - and  $V$ -band photometry for 717 of the VFTS targets. These were then supplemented by photometry for 68 stars from Parker (1993) and for 91 stars from

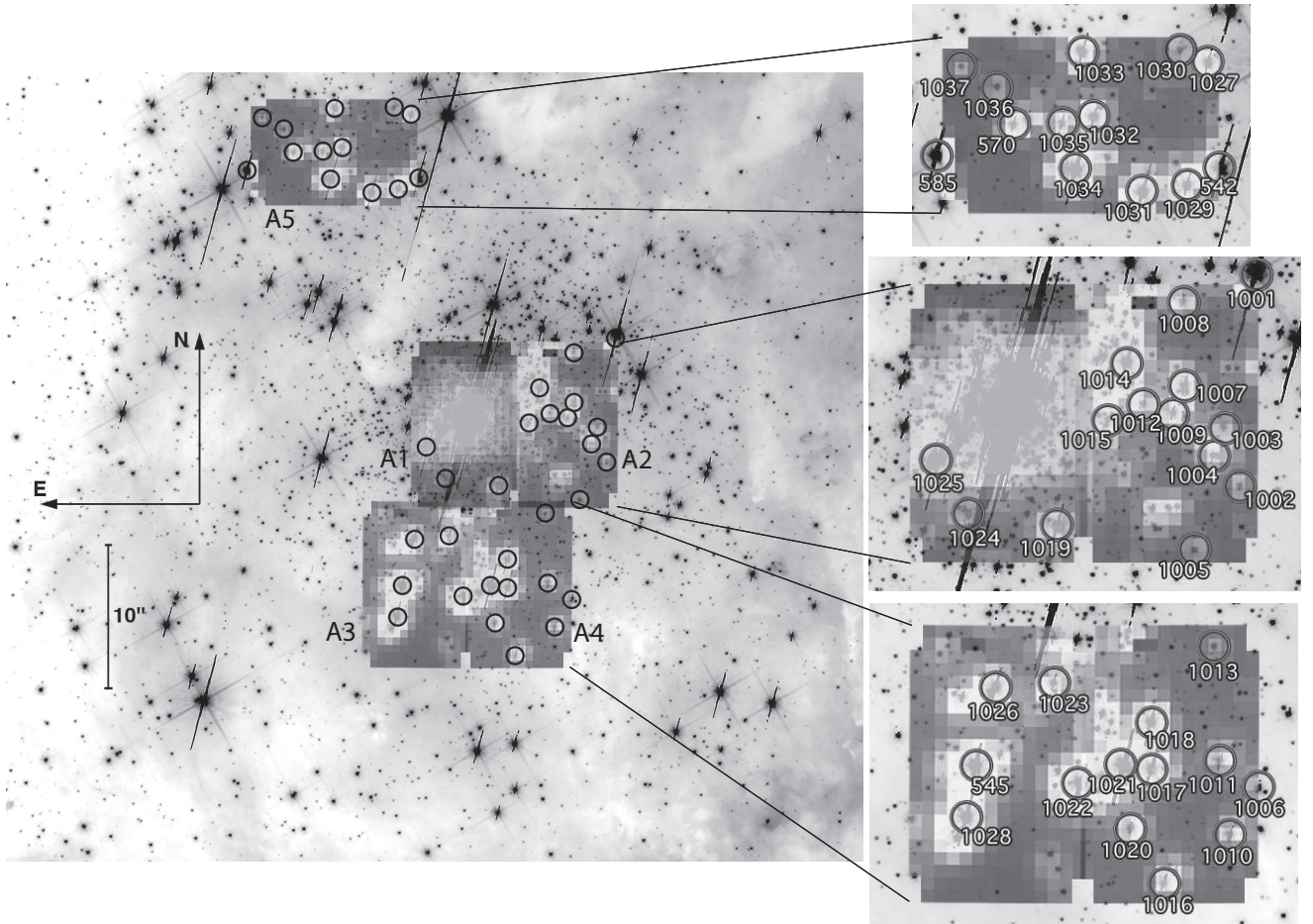


**Fig. 2.** Main image: the five ARGUS pointings overlaid on an F555W *HST*-WFC3 image. Right-hand panels: identification of individual extracted sources – upper panel: Field ‘A5’; central panel: Fields ‘A1’ (eastern pointing) and ‘A2’; lower panel: Fields ‘A3’ (eastern pointing) and ‘A4’.

new imaging at the Cerro Tololo Inter-American Observatory (CTIO), Chile. Each of these photometric sources is discussed briefly below.

Moreover, when undertaking quantitative spectral analysis of massive stars in regions of variable extinction, near-IR photometry can be a useful input towards the determination of accurate stellar luminosities (e.g. Crowther et al. 2010). Cross-matches of the VFTS targets with published near-IR data are discussed in Sections 3.6 and 3.7.

We note that there is a significant amount of imaging of selected regions of 30 Dor at better spatial resolution, principally from the *HST*. Our philosophy here is to compile optical photometry from seeing-limited, ground-based images, which are reasonably matched to the aperture of the Medusa fibres. Thus, even if our ‘stars’ are actually multiple objects, the light received by the fibre is comparable to that measured from the adopted imaging.

### 3.1. ‘Selman’ photometry

The data used for target selection in the central region were taken from the Selman–Skiff catalogue, which was obtained using the Superb-Seeing Imager (SUSI) on the 3.5 m New Technology Telescope (NTT) at La Silla, Chile. The conditions were photometric with sub-arcsecond seeing, and short exposures (10–30 s) were used to avoid saturation. The fine pixel scale of SUSI

( $0''.13/\text{pixel}$ ) means that crowding is less problematic than in the WFI frames. We therefore adopt the *B*- and *V*-band photometry from Selman et al. (1999) for the 167 stars observed from their catalogue, listed with the reference ‘S’ in Table 5. To illustrate the selection effects employed on the FLAMES sources (i.e.  $V \leq 17$  mag and no colour constraint), a colour–magnitude diagram for the 167 stars with photometry from Selman et al. is shown in Figure 3; their other sources ( $V \leq 18$  mag) are also shown.

### 3.2. WFI photometry

Our primary source of photometry is from point-spread function (PSF) fitting of sources in the WFI frames with the stand-alone version of DAOPHOT. We are mainly interested in the relatively bright population so we adopted a detection threshold of 20 times the root-mean-square noise of the local background to avoid spurious detections. We then applied a cut of  $0.2 < \text{sharpness} < 1$  to further filter those detections for extended objects, etc. The resulting *B*- and *V*-band catalogues were merged together using the DAOMATCH and DAOMASTER routines (Stetson 1994), i.e. the final catalogue includes only those sources detected in both bands.

Zero-points for the WFI photometry were determined with reference to 67 stars (within a search radius of less than  $0''.4$  and

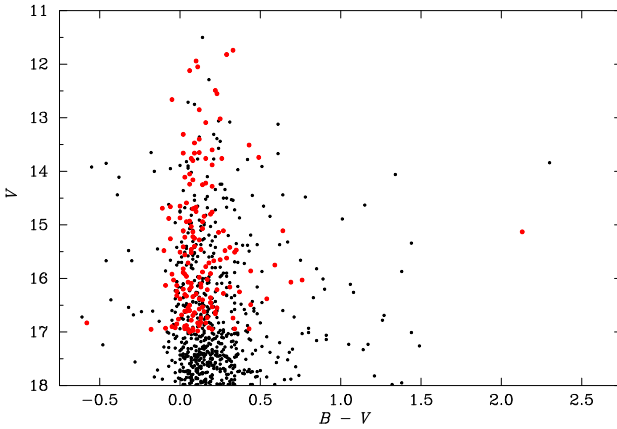


**Fig. 3.** FLAMES targets with photometry from Selman et al. (1999) (167 stars, red points) compared to all sources from their catalogue with  $V \leq 18$  (black).

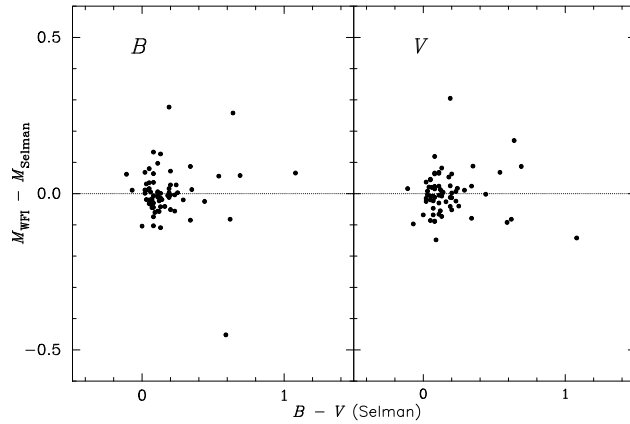


**Fig. 4.** Photometric residuals for the WFI data (where both are WFI – Selman) as a function of  $(B-V)_{\text{Selman}}$ .

$V \leq 18.0$  mag) that overlap with the Selman–Skiff catalogue. The resulting residuals for these matched sources are shown in Figure 4, with standard deviations of  $\leq 0.1$  mag in both bands. The second WFI pointing was bootstrapped from the first using the mean differences between overlapping stars.

Photometry of 550 stars is adopted from analysis of the WFI images (calibrated using the catalogue from Selman et al. 1999). These are listed with the reference ‘W’ in Table 5. Their colour–magnitude diagram is shown in Figure 5; also shown are the  $\sim 2000$  other WFI sources ( $V \leq 18$  mag) within a radius of  $12'$  from R136. There are ten sources with WFI photometry in Table 5 with  $V \leq 14.5$  mag, each of which agrees with the CTIO photometry (Section 3.5) to within 0.1 mag, i.e., within the dispersion of the calibrations in Figure 4.

### 3.3. ‘Parker’ photometry

To supplement the WFI and Selman photometry we first turned to the catalogue from Parker (1993) in 30 Dor, using the re-worked astrometry from Brian Skiff<sup>3</sup>. A comparison between the Parker results and the calibrated WFI photometry for 219 matched stars (within a radius of  $0''.5$ ) yielded only small residuals of  $\Delta V = 0.01$  ( $\sigma = 0.2$ ) and  $\Delta B = -0.03$  ( $\sigma = 0.2$ ) mag, as shown in Figure 6.

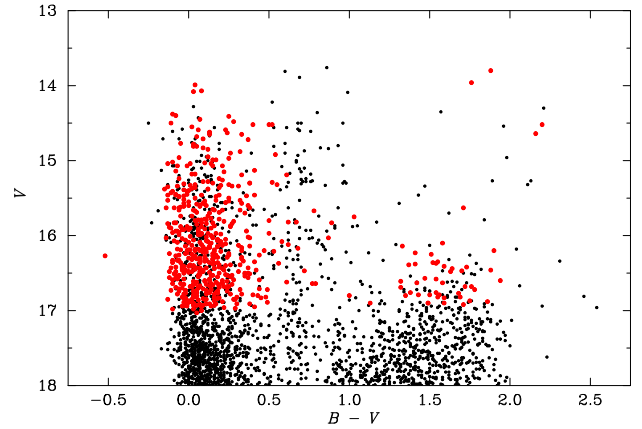


**Fig. 5.** FLAMES targets with WFI photometry (550 stars, red points) compared to all WFI sources with  $V \leq 18$  within a  $12'$  radius of the field centre (black).

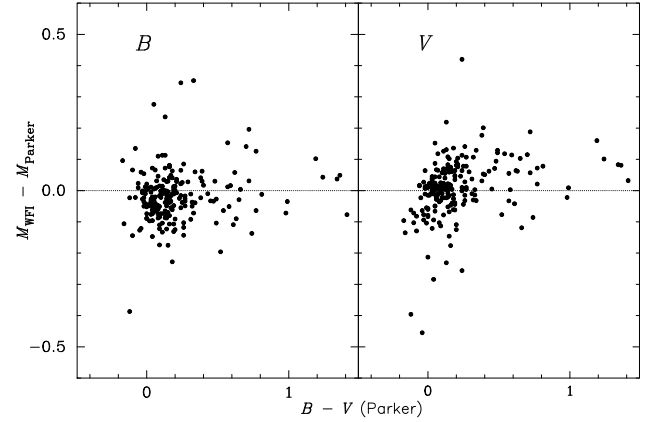


**Fig. 6.** Photometric residuals for the calibrated WFI data compared to those from Parker (1993) as a function of  $(B-V)_{\text{Parker}}$ .

A radial search (of  $0''.5$ ) and then visual matching of the VFTS targets without WFI or Selman photometry yielded 68 matches in the Parker catalogue (with a median radial offset of  $0''.11$ ). For our current purposes, we adopt his photometry for these 68 stars, listed with the reference ‘P’ in Table 5.

### 3.4. MCPS photometry

As a potential source of photometric information for the remaining 108 stars we turned to the LMC catalogue from the Magellanic Clouds Photometric Survey (MCPS; Zaritsky et al. 2004), which includes photometry of some of the bright sources from Massey (2002). However, we found large uncertainties on the MCPS photometry in the 30 Dor region.

We first considered cross-matched sources from the MCPS catalogue as an external check on the photometric calibration of the WFI frames. Adopting a search radius of less than  $1''.0$ , a total of 5726 ‘matches’ were found between the northeastern WFI frame and the MCPS. The residuals for  $B$  and  $V$  (in the sense of WFI – MCPS) are shown in Figure 7 as a function of MCPS colour. The standard deviation of the residuals in both bands is  $\sim 0.25$  mag, not unreasonable considering the potential for spurious matches and complications relating to blending and nebulosity in this field – the typical seeing from the MCPS is  $1''.5$

<sup>3</sup> [ftp://cdsarc.u-strasbg.fr/pub/cats/II/187A](http://cdsarc.u-strasbg.fr/pub/cats/II/187A)

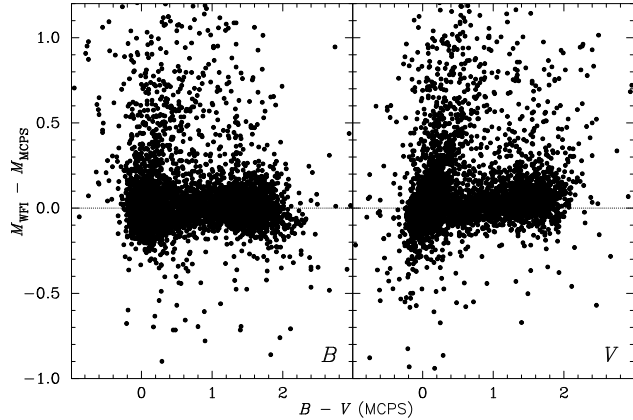


**Fig. 7.** Photometric residuals for the WFI data (where both are WFI – MCPS) as a function of  $(B - V)_{\text{MCPS}}$ .

(with  $0.^{\prime\prime}7$  pixels), but extended up to  $2.^{\prime\prime}5$  (Zaritsky et al. 2004), while the photometry from Massey (2002) used an aperture of  $16.^{\prime\prime}2$ . Although there is reasonable agreement in the zero-point calibrations between the WFI and MCPS data, the ‘plume’ to brighter MCPS magnitudes is particularly notable in Figure 7.

Concerned by the potential of inter-CCD calibration problems in the WFI data, we investigated the distribution of the residuals as a function of both declination and right ascension, as shown in Figures 8 and 9, respectively. The residuals between the WFI and MCPS photometry are noticeably larger over the main body of 30 Dor (centred at  $\alpha = 5^{\text{h}}645$ ,  $\delta = -69^{\circ}101$ , and with the densest nebulosity having a diameter of  $\sim 6'$ ). Larger residuals can also be seen in the region of  $\alpha = 5^{\text{h}}702$ , the centre of the dense cluster NGC 2100. The residuals are predominantly in the sense of brighter magnitudes from MCPS compared to the WFI frames, which suggests that they primarily arise from unresolved blends or nebular contamination.

### 3.5. CTIO photometry

Thus, to obtain optical photometry for the majority of the remaining FLAMES targets, we observed 30 Dor on 2010 December 27 with the Y4KCAM camera on the CTIO 1 m telescope, operated by the SMARTS consortium<sup>4</sup>. The camera is equipped with an STA  $4064 \times 4064$  CCD with  $15 \mu\text{m}$  pixels, yielding a scale of  $0.^{\prime\prime}29 \text{ pixel}^{-1}$  and total field-of-view of  $20' \times 20'$  at the Cassegrain focus.

Observations were obtained in photometric conditions with good seeing (less than  $1.^{\prime\prime}3$ ), using  $B$ - and  $V$ -band filters in the Kitt Peak system<sup>5</sup>. A range of exposure times in each band were used to avoid saturating bright stars (from 10 s up to a maximum of 400 and 300 s in the  $B$ - and  $V$ -bands, respectively). Instrumental magnitudes were obtained using PSF-fitting routines in DAOPHOT, then observations of standard stars taken on the same night in Selected Area 98 (Landolt 1992) were used to transform the photometry to the Johnson–Kron–Cousins system and to correct for atmospheric extinction. The standard observations spanned a range of airmass (from 1.05 to 2.60)

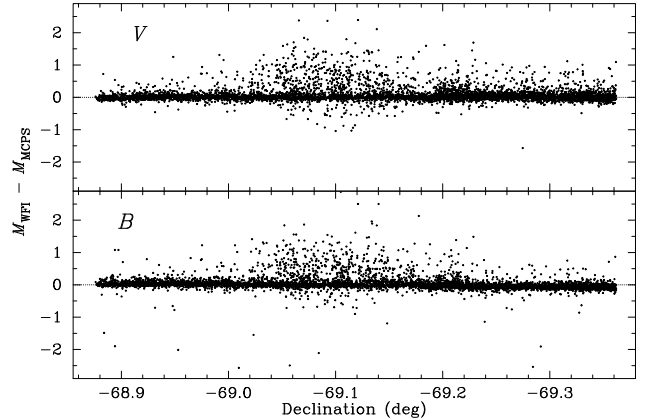


**Fig. 8.** Photometric residuals for the WFI data (where both are WFI – MCPS) as a function of declination.

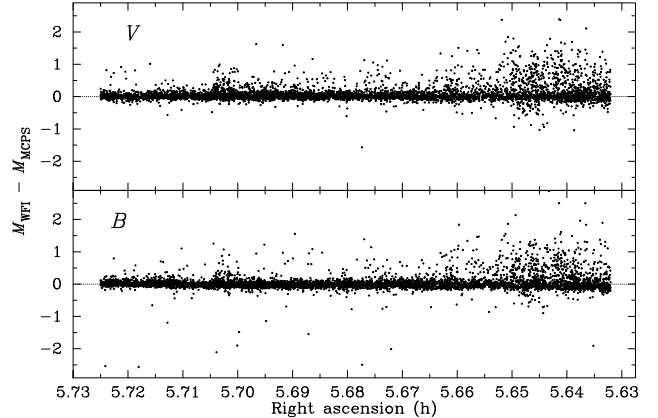


**Fig. 9.** Photometric residuals for the WFI data (where both are WFI – MCPS) as a function of right ascension.

and included stars over a broad range of colours ( $-0.3 \leq (B - V) \leq 1.7$  mag).

Robust matches were found for 91 of the remaining FLAMES targets, with photometry from the CTIO imaging listed in Table 5 with the reference ‘C’. Given the independent calibration using published standards, we do not attempt to transform the photometry of these stars onto the same exact system as the WFI photometry. However, they agree reasonably well – a comparison of nearly 800 matched stars yields mean residuals of  $\Delta V$  and  $\Delta B \leq 0.05$  mag (with  $\sigma \sim 0.2$  mag in both bands).

Seven of the remaining targets were beyond the western and southern extent of the CTIO images (VFTS 002, 003, 014, 016, 017, 739, and 764) and five did not have counterparts in the CTIO catalogue owing to nearby blends or the PSF-fitting criteria (VFTS 092, 172, 301, 776, and 835). Photometry is available from the MCPS catalogue for four of these (VFTS 016, 092, 739, 764), each of which is over  $8'$  from the core of 30 Dor, so the problems discussed in Section 3.4 should be minimised.

The last five targets without optical photometry (VFTS 145, 147, 150, 151, & 153) are in the dense ‘Brey 73 complex’, which was first resolved by Testor et al. (1988) and later observed with the *HST* by Walborn et al. (1995, 1999b). The *HST* photometry from Walborn et al. (1999b) is adopted in Table 5 for the three (visually) single stars: VFTS 145, 150, & 153. The two brightest members (#1 and #2 from Testor et al., VFTS 147 and 151) were resolved into separate bright components by the *HST* imaging, i.e. the Medusa fibres will contain contributions from these, and

<sup>4</sup> <http://www.astro.yale.edu/smarts>

<sup>5</sup> <http://www.astronomy.ohio-state.edu/Y4KCam/filters.html>

any future analysis will have to consider their relative fluxes (and colours).

### 3.6. Near-IR photometry

The extensive near-IR imaging survey of the Magellanic Clouds from Kato et al. (2007)<sup>6</sup> provides  $JHK_s$  photometry for nearly all of our FLAMES targets. The mean seeing at  $J$ ,  $H$ , and  $K_s$  was  $1''.3$ ,  $1''.2$ , and  $1''.1$ , respectively, i.e., well-matched to the on-sky Medusa fibre aperture.

To identify IRSF counterparts to the FLAMES targets we employed an astrometric search radius of  $0''.5$ , then overlaid the resulting list on the WFI  $V$ -band images to reject spurious matches. The IRSF magnitudes ( $JHK_s$ , and their associated photometric errors) are given for the FLAMES targets in Table 6 (published online). The IRSF ‘quality’ flag in the final column indicates the source detection in each of the three bands as follows (for further details see Kato et al. 2007): ‘1’, point-like; ‘2’, extended source; ‘3’, saturated; ‘4’, faint; ‘5’, odd shaped (e.g. double sources); ‘0’, no detection.

The Two Micron All Sky Survey (2MASS; Skrutskie et al. 2006) catalogue was used to calibrate the IRSF astrometry and to provide checks on the photometry (see Kato et al. 2007). However, we note that the IRSF–SIRIUS filter-set was designed to match that of the Mauna Kea Observatories near-IR filters (Tokunaga et al. 2002), and is therefore slightly different to that used by 2MASS. Transformation equations between the IRSF–SIRIUS and 2MASS systems are given by Kato et al. (2007) and Kucinskas et al. (2008); in practise, the corrections between the two are relatively small, with typical differences of less than  $0.05$  mag for  $(J - K_s)_{\text{IRSF}} < 1.7$  mag (Kucinskas et al. 2008).

There are five FLAMES targets without good IRSF matches within  $0''.5$ : VFTS 275, 503, 620, 823, and 828. Additionally, VFTS 151 has two potential matches, but is excluded following the discussion of multiplicity in Section 3.5. In some instances there were two potential matches both within a radius of less than  $0''.3$ . In approximately half of these one set of the IRSF measurements was obtained in the ‘periphery’ of the dither patterns (so the S/N is lower) and these values were omitted. However, for seven targets (VFTS 125, 330, 368, 374, 377, 383, 384) both IRSF detections are good spatial matches and not saturated. For these sources we compared the observational conditions of the relevant exposures (Table 2, Kato et al. 2007) and adopted the values obtained in the best seeing. As noted in Table 5, VFTS 240 appears slightly extended (or as a blended source) in the optical WFI image; the IRSF catalogue has a counterpart approximately  $0''.5$  from the FLAMES position, with  $J = 16.31 \pm 0.06$  mag, but it was not detected in the other two near-IR bands.

Similar comparisons were undertaken between the IRSF catalogue and the unique ARGUS targets (i.e. those numbered from 1001 to 1037, see Section 2.3). Good matches (all within  $0''.3$ ) were found for 31 sources, as summarised in Table 6. Six ARGUS sources are without IRSF photometry: VFTS 1012, 1014, 1015, 1019, 1024, and 1025.

### 3.7. Cross-references with 2MASS

Near-IR photometry for some of our targets is also available from the 2MASS catalogue. However, with a pixel size of  $2''.0$ ,

its spatial resolution is inferior to the IRSF data. Nonetheless, we include cross-identifications to 2MASS for the VFTS targets in the final column of Table 5 for completeness. Our approach was similar to the comparison with the IRSF catalogue, with visual inspection of potential matches to reject those notably blended in the WFI data or with positions offset by contributions from other nearby stars/nebulosity. In particular, given the crowding in the central region around R136 and the limited angular resolution of 2MASS, we did not attempt cross-matching within the central  $30''$ . Only cross-matches with 2MASS photometric qualities of either ‘A’ or ‘B’ (i.e.  $S/N \geq 7$ ) were retained, leading to 2MASS identifications for 227 of our targets.

## 4. Spectral classification

Following reduction, the first epoch of LR02 and LR03 spectra of each target were inspected; approximately 300 targets display He II absorption, which is indicative of an O (or B0) spectral type. However, the multi-epoch nature of the VFTS spectroscopy complicates precise classification and entails significant analysis, which is being undertaken as part of studies towards binarity and the determination of stellar radial velocities (Sana et al. and Dunstall et al., both in preparation). Detailed classifications of the O- and B-type spectra will therefore be given elsewhere. Here we present classifications for the two smaller spectral groups in the survey: the W–R/massive emission-line stars and the cooler stars (of A-type and later).

### 4.1. Wolf–Rayet and ‘slash’ stars

Massive emission-line stars in the LMC have been well observed over the years, from the seminal Radcliffe Observatory study by Feast et al. (1960), to narrow-band imaging surveys to identify W–R stars (e.g. Azzopardi & Breysacher 1979, 1980), comprehensive spectroscopic catalogues (e.g. Breysacher 1981; Breysacher et al. 1999), and monitoring campaigns to study binarity (e.g. Moffat 1989; Schnurr et al. 2008).

The W–R and transitional ‘slash’ stars (see Crowther & Walborn, in preparation) observed by the VFTS are summarised in Table 2 (and are highlighted in green in Figure 1). In addition to those in R136 (Crowther et al. 2010), these stars comprise some of the most massive stars in 30 Dor and will provide valuable insights into some of the most critical phases of massive-star evolution.

Previous spectral types are included in Table 2, with revised classifications in the final column if new features and/or evidence for companions are present in the FLAMES data. The new data reveal massive companions in at least three of these objects: VFTS 402 and 509 (BAT99-95 and 103, respectively). Quantitative analysis of these data is now underway. Note that VFTS 527 (*aka* R139), has been treated as a W–R star by some past studies; the VFTS observations have revealed it as an evolved, massive binary system comprised of two O Iaf supergiants (Taylor et al. 2011).

### 4.2. Discovery of a new W–R star in the LMC

The combined FLAMES spectrum of VFTS 682 is shown in Figure 10. Classified as WN5h (in which the ‘h’ suffix denotes the presence of hydrogen lines), this is a previously unknown W–R star. From qualitative comparisons of the individual spectra there is no evidence for significant ( $\Delta v \gtrsim 10 \text{ km s}^{-1}$ ) radial velocity variations.

<sup>6</sup> Obtained using the Simultaneous three-colour InfraRed Imager for Unbiased Survey (SIRIUS) camera ( $0''.45 \text{ pixel}^{-1}$ ) on the InfraRed Survey Facility (IRSF) 1.4 m telescope at Sutherland, South Africa.

**Table 2.** Summary of published and, where relevant, new spectral classifications for massive emission-line stars in the VLT-FLAMES Tarantula Survey (VFTS) observations. The spectral types adopted for the survey are given in bold font. Aliases to the Breysacher et al. (BAT99, 1999) and Breysacher (1981) catalogues are provided (other aliases are included in Table 5).

Identification				VFTS spectral types
VFTS	BAT99	Brey	Published spectral types	
002	85	67	WC4+OB [SSM90]	<b>WC4+O6-6.5 III</b>
019	86	69	WN4 [Brey]; WN3o+O9: [FMG03]	<b>WN3o</b>
079	88	70a	WN3-4 [MG87]; <b>WN4b/WCE</b> [FMG03]	—
108	89	71	WN7 [Brey]; <b>WN7h</b> [CS97]	—
136	90	74	WC5 [Brey]; <b>WC4</b> [SSM90]	—
147	91	73	WN6.5h and O7 V [W99]; WN6h:a [S08]	<b>WN6(h)</b>
180	93	74a	O3 If*/WN6 [TS90]	<b>O3 If*</b>
402	95	80	WN7 [F60]; WN7 [Brey]; WN6 [Mk]; WN7h [CS97]	<b>WN7h+OB</b>
427	96	81	WN8 [Brey]; WN8 [Mk]; <b>WN8(h)</b> [CS97]	—
457	97	—	O4 If [Mk]; O3 If*/WN7-A [WB97]	<b>O3.5 If*/WN7</b>
482	99	78	O4 If [Mk]; O3 If*/WN6-A [WB97]	<b>O2.5 If*/WN6</b>
507	101/102	87	WC5+WN4 [Mk]; <b>WC4+WN6</b> [M87];	—
509	103	87	WN4.5 [Mk]; WN6 [M87]; WN5.5 [B99]	<b>WN5(h)+O</b>
542	113	—	O3 If [Mk]; O3 If*/WN6-A [WB97]	<b>O2 If*/WN5</b>
545	114	—	O3 If [Mk]; O3 If*/WN6-A [WB97]	<b>O2 If*/WN5</b>
617	117	88	<b>WN5ha</b> [FMG03]	—
682	—	—	—	<b>WN5h</b>
695	119	90	WN6-7 [F60]; WN7 [Brey]; WN6 [Mk]; WN6 [B99]; WN6(h) [CS97]	<b>WN6h+?</b>
731	121	90a	WC4 [MG87]; <b>WC4</b> [SSM90]; WC7-9 [B99]	—
758	122	92	WN5+ [F60]; WN6 [Brey]; WN5(h) [FMG03]	<b>WN5h</b>

**Notes.** Previous classifications are from F60 (Feast et al. 1960); Brey (Breysacher 1981); W84 (Walborn 1984); Mk (Melnick 1985); MG87 (Morgan & Good 1987); M87 (Moffat et al. 1987); SSM90 (Smith et al. 1990); TS90 (Testor & Schild 1990); CS97 (Crowther & Smith 1997); WB97 (Walborn & Blades 1997); B99 (Bosch et al. 1999); W99 (Walborn et al. 1999b); FMG03 (Foellmi et al. 2003); S08 (Schnurr et al. 2008).

In their analysis of the *Spitzer*-SAGE survey of the LMC (Meixner et al. 2006), VFTS 682 is included by Gruendl & Chu (2009, hereafter GC09) in their list of ‘definite’ young stellar objects (YSOs). Near-IR (from the IRSF catalogue) and *Spitzer* photometry for VFTS 682 are summarised in Table 4. Near-IR photometry is also available from Hyland et al. (1992, infrared source 153) and 2MASS. The evolutionary status of VFTS 682 and the origins of its mid-IR excess are discussed by Bestenlehner et al. (in preparation).

#### 4.2.1. A new B[e]-type star adjacent to R136

The ARGUS spectrum of VFTS 1003 (Figure 11) is particularly striking owing to a large number of Fe II emission lines. It is similar to that of GG Carinae (see Walborn & Fitzpatrick 2000) but with emission lines from [Fe II]; some weak He I absorption lines are also present. There is forbidden [S II] and [O III] emission at  $\lambda$ 4069 and  $\lambda$ 4363, respectively, although from the present data it is not clear if these are from the local nebulosity or are intrinsic to the star. There do not appear to be any significant radial velocity shifts between the individual spectra. Its near-IR colours ( $J - H = 0.54$  and  $(H - K_s) = 1.43$  mag (from the IRSF catalogue) place it in a comparable region to the B[e] stars from Gummersbach et al. (1995). We also note that it is a single, isolated source in the high angular-resolution near-IR images from the Multiconjugate Adaptive-optics Demonstrator (MAD) from Campbell et al. (2010).

Lamers et al. (1998) presented a classification framework for B[e]-type stars, with GG Car classified as a B[e] supergiant. The spectrum of VFTS 1003 warrants a B[e] classification, but does not allow us to distinguish between an evolved B[e] supergiant and a pre-main sequence (‘Herbig’) B[e] star (cf. the criteria

from Lamers et al.). Nevertheless, the presence of such a rare object a mere 8''.5 from the core of R136 certainly warrants further study. In particular, photometric monitoring would help to distinguish between the two evolutionary scenarios: small variations ( $\sim 0.2$  mag) would be expected for a B[e]-type supergiant, whereas much larger and irregular variations (related to accretion processes) would be expected for a ‘Herbig’ object (Lamers et al. 1998).

#### 4.3. Classification of later-type stars

There are 91 stars with classifications of A-type or later that were retained as likely members of the LMC. For the purposes of classification these were assumed to be single stars, i.e. all of the available LR02 and LR03 spectra were stacked and co-added; classifications are given in Table 3.

The small number of A-type spectra were classified with reference to the standards presented by Evans & Howarth (2003) and the metal-poor A-type stars from Evans et al. (2006). The new FLAMES data do not include the Ca K line, so the primary temperature diagnostic is the intensity of the metal lines; luminosity types were assigned on the basis of the H $\gamma$  equivalent-width criteria from Evans et al. (2004).

Except for a small number of G-type stars (that were classified following the criteria from Evans & Howarth 2003) we employ broad classification bins for the cooler types. These are not a key component of our scientific motivations and due to their red colours have relatively low S/N ratios. The spectral bins adopted in Table 3 encompass a range of types: ‘Early G’ (G0-G5); ‘Late G/Early K’ (G5-K3); ‘Mid-late K’ (K3-M0); and

'Early M'. Three carbon stars with strong C<sub>2</sub> Swan bands are also included in the sample.

We do not attempt luminosity classifications for stars of F-type and later. On the basis that their radial velocities are consistent with membership of the LMC, from distance arguments they are notionally supergiants or bright giants (i.e. classes I and II). Indeed, five stars in Table 5 are sufficiently bright<sup>7</sup> to be considered 'red supergiants': VFTS 081, 198, 236, 289, and 793, each of which is encircled in red in Figure 1.

## 5. Spitzer YSO candidates

Prompted by the mid-IR behaviour of VFTS 682 (Section 4.2), we cross-matched the survey targets with the catalogues of 'definite' and 'probable' YSOs from GC09 to investigate their spectral properties.

The SAGE data comprise imaging with two *Spitzer* instruments: the InfraRed Array Camera (IRAC) at 3.6, 4.5, 5.8, and 8.0  $\mu\text{m}$ , and the Multiband Imaging Photometer for Spitzer (MIPS) at 24, 70, and 160  $\mu\text{m}$ . The angular resolution of the IRAC images ranges from 1''.7 to 2''.0, with coarser resolution of 6'', 18'', and 40'', at 24, 70, and 160  $\mu\text{m}$ , respectively (Meixner et al. 2006). To compare our targets with the GC09 catalogues, we employed a conservative search radius (compared to the IRAC resolution) of  $r < 2''.5$ , which yielded five potential matches in the 'definite' YSO list, and 11 potential matches in the 'probable' YSO list. Each potential match was then examined using the optical WFI images and, where possible, the MAD near-IR imaging from Campbell et al. (2010), and the imaging from the High Acuity Wide-field K-band Imager (HAWK-I) which was used to calibrate the MAD data.

The near-IR images are particularly helpful to identify robust counterparts. A notable false match at a distance of 1''.2 from VFTS 476 is GC09 053839.69–690538.1. The optical WFI image reveals only the VFTS target whereas, as shown by Figure 13 from Campbell et al. (2010), there is a very red source at the GC09 position, with VFTS 476 the object to the south<sup>8</sup>. Near- and mid-IR photometry of matched sources from GC09 are summarised in Table 4, each of these is now discussed in turn.

**VFTS 016:** This is the massive 'runaway' star from Evans et al. (2010, '30 Dor 016', classified as O2 III-If\*), which features in the list of probable YSOs from GC09.

Mid-IR observations have been used by, e.g., Gvaramadze & Bomans (2008) and Gvaramadze et al. (2010, 2011) to identify bow shocks associated with runaway stars. For instance, the SAGE 24  $\mu\text{m}$  images were used to investigate six O2-type stars in the LMC thought to be runaways, including VFTS 016 (Gvaramadze et al. 2010). Of the six candidate runaways, only BI 237 was reported to have a bow shock from inspection of the MIPS images, consistent with the expectation from Gvaramadze & Bomans (2008) that approximately 20% of runaways have an associated bow shock.

Although the *Spitzer* resolution at 24  $\mu\text{m}$  is less than ideal in a region as crowded as 30 Dor, VFTS 016 is relatively isolated at a projected distance of 120 pc from the core of R136. The 24  $\mu\text{m}$  magnitude from GC09 for VFTS 016 (see Table 4) suggests a

strong mid-IR excess – perhaps associated with a bow shock (but not extended sufficiently to be detected by Gvaramadze et al.).

**VFTS 178:** A visually bright star, the spectrum of VFTS 178 appears as a relatively unremarkable supergiant, classified O9.7 Iab (see Figure 12). The star was previously classified as B0.5 I by Schild & Testor (1992), with the new high-quality data revealing sufficiently strong He II  $\lambda 4542$  absorption that a slightly earlier type is required. No obvious radial velocity variations are apparent from inspection of the FLAMES data.

**VFTS 320:** This was the closest match to GC09 053821.10–690617.2 (with VFTS 316 at a distance of only 1''.2). As noted in Table 5, the spectrum of VFTS 320 suffers from contamination from an adjacent fibre on the detector (see Section 2.2.2), manifested by a broad emission bump (approximately 4% above the continuum) at  $\lambda 4686$ . Aside from this wavelength region, the spectrum is that of an early B-type star with considerable nebular contamination plus weak Fe II emission, which resembles that from a Be-type star. The adjacent object on the detector was VFTS 147, classified in Section 4.1 as WN6(h). This does not display Fe II emission (indeed, the He II  $\lambda 4686$  emission is by far the strongest line), i.e., the Fe II features seen in VFTS 320 are genuine. The spectrum (with the  $\lambda 4686$  region omitted) is shown in Figure 12.

**VFTS 345:** A single object in the WFI and HAWK-I frames, the co-added spectrum of VFTS 345 is shown in Figure 12 and is classified as O9.7 III(n) (cf. the published classification of B0 V from Bosch et al. 1999).

**VFTS 410:** This target is P93-409 (Parker 1993), located in 'Knot 3' to the west of R136 (Walborn 1991). Classified as O3-6 V by Walborn & Blades (1997), *HST* imaging and spectroscopy by Walborn et al. (1999a, 2002) resolved two bright components with spectral types of O8.5 V and O9 V. A third, much redder (visually fainter) source was reported just 0''.4 northwest of the two massive stars by Walborn et al. (1999a), as well as several very compact nebulosities to the northeast. This complex would be resolved poorly by the *Spitzer* observations, but is clearly an active site of star formation.

For completeness, we show the combined spectrum of VFTS 410 in Figure 12; there is significant nebular emission superimposed on the stellar profiles. Given the knowledge that there are two luminous components contributing to these data, it is worth noting that no radial velocity variations are seen from a comparison of the available spectra. Even if these are not in a bound binary system, their proximity in such a star-formation complex suggests they are associated. This object highlights the benefit of high-resolution imaging for some systems (from *HST*, MAD, etc.) when attempting to interpret the new spectroscopy.

**VFTS 464:** This is the star at the centre of the impressive bow-shock feature discovered by Campbell et al. (2010) from the MAD images. In Figure 13 we show new combined colour images from MAD (with different intensity scalings). There is a source 0''.4 from the central object that is approximately three times fainter – given the 1''.2 aperture of the Medusa fibres, the spectra of the central star are likely contaminated by the companion.

As one might expect, the FLAMES spectra are heavily contaminated by nebular emission, which appears to include forbidden lines such as [S II]  $\lambda\lambda 4069$ -76, [Fe III]  $\lambda 4702$ , and

<sup>7</sup> Assuming  $M_V \sim -4.5$  to 5.0 for late-type Ib supergiants.

<sup>8</sup> Campbell et al. (2010) argued that the star was likely a massive star on the basis of its near-IR photometry. Indeed, the FLAMES spectra of VFTS 476 reveal it as a late O-type star.

**Table 3.** Spectral classifications for cool-type stars (A-type or later) from the VLT-FLAMES Tarantula Survey (VFTS).

Star	Sp. Type	Star	Sp. Type	Star	Sp. Type
006	Mid-late K	323	A5 II	773	Late G/Early K
011	Late G/Early K	341	Mid-late K	776	Carbon star
023	Late G/Early K	344	Mid-late K	783	Late G/Early K
026	Late G/Early K	357	Late G/Early K	785	Mid-late K
032	Late G/Early K	372	Late G/Early K	790	F0
057	Mid-late K	379	Mid-late K	791	Late G/Early K
081	Mid-late K	437	Mid-late K	793	Late G/Early K
092	Late F	439	Late G/Early K	803	Late G/Early K
115	Late G/Early K	454	Late G/Early K	805	Mid-late K
129	Mid-late K	490	Late G/Early K	808	Late G/Early K
139	Late F	524	G0	809	Late G/Early K
175	A2-3 II	544	Late G/Early K	816	G2
182	F0	595	Mid-late K	818	Mid-late K
193	Late G/Early K	614	Early G	820	A0 Ia
198	Mid-late K	655	Late G/Early K	828	Early M
222	G0	658	A7 II	839	G
236	Mid-late K	674	A2-3 II	844	Mid-late K
245	Mid-late K	680	Early G	852	Late F
260	Early G	691	A2-3 II	856	A7 II
262	F0	693	Late G/Early K	858	A7 II
264	Mid-late K	694	Mid-late K	861	Late G/Early K
265	A2-3 II	700	Mid-late K	862	Early G
271	A7 II	708	Late G/Early K	863	A5 II
275	Early M	721	A9 II	865	Late G/Early K
281	Mid-late K	744	Early M	870	F0
289	Late G/Early K	759	Mid-late K	871	A7 II
294	A0 Ib	760	A9-F0 II	873	A2-3 II
311	Carbon star	763	G5:	878	G2
312	Mid-late K	765	Early M	884	Carbon star
317	A9 II	767	Late G/Early K	893	A7: II
319	Mid-late K				

**Notes.** Previous classifications are available for 11 stars, primarily from Melnick (1985, Mk) and Schild & Testor (1992, ST92): 057: G8-K2 [ST92]; 129: G8-K3 [ST92]; 193: late G [ST92]; 198: G,K [ST92]; 222: G,K [ST92]; 271: A Ib [Mk]; 294: A0 Ib [Mk]; 317: A5 Ib [Mk]; 437: G8 III (Bosch et al. 1999); 691: A I (Walborn & Blades 1997), A2-3 I (Bosch et al. 1999); 793: early K I (Parker 1993).

[Ar IV]  $\lambda$ 4711. The combined blue-region spectrum is shown in Figure 12 – note the weak He II absorption, leading to a provisional classification of B0:, with the uncertainty reflecting the problems of nebular contamination and the potential contribution from the nearby object.

The He II absorption at  $\lambda$ 4542 and  $\lambda$ 4686 appears consistent with the systemic radial velocity of 30 Dor, i.e., the object does not appear to be a candidate runaway in the radial direction. Indeed, as noted by Campbell et al. (2010), the bow shock is orientated towards R136 (and Brey 75/BAT99-100), suggesting it might well be related to an ionization front (with associated triggered star-formation) rather than a dynamical shock.

**VFTS 500:** This object appears as a single source in the HAWK-I imaging, as shown in Figure 14 (in which the slight northern extension of the star is an artefact of the dither pattern used for the observations)<sup>9</sup>; the FLAMES spectroscopy reveals it as a double-lined binary. Observed in Medusa Field A, the first LR03 epoch was obtained on the same night as the first three LR02 spectra. The co-added spectrum from these epochs is shown in Figure 12, displaying twin components in the He I and II lines. The nebular contamination thwarts precise

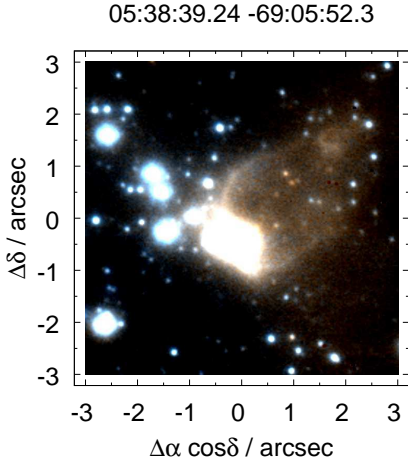
<sup>9</sup> The two sources  $\sim$ 2''.75 to the SSE comprise VFTS 504, and the two at the SE edge are VFTS 530. Both appear as probable blends in the WFI imaging.

classification, but both of the He I  $\lambda$ 4026 components are greater in intensity than the He II  $\lambda$ 4200 features, requiring a type of later than O6. Similarly, the intensity of the He II  $\lambda$ 4200 profiles suggests a type of earlier than B0 for both components.

**VFTS 586:** The combined blue-region spectrum is shown in Figure 12. The spectrum is classified O4 V((n))((fc))z, in which the ‘c’ suffix refers to C III emission at  $\lambda\lambda$ 4647-50-52 (Walborn et al. 2010).

**VFTS 631:** Inspection of the spectra of VFTS 631 reveals a single-lined binary, with radial velocity shifts of the order of  $70 \text{ km s}^{-1}$  in the final LR02 observation compared to the first epoch. To estimate the spectral type, the first three LR02 epochs (taken on the same night) were combined with the LR03 data, as shown in Figure 12. The combined spectrum is classified as O9.7 III(n), in good agreement with published types of O9-B0 II (Walborn & Blades 1997) and O9.5 II (Bosch et al. 1999).

There are two obvious components to the nebular emission in the LR02 and LR03 spectra (e.g. twin-peaked emission in the [O III] lines). One of the components is consistent with the typical systemic velocity of 30 Dor ( $\sim$ 270–280  $\text{km s}^{-1}$ ), with the other blueshifted by approximately 50–60  $\text{km s}^{-1}$ ). These are most likely from separate components of gas emission, but could also be indicative of a wind-blown bubble around the



05:38:39.24 -69:05:52.3

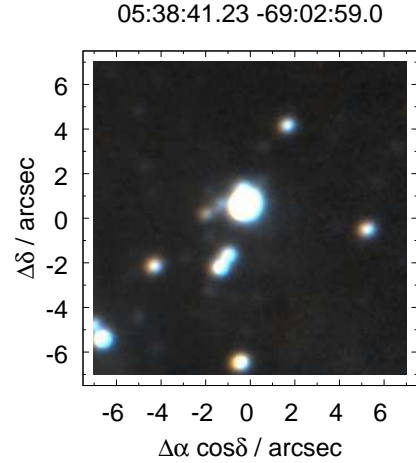
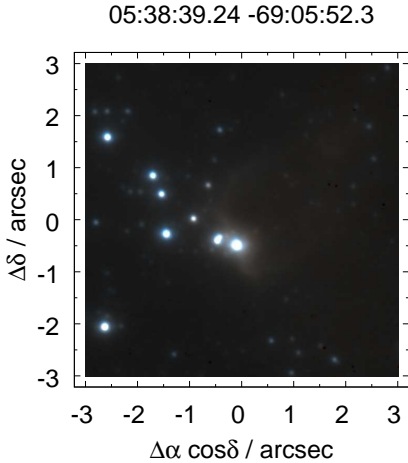


**Fig. 14.** Combined  $14'' \times 14''$   $J$ - and  $K_s$ -band HAWK-I image of the candidate young stellar object 053841.23–690259.0, centred at the position from Gruendl & Chu (2009). The (near-) central bright source is VFTS 500, a double-lined binary comprised of two late O-type stars.



05:38:48.86 -69:08:28.0

**Fig. 13.** Combined  $6'' \times 6''$   $H$ - and  $K_s$ -band MAD image of the candidate young stellar object 053839.24–690552.3 from the catalogue of Gruendl & Chu (2009, centred on their position). The intensity is scaled to bring out the bow shock and the source at its centre, VFTS 464, in the upper and lower panels, respectively.

**Fig. 15.** Combined  $14'' \times 14''$   $J$ - and  $K_s$ -band HAWK-I image of the candidate young stellar object 053848.86–690828.0, centred at the position from Gruendl & Chu (2009). The (near-) central bright source is VFTS 631, a single-lined massive binary.

binary, depending on the systemic velocity of the system. A third (weaker), longer-wavelength nebular component is also visible in the [N II] and [S II] lines in the HR15N spectra.

**VFTS 702:** As with VFTS 631, radial velocity shifts are seen between the LR02 observations. To estimate the spectral type we combined the second and third LR02 epochs with the LR03 observations (all obtained on the same night), shown in Figure 12 and classified as O8.5 V.

**VFTS 751:** An apparently single star, with the combined spectrum shown in Figure 12. The stellar lines appear broadened by rotation, leading to a classification of O7-8 Vnnz.

### 5.1. Discussion

All of the spectra in Figure 12 (except VFTS 178) contain some degree of nebular contribution; this is not surprising given the spatial extent of the H II region in 30 Dor. However, the most intense [O III] emission is seen in VFTS 410, 464, and 702, the three sources identified by GC09 as clear YSO candidates. Both VFTS 410 and 464 are located immediately to the west of R136, while VFTS 702 is  $2'$  to the northeast. Echoing the discussion from Campbell et al. (2010) regarding the location of the candidate high-mass YSOs (which included VFTS 464), all three objects are in regions associated with molecular gas (Werner et al. 1978; Johansson et al. 1998) that comprise the second genera-

**Table 4.** Summary of matches between targets in the VLT-FLAMES Tarantula Survey (VFTS) and candidate young stellar objects (YSOs) from Gruendl & Chu (2009, ‘GC09’). The fourth column is the source classification from GC09: ‘C’ – candidate YSO; ‘CS’ – probable YSO, but could possibly be a star; ‘SD’ – stars with photometric contamination from diffuse emission. Near-IR photometry ( $JHK_s$ ) is from the IRSF catalogue (Kato et al. 2007), with mid-IR photometry from GC09.

Star [VFTS]	VFTS Sp. Type	Identification [GC09]	Type	$\Delta r$ [”]	$J$	$H$	$K_s$	[3.6]	[4.5]	[5.8]	[8.0]	[24.0]		
016	O2 III-If*	053708.79–690720.3	CS	0.5	13.39	13.37	13.35	12.99	12.20	10.61	8.73	3.82		
178	O9.7 Iab	053751.03–690934.0	CS	0.1	12.84	12.83	12.81	12.71	12.48	11.69	9.76	3.87		
320	Be	053821.10–690617.2	CS	0.4	15.19	14.98	14.64	13.21	12.86	11.85	10.04	—		
345	O9.7 III(n)	053827.39–690809.0	CS	0.4	15.48	15.47	15.37	13.82	12.88	11.48	9.70	—		
410	Late O	053834.77–690606.1	C	0.9	Multiple components – see Walborn et al. (1999a, 2002)									
464	B0:	053839.24–690552.3	C	1.2	14.55	14.26	13.63	11.27	10.40	8.98	6.93	—		
500	Late O+ late O	053841.23–690259.0	CS	0.7	13.80	13.73	13.68	13.27	12.52	10.89	8.74	3.02		
586	O4 V((n))((fc))z	053845.33–690251.6	CS	0.4	14.96	14.91	14.88	14.51	13.34	11.62	9.51	2.82		
631	O9.7 III(n) (SB1)	053848.86–690828.0	CS	0.1	15.76	15.66	15.66	14.60	13.53	12.37	11.13	—		
682	WN5h	053855.56–690426.5	CS	0.3	13.53	12.96	12.48	11.69	11.37	10.48	9.15	—		
702	O8.5 V (SB1)	053858.42–690434.7	C	0.5	15.35	15.12	14.91	12.57	11.74	9.59	7.71	—		
751	O7-8 Vnnz	053909.13–690128.7	CS	0.9	15.62	15.48	15.31	13.87	13.07	—	10.37	3.75		
152	B2 V	053746.64–690619.8	SD	0.4	14.66	14.47	14.30	14.05	13.99	13.26	11.76	—		
323	A5 II	053821.78–691042.9	SD	0.1	14.26	14.07	13.91	13.81	13.86	13.15	11.57	—		
641	B0.5: I:	053849.81–690643.3	SD	0.5	12.63	12.58	12.48	11.46	10.54	9.67	7.34	0.06		
842	Be	053942.66–691151.6	SD	0.3	15.08	14.85	14.53	13.58	13.40	—	10.98	—		

**Notes.** VFTS 410 = P93-409; the two major components were classified by Walborn et al. (2002) as O8.5 V and O9 V.

tion of star-formation around R136 (Walborn & Blades 1997; Walborn et al. 1999a, 2002).

Closer scrutiny of the correlation between H $\alpha$  emission (from archival *HST* images) and the GC09 sources was provided by Vaidya et al. (2009), in which they discussed four of the VFTS sources: VFTS 464 was identified as a Type II YSO (cf. the criteria from Chen et al. 2009) in a bright-rimmed dust pillar, and VFTS 320, 682 and 702 were each classified as Type III YSOs in H II regions. Vaidya et al. noted each of the latter three as comprising multiple sources in the *Spitzer* PSF. The close companions to VFTS 320 have already been noted above, while there are no obvious nearby companions to VFTS 702 in the HAWK-I images, nor in the IRSF catalogue. There is a faint IRSF source approximately 2” from VFTS 682: 05385578–6904285, with  $H = 17.56 \pm 0.09$  mag and no detections in  $J$  and  $K_s$ . Intriguingly, VFTS 682 is only  $\sim 17.5'$  from VFTS 702, both of which appear to be co-located with the most intense CO-emission in the region (see Fig. 1 from Johansson et al. 1998). This poses additional evolutionary questions regarding VFTS 682 (Bestenlehner et al. in preparation).

From their multi-band approach, Vaidya et al. (2009) reported VFTS 016 and 631 as non-YSOs. They describe VFTS 016 (GC09 053708.79–690720.3) as a bright star, consistent with the mid-IR excess perhaps arising from a bow shock. However, they flag VFTS 631 (GC09 053848.86–690828.0) as a galaxy. Notwithstanding the discussion of the spectroscopy of VFTS 631, the combined  $J$ - and  $K_s$ -band HAWK-I image appears unremarkable (Figure 15), nor is it obviously extended in the WFI images.

Analysis of the SAGE data by Whitney et al. (2008) identified 1197 candidate YSOs using different selection criteria to GC09. The relative merits of the selection criteria were discussed by GC09, who note that 72.5% of their ‘probable’ YSOs were not in the Whitney et al. catalogue owing to conservative identification criteria. While the nine probable YSOs from GC09 with VFTS spectroscopy in Table 4 are all interesting objects in the context of their mid-IR behaviour, none appear to be genuine

high-mass YSOs. However, two of the more secure candidates (VFTS 410 and 464) appear to be genuine high-mass YSOs, and are not included in the Whitney et al. catalogue. Indeed, there is only one matched source between the VFTS targets and those from Whitney et al.: VFTS 178.

One potential explanation for the photometric properties of some of the (non-YSO) stars in Table 4 is that they are LMC analogues of the ‘dusty’ B-type stars with 24  $\mu$ m excesses discovered by Bolatto et al. (2007) in the SMC. They suggested that these might be caused by remnant accretion discs, planetary debris discs, or hot spots in the local interstellar cirrus; similar excesses for SMC stars have also been found by Ita et al. (2010) and Bonanos et al. (2010). However, Bolatto et al. (2007) report  $K_s - [24]$  colours of  $\sim 6.5$  mag. In contrast, the sources with 24  $\mu$ m detections in Table 4 have larger  $K_s - [24]$  colours.

A range of physical explanations likely lie behind the mid-IR excesses in the sources listed in Table 4. One plausible explanation for some of the otherwise normal O- and early B-type stars could be the dusty shocks seen to be associated with massive stars in the Carina nebula (Smith et al. 2010). At the distance of the LMC these diffuse emission regions, depending on their spatial scales, can sometimes be within the resolution of the *Spitzer* observations.

Also included in Table 4 are four VFTS targets that GC09 classified as stellar sources with mid-IR excesses, VFTS 152 (classified here as B2 V), VFTS 323 (A5 II), VFTS 641 (B0.5: I:), and VFTS 842 (Be). VFTS 641 (*aka* Mk 11 Melnick 1985) is particularly bright at 24  $\mu$ m ( $[24] = 0.06 \pm 0.12$  mag from GC09), but we note that VFTS 655 is nearby ( $\sim 8''$ , cf. the angular resolution at 24  $\mu$ m of 6”) and is classified as late G/early K (Table 3), so confusion/crowding might be a factor. We only have UVES spectroscopy of VFTS 641, so the uncertainty in its classification arises from the lack of observations around 4100 Å; nevertheless this agrees well with previous classifications: B0.5 Ia (Melnick 1985); B0-0.5 Ia (Walborn 1986); B0 Ib (Walborn & Blades 1997); B0.2 III (Bosch et al. 1999).

## 6. Summary

We have introduced the VLT-FLAMES Tarantula Survey, which has provided high-quality spectroscopy of over 800 massive stars in the 30 Doradus region of the LMC. The survey targets are presented in Table 5, including  $B$ - and  $V$ -band optical photometry, and extensive cross-references with previous identifications in this well-studied region. Near-IR ( $JHK_s$ ) magnitudes for our targets from the IRSF catalogue by Kato et al. (2007) are given in Table 6.

Spectral classifications are given for the massive emission-line stars in Section 4.1, including the discovery of a new WN5h star (VFTS 682) 2' from R136, and a new B[e]-type star (VFTS 1003) just 8.5'' to the west of R136. Classifications are also given for the cool-type stars observed by the survey that have radial velocities consistent with them being members of the LMC.

In Section 5 we investigated the spectral properties of 12 stars identified as definite or probable YSOs by GC09, finding an eclectic mixture of objects. VFTS 410 and 464 appear to be embedded massive stars, (i.e. *bona fide* high-mass YSOs), but others include the runaway star (VFTS 016), the new W-R star (VFTS 682), and three massive binaries. There are four additional stars in the survey with mid-IR excesses flagged by GC09, one of which is VFTS 641 (Mk 11), an early B-type supergiant that is particularly bright at 24  $\mu\text{m}$ .

Analysis of the stellar radial velocities and multiplicity of the high-mass stars in the survey will be presented by Sana et al. and Dunstall et al. (both in preparation), but the power of the multi-epoch strategy has already been illustrated by two recent results. Namely, the discovery of VFTS 527 (R139) as an intriguing OIf+OIfc binary system (Taylor et al. 2011), and the lack of a detected companion to VFTS 016, which suggest that its peculiar radial velocity is caused by it being a massive runaway from the core of 30 Dor (Evans et al. 2010).

Analysis of the spectroscopy will be complemented in the future by two additional sources of photometry. Monitoring of selected fields across 30 Dor is part of an ongoing variability campaign with the 2 m Faulkes Telescope South at the Siding Spring Observatory, Australia. This builds on previous (and still ongoing) follow-up of the FLAMES fields from Evans et al. (2006) to determine periods for notable binaries (e.g. Ritchie et al. in preparation). The 30 Dor region was also one of the first fields observed by the ongoing VISTA Magellanic Clouds Survey (Cioni et al. 2011), with time-linked  $K_s$ -band observations to investigate variability.

The Tarantula Survey is by far the largest homogeneous spectroscopic study of extragalactic early-type stars undertaken to date. The 30 Dor region is the only ‘super star-cluster’ at a well-known distance in which individual objects can be resolved spatially in optical light. This makes it the perfect target for the comprehensive studies required to address some of the fundamental questions that remain in our understanding of massive-star evolution, relying on the analysis of a statistically-significant and unbiased sample. The results of these studies will be presented in a series of forthcoming papers.

**Acknowledgements.** Based on observations at the European Southern Observatory Very Large Telescope in programme 182.D-0222. We are indebted to Claudio Melo and the other ESO staff who have provided invaluable assistance with this programme, and to Brian Skiff for his dedicated and careful refinements of the published source catalogues. We are also grateful to Yuri Beletsky for his astrometric calibration, to Simone Zaggia for his advice on the WFI data, to Ian Hunter for his input to the original proposal, and to the referee for their helpful comments. STScI is operated by the Association of

Universities for Research in Astronomy, under NASA contract NAS 5-26555, and SdM acknowledges NASA Hubble Fellowship grant HST-HF-51270.01-A awarded by STScI. MG acknowledges the Royal Society for financial support. AH and SSD acknowledge funding from the Spanish MICINN (AYA2008-06166-03-01, AYA2010-21697-C05-04, Consolider Ingenio 2010 CSD2006-70) and Gobierno de Canarias (ProID2010119). JSV and PRD acknowledge support from the Science and Technology Facilities Council. NM acknowledges the Bulgarian National Science Fund under grant DO02-85. VHB acknowledges support from the Scottish Universities Physics Alliance (SUPA) and the Natural Sciences and Engineering Research Council of Canada (NSERC). JMA acknowledges support from the Spanish Government through grants AYA2010-15081 and AYA2010-17631 and the Junta de Andalucía through grant P08-TIC-4075. AZB acknowledges research and travel support from the European Commission FP7 under Marie Curie International Re-integration Grant PIRG04-GA-2008-239335.

## References

- Azzopardi, M. & Breysacher, J. 1979, A&A, 75, 243
- Azzopardi, M. & Breysacher, J. 1980, A&AS, 39, 19
- Bastian, N., Emsellem, E., Kissler-Patig, M., & Maraston, C. 2006, A&A, 445, 471
- Bolatto, A. D., Simon, J. D., Stanimirović, S., et al. 2007, ApJ, 655, 212
- Bonanos, A. Z., Lennon, D. J., Köhlinger, F., et al. 2010, AJ, 140, 416
- Bosch, G., Terlevich, E., & Terlevich, R. 2009, AJ, 137, 3437
- Bosch, G. L., Terlevich, R., Melnick, J., & Selman, F. 1999, A&AS, 137, 21
- Bouwens, R. J., Illingworth, G. D., Labbe, I., et al. 2011, Nature, 469, 504
- Bresolin, F., Pietrzynski, G., Urbaneja, M. A., et al. 2006, ApJ, 648, 1007
- Bresolin, F., Urbaneja, M. A., Gieren, W., Pietrzynski, G., & Kudritzki, R. 2007, ApJ, 671, 2028
- Breysacher, J. 1981, A&AS, 43, 203
- Breysacher, J., Azzopardi, M., & Testor, G. 1999, A&AS, 137, 117
- Brott, I., Evans, C. J., Hunter, I., et al. 2011, A&A, arXiv:1102.0766
- Brunet, J. P., Imbert, M., Martin, N., et al. 1975, A&AS, 21, 109
- Campbell, M. A., Evans, C. J., Mackey, A. D., et al. 2010, MNRAS, 405, 421
- Chen, C.-H. R., Chu, Y.-H., Gruendl, R. A., Gordon, K. D., & Heitsch, F. 2009, ApJ, 695, 511
- Chu, Y.-H., Kennicutt, R. C., Schommer, R. A., & Laff, J. 1992, AJ, 103, 1545
- Cioni, M.-R., Clementini, G., & Girardi, L. . et al. 2011, A&A, 527, A116
- Crowther, P. A., Schnurr, O., Hirschi, R., et al. 2010, MNRAS, 731
- Crowther, P. A. & Smith, D. J. 1997, A&A, 320, 500
- de Koter, A., Heap, S. R., & Hubeny, I. 1998, ApJ, 509, 879
- de Koter, A., Smith, L. J., & Waters, L. B. F. M. 2008, in Mass Loss from Stars and the Evolution of Stellar Clusters, ed. A. de Koter, L. J. Smith, & L. B. F. M. Waters, Vol. 388 (Astronomical Society of the Pacific)
- Douglas, L. S., Bremer, M. N., Lehnert, M. D., Stanway, E. R., & Milvang-Jensen, B. 2010, MNRAS, 409, 1155
- Erb, D. K., Shapley, A. E., Pettini, M., et al. 2006, ApJ, 644, 813
- Evans, C. J., Bresolin, F., Urbaneja, M. A., et al. 2007, ApJ, 659, 1198
- Evans, C. J. & Howarth, I. D. 2003, MNRAS, 345, 1223
- Evans, C. J., Howarth, I. D., Irwin, M. J., Burnley, A. W., & Harries, T. J. 2004, MNRAS, 353, 601
- Evans, C. J., Lennon, D. J., Smartt, S. J., & Trundle, C. 2006, A&A, 456, 623
- Evans, C. J., Smartt, S. J., Lee, J., et al. 2005, A&A, 437, 467
- Evans, C. J., Walborn, N. R., Crowther, P. A., et al. 2010, ApJ, 715, L74
- Feast, M. W., Thackeray, A. D., & Wesselink, A. J. 1960, MNRAS, 121, 337
- Foellmi, C., Moffat, A. F. J., & Guerrero, M. A. 2003, MNRAS, 338, 1025
- Gibson, B. K. 2000, Mem. Soc. Astron. Ital., 71, 693
- Gieren, W., Pietrzynski, G., Bresolin, F., et al. 2005, Msngr, 121, 23
- Grebel, E. K. & Chu, Y.-H. 2000, AJ, 119, 787
- Gruendl, R. A. & Chu, Y.-H. 2009, ApJS, 184, 172 [GC09]
- Gummersbach, C. A., Zickgraf, F.-J., & Wolf, B. 1995, A&A, 302, 409
- Gvaramadze, V. V. & Bomans, D. J. 2008, A&A, 490, 1071
- Gvaramadze, V. V., Kroupa, P., & Pfleiderer-Altenburg, J. 2010, A&A, 519, A33
- Gvaramadze, V. V., Pfleiderer-Altenburg, J., & Kroupa, P. 2011, A&A, 525, A17
- Haiman, Z. & Loeb, A. 1997, ApJ, 483, 21
- Herrero, A., Puls, J., & Najarro, F. 2002, A&A, 396, 949
- Herrero, A., Puls, J., & Villamariz, M. R. 2000, A&A, 354, 193
- Hodge, P. 1988, PASP, 100, 1051
- Howarth, I. D. & Prinja, R. K. 1989, ApJS, 69, 527
- Howarth, I. D., Siebert, K. W., Hussain, G. A. J., & Prinja, R. K. 1997, MNRAS, 284, 265
- Hunter, I., Brott, I., Langer, N., et al. 2009, A&A, 496, 841
- Hunter, I., Brott, I., Lennon, D. J., et al. 2008, ApJ, 676, L29
- Hyland, A. R., Straw, S., Jones, T. J., & Gatley, I. 1992, MNRAS, 257, 391
- Ita, Y., Onaka, T., Tanabé, T., et al. 2010, PASJ, 62, 273
- Johansson, L. E. B., Greve, A., Booth, R. S., et al. 1998, A&A, 331, 857

- Kato, D., Nagashima, C., Nagayama, T., et al. 2007, PASJ, 59, 615
- Kucinskas, A., Dobrovolskas, V., Lazauskaité, R., Lindegren, L., & Tanabé, T. 2008, BaltA, 17, 283
- Kudritzki, R. P., Urbaneja, M. A., Bresolin, F., & Przybilla, N. 2008, Phys. Scr., T133, 014039
- Lamers, H. J. G. L. M., Zickgraf, F.-J., de Winter, D., Houziaux, L., & Zorec, J. 1998, A&A, 340, 117
- Landolt, A. U. 1992, AJ, 104, 340
- Langer, N., Cantiello, M., Yoon, S., et al. 2008, in IAU Symp. 250, Massive Stars as Cosmic Engines, ed. F. Bresolin, P. A. Crowther, & J. Puls (Cambridge Univ. Press), 167
- Leitherer, C., Ortiz Otálvaro, P. A., Bresolin, F., et al. 2010, ApJS, 189, 309
- Leitherer, C., Schaerer, D., Goldader, J. D., et al. 1999, ApJS, 123, 3
- Massey, P. 2002, ApJS, 141, 81
- Massey, P. & Hunter, D. A. 1998, ApJ, 493, 180
- Massey, P., Zangari, A. M., Morrell, N. I., et al. 2009, ApJ, 692, 618
- Meixner, M., Gordon, K. D., Indebetouw, R., et al. 2006, AJ, 132, 2268
- Melnick, J. 1985, A&A, 153, 235
- Moffat, A. F. J. 1989, ApJ, 347, 373
- Moffat, A. F. J., Niemela, V. S., Philips, M. M., Chu, Y.-H., & Seggewiss, W. 1987, ApJ, 312, 612
- Mokiem, M. R., de Koter, A., Evans, C. J., et al. 2007, A&A, 465, 1003
- Mokiem, M. R., de Koter, A., Evans, C. J., et al. 2006, A&A, 456, 1131
- Mokiem, M. R., de Koter, A., Puls, J., et al. 2005, A&A, 441, 711
- Morgan, D. H. & Good, A. R. 1987, MNRAS, 224, 435
- Nesvadba, N. P. H., Lehnert, M. D., Davies, R. I., Verma, A., & Eisenhauer, F. 2008, A&A, 479, 67
- Parker, J. W. 1993, AJ, 106, 560
- Pasquini, L., Avila, G., Blecha, A., et al. 2002, Msngr, 110, 1
- Penny, L. R. 1996, ApJ, 463, 737
- Penny, L. R. & Gies, D. R. 2009, ApJ, 700, 844
- Portegies Zwart, S., McMillan, S. L. W., & Gieles, M. 2010, ARA&A, 48, 431
- Prinja, R. K., Barlow, M. J., & Howarth, I. D. 1990, ApJ, 361, 607
- Puls, J., Sundqvist, J. O., & Rivero González, J. G. 2011, in IAU Symp. 272, Active OB stars: structure, evolution, mass loss & critical limits, ed. C. Neiner, G. Wade, G. Meynet, & G. Peters (Cambridge Univ. Press), arXiv:1009.0364
- Puls, J., Urbaneja, M. A., Venero, R., et al. 2005, A&A, 435, 669
- Repolust, T., Puls, J., & Herrero, A. 2004, A&A, 415, 349
- Sana, H. & Evans, C. J. 2011, in IAU Symp. 272, Active OB stars: structure, evolution, mass loss & critical limits, ed. C. Neiner, G. Wade, G. Meynet, & G. Peters (Cambridge Univ. Press), arXiv:1009.4197
- Sanduleak, N. 1970, Contrib. Cerro Tololo Inter-American Obs., No. 89
- Schild, H. & Testor, G. 1992, A&AS, 92, 729
- Schnurr, O., Moffat, A. F. J., St-Louis, N., Morrell, N. I., & Guerrero, M. A. 2008, MNRAS, 389, 806
- Selman, F., Melnick, J., Bosch, G., & Terlevich, R. 1999, A&A, 341, 98
- Shapley, H. & Lindsay, E. M. 1963, IrAJ, 6, 74
- Skrutskie, M. F., Cutri, R. M., Stiening, R., et al. 2006, AJ, 131, 1163
- Smith, L. F., Shara, M. M., & Moffat, A. F. J. 1990, ApJ, 348, 471
- Smith, N., Povich, M. S., Whitney, B. A., et al. 2010, MNRAS, 406, 952
- Stetson, P. B. 1987, PASP, 99, 191
- Stetson, P. B. 1994, PASP, 106, 250
- Taylor, W. D., Evans, C. J., & Sana, H. et al. 2011, A&A, arXiv:1103.5387
- Testor, G., Llebaria, A., & Debray, B. 1988, Msngr, 54, 43
- Testor, G. & Schild, H. 1990, A&A, 240, 299
- Tokunaga, A., Simons, D. A., & Vacca, W. D. 2002, PASP, 114, 180
- Vaidya, K., Chu, Y.-H., Gruendl, R. A., Chen, C.-H. R., & Looney, L. W. 2009, ApJ, 707, 1417
- Walborn, N. R. 1984, in IAU Symp. 108, Structure and Evolution of the Magellanic Clouds, ed. S. van den Bergh & K. S. de Boer (Dordrecht: Reidel), 243
- Walborn, N. R. 1986, in IAU Symp. 116, Luminous Stars and Associations in Galaxies, ed. C. W. H. de Loore, A. J. Willis, & P. Laskarides (Dordrecht: Reidel), 185
- Walborn, N. R. 1991, in Massive Stars in Starbursts, ed. C. Leitherer, N. Walborn, T. Heckman, & C. Norman (Cambridge University Press), 145
- Walborn, N. R., Barbá, R. H., Brandner, W., et al. 1999a, AJ, 117, 225
- Walborn, N. R. & Blades, J. C. 1997, ApJS, 112, 457
- Walborn, N. R., Drissen, L., Parker, J. W., et al. 1999b, AJ, 118, 1684
- Walborn, N. R. & Fitzpatrick, E. L. 2000, PASP, 112, 50
- Walborn, N. R., MacKenty, J. W., Saha, A., White, R. L., & Parker, J. W. 1995, ApJ, 439, L47
- Walborn, N. R., Maíz-Apellániz, J., & Barbá, R. H. 2002, AJ, 124, 1601
- Walborn, N. R., Sota, A., Maíz Apellániz, J., et al. 2010, ApJ, 711, L143
- Werner, M. W., Becklin, E. E., Gatley, I., et al. 1978, MNRAS, 184, 365
- Whitney, B. A., Sewilo, M., Indebetouw, R., et al. 2008, AJ, 136, 18
- Zacharias, N., Urban, S. E., Zacharias, M. I., et al. 2004, AJ, 127, 3043
- Zaritsky, D., Harris, J., Thompson, I. B., & Grebel, E. K. 2004, AJ, 128, 1606

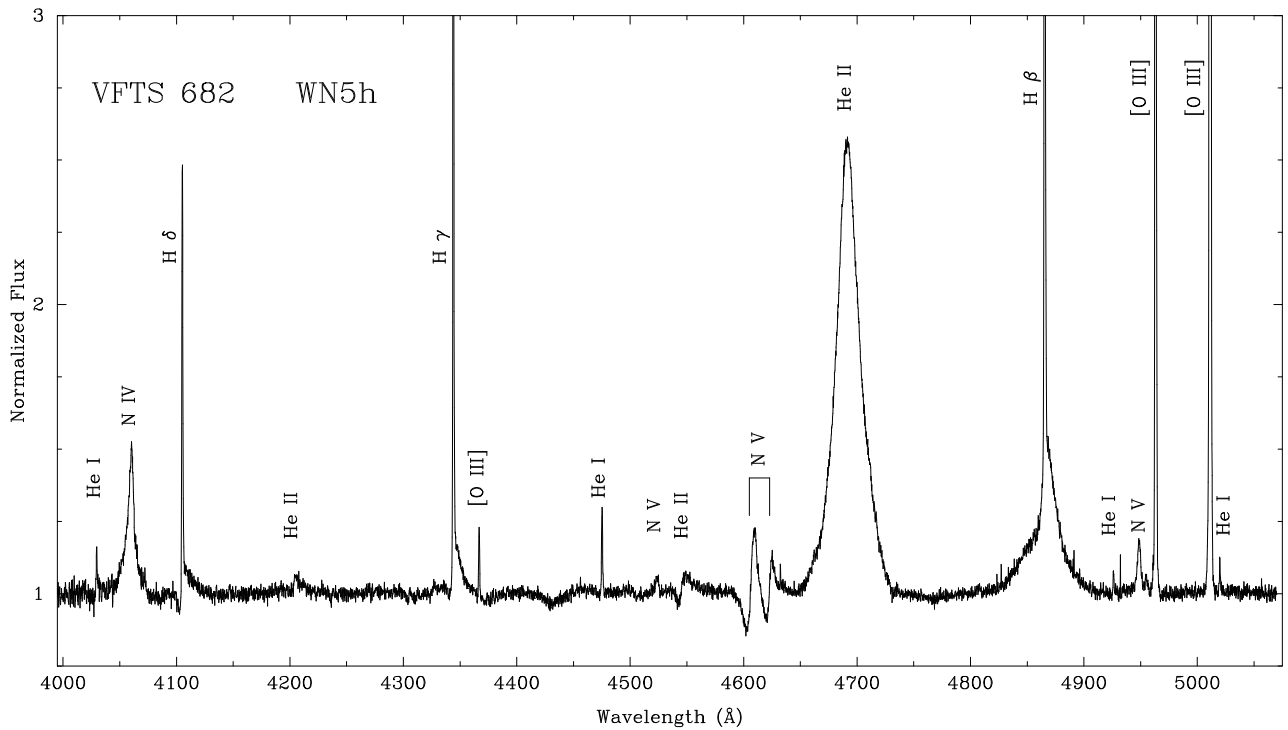


**Fig. 10.** Combined FLAMES–Medusa spectrum of VFTS 682, a newly discovered Wolf-Rayet star. Identified lines are, from left-to-right by species: H $\delta$ , H $\gamma$ , and H $\beta$  (each with super-imposed nebular emission); He I  $\lambda\lambda$ 4026, 4471, 4922, 5015 (each from nebular emission); He II  $\lambda\lambda$ 4200, 4542, 4686; N IV  $\lambda$ 4058; N V  $\lambda\lambda$ 4520, 4604-4620, 4944; and the [O III] nebular lines at  $\lambda\lambda$ 4363, 4959, 5007.

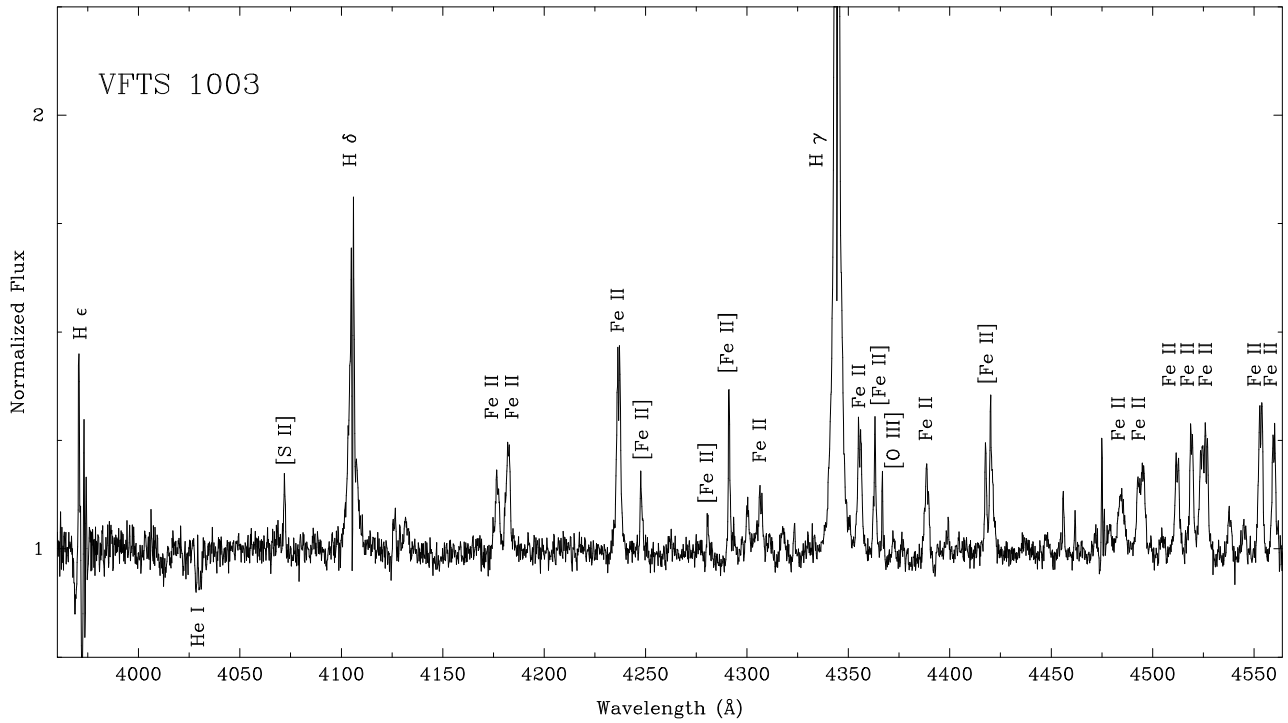


**Fig. 11.** Combined FLAMES–ARGUS spectrum of VFTS 1003, a newly discovered B[e]-type star. There appears to be weak stellar absorption at  $\text{He I } \lambda\lambda 4009, 4026, 4388, 4471$ , combined with weak nebular emission components, particularly at  $\lambda 4471$ . In addition to the Balmer lines, the identified lines are [S II]  $\lambda 4069$ ; [O III]  $\lambda 4363$ ; Fe II  $\lambda\lambda 4173, 4179, 4233, 4303, 4352, 4385, 4481, 4491, 4508, 4515, 4520-23, 4549, 4556$ ; [Fe II]  $\lambda\lambda 4244, 4277, 4287, 4358-59, 4414-16$ .

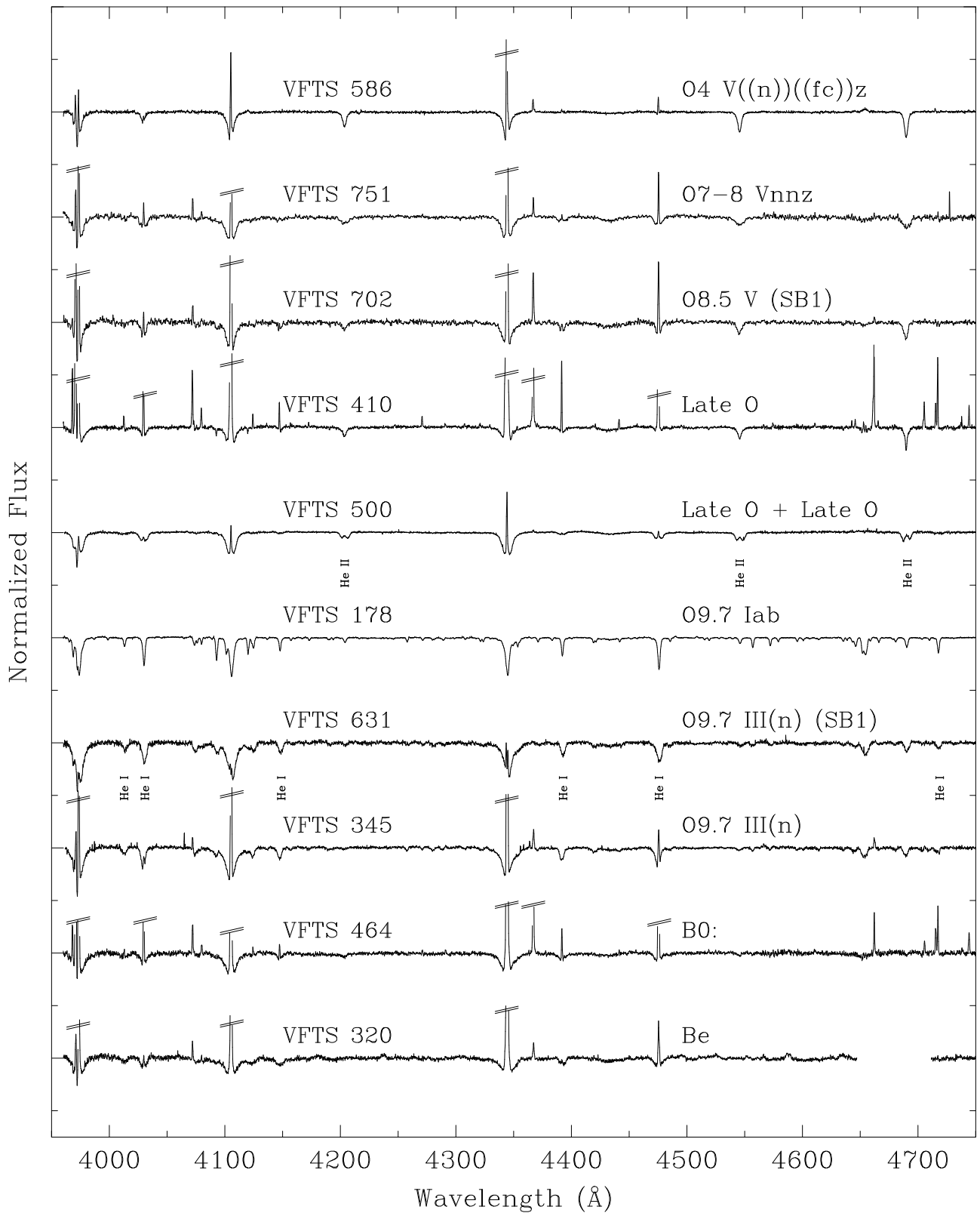


**Fig. 12.** FLAMES–Giraffe spectroscopy of ten candidate YSOs from Gruendl & Chu (2009), as summarised in Table 4. Strong nebular lines have been truncated as indicated. The He II lines identified in VFTS 500 (a double-lined spectroscopic binary) are:  $\lambda\lambda 4200, 4542, 4686$ ; He I lines identified in VFTS 631 are:  $\lambda\lambda 4009, 4026, 4144, 4388, 4471, 4713$ .

**Table 5.** Observational information for the VLT-FLAMES Tarantula Survey (VFTS) targets. The FLAMES–Medusa configuration ('A' to 'T') or FLAMES–ARGUS pointing ('A1' to 'A5') used to observe each target is listed in the second column; 'U' indicates those observed with the fibre-feed to UVES. The fifth and sixth columns give radial distances (in arcmin and pc) to the core of R136 (specifically, R136-a1:  $\alpha = 5^{\text{h}} 38^{\text{m}} 42\overset{\text{s}}{.}39$ ,  $\delta = -69^{\circ} 06' 02\overset{\text{s}}{.}91$ , J2000.0). Sources of photometry are: C (CTIO data, current study); P (Parker 1993); S (Selman et al. 1999); W (WFI data, current study); Z (Zaritsky et al. 2004). Aliases/previous identifications of the targets are given in the final column. Sources of identifications are: R (Feast et al. 1960); Sk (Sanduleak 1970); BI (Brunet et al. 1975); Brey (Breysacher 1981); Mk (Melnick 1985); M87 (Moffat et al. 1987); T88 (Testor et al. 1988); ST92 (Schild & Testor 1992); P93 (Parker 1993); WB97 (Walborn & Blades 1997); BAT99 (Breysacher et al. 1999); S99 (Selman et al. 1999); GC00 (Grebel & Chu 2000); 2MASS (Skrutskie et al. 2006). A total of 22 stars have some degree of cross-contamination from adjacent spectra on the detector (noted in final column), see Section 2.2.4 for details.

Star [VFTS]	Field	$\alpha$ (2000)	$\delta$ (2000)	$r_d$ ['']	$V$	$B - V$	Ref.	Aliases (& comments)
				[pc]				
001	H	05 36 53.39	-69 08 18.29	9.98	145.1	16.93	0.05	W
002	C	05 36 54.73	-69 11 38.18	11.11	161.6	—	—	HD 38029a, Sk-69° 223, Brey 67, BAT99-085; blend of (at least) two components in WFI image
003	B	05 36 55.24	-69 11 37.58	11.06	160.9	—	—	HD 38029b, Sk-69° 224
004	I	05 36 58.45	-69 06 47.26	9.30	135.2	16.87	0.16	W
005	H	05 37 01.74	-69 08 16.23	9.25	134.5	16.25	0.02	W
006	G	05 37 02.50	-69 06 43.75	8.93	129.9	16.72	1.78	W 2MASS J05370250-6906436
007	H	05 37 02.96	-69 02 04.17	9.72	141.4	16.74	0.03	W
008	G	05 37 03.11	-69 08 22.57	9.15	133.2	16.92	0.07	W
009	G	05 37 04.26	-69 08 05.65	8.99	130.7	16.18	0.11	W
010	I	05 37 04.72	-69 08 56.65	9.18	133.5	16.79	0.04	W
011	G	05 37 04.96	-69 04 58.66	8.75	127.3	16.25	1.51	W 2MASS J05370496-6904585
012	I	05 37 05.64	-69 09 12.42	9.19	133.6	15.83	0.15	W
013	G	05 37 06.30	-69 04 41.39	8.68	126.2	16.36	0.13	W
014	H	05 37 07.51	-69 05 06.88	8.51	123.8	—	—	—
015	G	05 37 08.56	-69 05 10.03	8.41	122.4	16.20	0.04	W
016	G	05 37 08.88	-69 07 20.36	8.44	122.7	13.55	0.04	Z 2MASS J05370888-6907203
017	I	05 37 11.44	-69 05 04.24	8.17	118.8	—	—	—
018	I	05 37 11.46	-69 10 30.97	9.26	134.7	16.62	0.17	W
019	G	05 37 11.48	-69 07 38.13	8.26	120.2	16.31	0.05	W Brey 69, BAT99-086
020	H	05 37 14.12	-69 04 02.72	8.12	118.1	16.70	0.06	W
021	F	05 37 14.38	-69 06 32.51	7.86	114.4	15.57	0.09	W
022	H	05 37 15.03	-69 08 43.09	8.24	119.8	16.67	0.55	C Multiple in WFI image, fibre centred on brighter (southern) source
023	I	05 37 16.08	-69 08 52.86	8.20	119.3	15.63	1.97	C 2MASS J05371608-6908528
024	H	05 37 16.68	-69 08 50.36	8.14	118.4	16.02	0.37	W
025	I	05 37 16.97	-69 07 54.36	7.84	114.0	16.18	0.06	W
026	G	05 37 17.05	-69 06 59.90	7.67	111.6	16.83	1.59	W 2MASS J05371705-6906598
027	F	05 37 17.37	-69 07 48.05	7.78	113.2	14.71	0.09	W 2MASS J05371734-6907479
028	H	05 37 17.86	-69 09 46.26	8.41	122.3	13.48	0.24	C 2MASS J05371785-6909461
029	G	05 37 18.30	-69 03 04.57	8.07	117.3	16.73	-0.02	W
030	I	05 37 18.81	-69 02 13.02	8.38	121.9	16.34	0.10	W
031	H	05 37 20.50	-68 59 52.23	9.57	139.1	16.41	0.00	W
032	G	05 37 20.52	-69 01 37.78	8.53	124.1	16.90	1.49	W 2MASS J05372050-6901378
033	F	05 37 22.05	-69 07 55.13	7.40	107.7	16.20	0.07	W
034	F	05 37 22.32	-69 07 16.10	7.24	105.4	16.14	0.13	W
035	I	05 37 22.77	-69 12 09.88	9.37	136.3	16.91	0.17	W
036	F	05 37 23.63	-69 04 29.80	7.19	104.6	16.61	0.10	W

continued on next page

**Table 5.** *continued*

Star [VFTS]	Field	$\alpha$ (2000)	$\delta$ (2000)	$r_d$ [']	$V$	$B - V$	Ref.	Aliases (& comments)
				[pc]				
037	I	05 37 23.95	-69 12 21.27	9.42	137.0	15.79	0.06	W
038	I	05 37 24.34	-69 07 17.12	7.07	102.8	16.54	0.06	W
039	H	05 37 24.65	-69 09 52.96	7.92	115.2	14.52	0.52	W ST92 1-01, 2MASS J05372465-6909528
040	F	05 37 24.75	-69 08 27.73	7.33	106.6	16.85	0.10	W ST92 1-02
041	F	05 37 24.89	-69 04 15.73	7.14	103.8	16.94	0.14	W
042	H	05 37 25.12	-69 07 42.63	7.09	103.1	14.66	-0.12	C
043	G	05 37 25.84	-69 07 28.49	6.97	101.4	16.49	-0.06	C
044	F	05 37 26.06	-69 07 29.29	6.96	101.2	16.62	-0.07	C
045	G	05 37 26.19	-69 08 56.54	7.39	107.4	15.30	0.38	W ST92 1-04, 2MASS J05372617-6908565
046	F	05 37 26.19	-69 09 53.07	7.80	113.5	14.65	0.13	W ST92 1-05, 2MASS J05372619-6909529
047	G	05 37 26.55	-69 10 40.78	8.20	119.2	16.91	0.28	C
048	I	05 37 26.56	-69 07 01.77	6.83	99.4	16.72	0.14	W
049	G	05 37 26.92	-69 03 44.15	7.12	103.5	16.07	0.11	W
050	H	05 37 27.43	-69 10 40.15	8.13	118.2	16.77	0.18	W
051	I	05 37 27.83	-69 08 02.88	6.94	101.0	15.88	0.26	W ST92 1-06, 2MASS J05372782-6908028
052	E	05 37 28.87	-69 07 06.49	6.64	96.6	14.55	-0.07	C 2MASS J05372886-6907064
053	E	05 37 28.92	-69 06 52.84	6.60	96.1	15.28	0.09	W
054	I	05 37 29.08	-69 13 03.98	9.59	139.5	16.60	0.21	W
055	H	05 37 29.08	-69 03 44.53	6.93	100.8	15.56	0.23	W 2MASS J05372905-6903445
056	F	05 37 29.11	-69 08 41.47	7.05	102.5	16.23	0.30	C ST92 1-07, 2MASS J05372909-6908414
057	G	05 37 29.85	-69 11 11.10	8.26	120.1	16.79	1.56	W ST92 1-08, 2MASS J05372984-6911111
058	F	05 37 30.10	-69 09 51.01	7.48	108.9	15.65	0.15	W ST92 1-09
059	I	05 37 30.40	-69 10 00.54	7.54	109.7	16.42	0.19	W ST92 1-10
060	G	05 37 30.63	-69 09 12.91	7.14	103.9	16.12	0.62	W 2MASS J05373060-6909129
061	E	05 37 30.76	-69 05 17.53	6.43	93.6	15.15	0.22	W 2MASS J05373075-6905175
062	G	05 37 30.83	-69 03 21.90	6.92	100.7	16.27	0.15	W
063	B	05 37 30.89	-69 11 48.56	8.59	125.0	14.23	0.00	C ST92 1-11, 2MASS J05373087-6911485
064	H	05 37 30.93	-69 11 07.09	8.14	118.4	14.62	0.13	W ST92 1-12, 2MASS J05373092-6911070
065	E	05 37 32.62	-69 06 40.75	6.25	91.0	15.99	0.06	W
066	F	05 37 33.10	-69 04 34.71	6.35	92.4	15.54	0.10	W
067	H	05 37 33.36	-69 02 47.57	6.96	101.3	16.83	0.16	W
068	E	05 37 33.54	-69 07 13.99	6.25	91.0	15.65	0.77	C
069	C	05 37 33.76	-69 08 13.23	6.49	94.5	13.59	0.17	C ST92 1-17, 2MASS J05373375-6908132
070	E	05 37 33.89	-69 08 58.30	6.77	98.5	16.85	0.28	W
071	F	05 37 34.21	-69 06 39.27	6.11	88.9	16.65	0.03	W
072	H	05 37 34.47	-69 01 10.20	7.78	113.1	13.70	-0.14	C BI 253, 2MASS J05373446-6901102
073	E	05 37 34.47	-69 09 09.48	6.81	99.0	16.14	0.38	W ST92 1-19
074	H	05 37 34.56	-69 10 10.26	7.32	106.5	16.53	0.14	W ST92 1-20
075	F	05 37 34.69	-69 07 13.33	6.15	89.5	16.93	0.03	W
076	F	05 37 34.81	-69 08 01.31	6.34	92.2	15.24	0.19	W ST92 1-21, 2MASS J05373478-6908013
077	F	05 37 35.14	-69 09 41.29	7.02	102.0	16.64	0.14	W ST92 1-22
078	G	05 37 35.44	-69 07 57.14	6.27	91.1	16.63	0.21	W
079	E	05 37 35.70	-69 08 40.34	6.50	94.5	16.90	1.13	W MG4, Brey 70a, BAT99-088, 2MASS J05373571-6908402
080	H	05 37 35.74	-69 08 07.52	6.30	91.6	16.26	0.25	W ST92 1-23
081	B	05 37 35.99	-69 12 29.93	8.76	127.4	13.71	1.97	C 2MASS J05373597-6912298
082	A	05 37 36.08	-69 06 45.37	5.96	86.6	13.61	-0.06	C
083	D	05 37 36.34	-69 05 01.14	5.98	87.0	15.91	0.10	W
084	G	05 37 36.52	-69 09 59.36	7.07	102.9	16.84	0.18	W
085	F	05 37 36.52	-69 01 41.35	7.32	106.4	16.48	-0.08	W
086	B	05 37 36.55	-69 10 32.57	7.39	107.5	14.47	0.12	C ST92 1-24, 2MASS J05373597-6912298
087	A	05 37 36.66	-69 07 31.87	6.05	87.9	13.58	-0.14	C 2MASS J05373664-6907318
088	E	05 37 36.82	-69 06 33.23	5.87	85.4	15.24	-0.06	W 2MASS J05373681-6906331
089	H	05 37 36.87	-69 08 22.82	6.29	91.5	16.08	0.20	W ST92 1-25

continued on next page

**Table 5.** *continued*

Star [VFTS]	Field	$\alpha$ (2000)	$\delta$ (2000)	$r_d$ [']	$V$	$B - V$	Ref.	Aliases (& comments)
090	I	05 37 37.15	-69 10 18.15	7.21	104.8	15.78	0.19	W ST92 1-26
091	G	05 37 37.53	-69 08 20.51	6.22	90.5	15.98	0.20	W ST92 1-27
092	H	05 37 37.68	-68 58 55.57	9.17	133.3	16.80	1.73	Z 2MASS J05373768-6858555
093	D	05 37 37.81	-69 05 45.52	5.77	83.9	15.03	0.10	W 2MASS J05373778-6905455
094	B	05 37 37.97	-69 10 14.85	7.12	103.5	14.12	0.11	C ST92 1-28 , 2MASS J05373797-6910147
095	F	05 37 38.53	-69 06 04.47	5.70	82.8	16.06	-0.02	W
096	C	05 37 38.54	-69 10 19.99	7.13	103.6	13.91	0.00	C ST92 1-29, 2MASS J05373854-6910199
097	F	05 37 38.75	-69 10 27.70	7.19	104.6	16.21	0.16	W ST92 1-31
098	G	05 37 38.78	-69 08 08.67	6.05	88.0	15.07	0.15	W ST92 1-30, 2MASS J05373879-6908085
099	I	05 37 38.80	-68 58 31.83	9.42	137.0	16.78	-0.03	W
100	H	05 37 38.92	-69 10 08.34	6.98	101.6	16.68	0.22	W
101	G	05 37 39.19	-69 08 40.92	6.22	90.5	16.39	0.32	W ST92 1-33, 2MASS J05373918-6908409
102	E	05 37 39.24	-69 09 51.12	6.80	98.8	15.70	0.35	W ST92 1-32, 2MASS J05373924-6909510
103	G	05 37 39.25	-69 11 34.45	7.89	114.7	16.20	0.47	W 2MASS J05373923-6911343
104	F	05 37 39.90	-69 05 46.76	5.58	81.1	16.20	-0.01	W
105	C	05 37 40.19	-69 10 46.16	7.28	105.9	15.46	0.10	C ST92 1-37
106	E	05 37 40.22	-69 04 12.11	5.84	85.0	16.43	0.05	W
107	E	05 37 40.41	-69 05 54.09	5.53	80.4	16.68	0.06	W
108	D	05 37 40.50	-69 07 57.71	5.84	85.0	14.02	0.06	C HDE 269883, Brey 71, BAT99-089, 2MASS J05374049-6907577
109	F	05 37 40.75	-69 08 01.20	5.84	84.9	16.37	0.16	W ST92 1-38
110	A	05 37 40.87	-69 10 48.44	7.26	105.6	15.69	0.07	C ST92 1-40
111	G	05 37 40.87	-69 00 04.20	8.11	118.0	14.40	-0.08	W 2MASS J05374084-6900041
112	D	05 37 40.89	-69 04 41.52	5.65	82.2	16.19	0.08	W
113	E	05 37 40.91	-69 08 44.27	6.11	88.8	16.69	0.19	W ST92 1-39
114	I	05 37 41.12	-69 10 37.92	7.13	103.7	15.97	0.17	W ST92 1-41
115	I	05 37 41.42	-69 06 10.51	5.44	79.1	16.38	1.41	W 2MASS J05374141-6906105
116	H	05 37 41.45	-69 09 19.23	6.34	92.3	16.44	0.21	W ST92 1-42
117	G	05 37 41.47	-69 10 46.96	7.21	104.8	16.64	0.18	W
118	D	05 37 41.60	-69 08 08.73	5.81	84.5	16.21	0.20	W Some cross-contamination
119	D	05 37 41.72	-69 07 28.19	5.59	81.4	16.36	0.07	W
120	F	05 37 41.96	-69 08 33.47	5.94	86.5	14.95	0.12	W ST92 1-43, 2MASS J05374194-6908335
121	C	05 37 42.23	-69 07 14.37	5.50	79.9	15.96	0.06	W
122	I	05 37 42.28	-69 09 41.59	6.48	94.3	16.53	0.24	W
123	H	05 37 42.45	-69 12 21.58	8.27	120.3	15.78	0.10	W
124	F	05 37 42.61	-69 09 19.26	6.26	91.0	16.61	0.24	W ST92 1-46
125	H	05 37 42.95	-69 10 35.12	6.98	101.5	16.54	0.33	C ST92 1-47
126	G	05 37 42.96	-69 01 05.34	7.26	105.6	16.78	-0.07	W
127	F	05 37 43.37	-69 10 45.91	7.07	102.8	16.93	0.07	C
128	E	05 37 43.41	-69 09 59.11	6.57	95.6	16.29	0.03	W ST92 1-49
129	E	05 37 43.66	-69 10 15.18	6.72	97.7	16.46	1.88	W ST92 1-50, 2MASS J05374366-6910150
130	G	05 37 43.68	-69 10 50.47	7.10	103.2	16.67	0.16	C
131	F	05 37 43.76	-69 10 22.21	6.78	98.7	16.77	0.11	W
132	H	05 37 43.96	-69 09 39.09	6.34	92.1	16.09	0.07	W ST92 1-51
133	D	05 37 43.98	-69 06 34.41	5.24	76.1	16.03	-0.02	C
134	E	05 37 44.08	-69 05 27.06	5.23	76.1	16.85	0.02	W
135	G	05 37 44.21	-69 06 37.29	5.22	75.9	16.01	0.01	W
136	A	05 37 44.63	-69 14 25.72	9.84	143.1	14.53	0.11	C HDE 269888, Sk-69° 234, Brey 74, BAT99-090, 2MASS J05374463-6914256
137	I	05 37 44.72	-69 09 18.33	6.09	88.5	16.85	0.11	W ST92 1-55
138	H	05 37 45.05	-69 02 29.66	6.23	90.6	15.63	-0.09	W
139	H	05 37 45.21	-68 58 48.75	8.85	128.8	16.82	1.55	W 2MASS J05374520-6858487
140	B	05 37 45.25	-69 10 13.72	6.59	95.9	16.05	0.23	W ST92 1-56
141	C	05 37 45.74	-69 09 13.33	5.97	86.8	15.32	0.04	W T88-6
142	F	05 37 45.90	-69 10 22.07	6.64	96.5	16.39	0.19	W ST92 1-58

continued on next page

**Table 5.** *continued*

Star [VFTS]	Field	$\alpha$ (2000)	$\delta$ (2000)	$r_d$ [']	$V$	$B - V$	Ref.	Aliases (& comments)
				[pc]				
143	G	05 37 45.91	-69 11 09.34	7.17	104.3	15.36	0.19	W ST92 1-60
144	H	05 37 46.08	-69 09 14.37	5.95	86.5	16.81	0.00	C T88-10
145	A	05 37 46.08	-69 09 08.85	5.90	85.8	14.30	0.19	— T88-3; <i>HST</i> photometry from Walborn et al. (1999b)
146	F	05 37 46.10	-69 06 34.93	5.05	73.4	16.24	0.25	W
147	D	05 37 46.19	-69 09 10.44	5.91	85.9	—	—	Brey 73, BAT99-091, T88-1; multiple bright components (Walborn et al. 1995)
148	I	05 37 46.28	-69 00 06.29	7.77	113.0	16.04	-0.04	W
149	F	05 37 46.31	-69 08 20.76	5.50	80.0	16.44	0.16	W ST92 1-61
150	B	05 37 46.41	-69 09 12.15	5.91	85.9	15.30	0.12	— T88-4; <i>HST</i> photometry from Walborn et al. (1999b)
151	G	05 37 46.52	-69 09 08.79	5.87	85.3	—	—	T88-2; multiple bright components (Walborn et al. 1995)
152	D	05 37 46.70	-69 06 19.58	4.97	72.3	15.32	0.25	W 2MASS J05374669–6906196
153	E	05 37 46.71	-69 09 11.27	5.87	85.4	15.30	0.06	— T88-5; <i>HST</i> photometry from Walborn et al. (1999b)
154	F	05 37 47.09	-69 09 07.70	5.81	84.6	14.94	0.05	C T88-7
155	H	05 37 47.18	-69 13 13.60	8.70	126.6	16.95	0.08	W
156	H	05 37 47.20	-69 09 03.03	5.77	83.9	16.26	0.44	W T88-11, ST92 1-64
157	I	05 37 47.23	-68 58 49.25	8.74	127.2	16.69	-0.08	W
158	C	05 37 47.43	-69 04 12.71	5.23	76.1	15.33	0.20	W 2MASS J05374741–6904127
159	F	05 37 47.67	-69 00 35.10	7.33	106.5	15.61	-0.03	W
160	C	05 37 47.80	-69 09 14.86	5.83	84.7	14.17	0.03	C
161	E	05 37 47.91	-69 10 41.13	6.72	97.7	16.69	0.24	W
162	H	05 37 48.06	-69 09 59.88	6.25	90.9	16.49	0.07	W
163	E	05 37 48.06	-69 09 26.43	5.91	86.0	16.21	0.53	W 2MASS J05374805–6909263
164	D	05 37 48.21	-69 09 31.56	5.95	86.6	16.54	0.35	W ST92 1-67
165	A	05 37 48.33	-69 09 15.22	5.79	84.2	13.72	0.07	C ST92 1-68
166	G	05 37 48.38	-69 02 37.65	5.91	85.9	16.93	0.16	W
167	D	05 37 48.81	-69 09 15.88	5.76	83.8	16.07	0.01	C
168	G	05 37 49.52	-69 12 33.17	8.03	116.8	15.46	0.08	W
169	A	05 37 49.91	-69 10 27.98	6.44	93.6	14.59	0.03	C ST92 1-71, 2MASS J05374991–6910279
170	C	05 37 50.00	-69 07 42.17	4.96	72.1	16.03	0.15	W
171	A	05 37 50.02	-69 09 59.94	6.12	89.0	14.06	-0.05	C ST92 1-72, 2MASS J05375001–6909599
172	E	05 37 50.13	-69 10 01.58	6.13	89.1	—	—	—
173	D	05 37 50.39	-69 08 54.43	5.45	79.2	16.16	0.33	W ST92 1-73
174	A	05 37 50.66	-69 08 48.44	5.38	78.2	15.50	0.25	W ST92 1-75
175	F	05 37 50.79	-69 11 35.60	7.21	104.8	15.94	0.36	W ST92 1-74
176	E	05 37 50.97	-69 11 00.31	6.75	98.2	14.78	0.03	W ST92 1-77, 2MASS J05375095–6911003
177	C	05 37 51.03	-69 06 10.60	4.58	66.6	14.63	0.24	W 2MASS J05375102–6906106
178	B	05 37 51.05	-69 09 34.01	5.77	84.0	12.91	-0.05	C ST92 1-76, 2MASS J05375103–6909339
179	D	05 37 51.18	-69 09 37.44	5.80	84.4	16.93	0.09	W
180	B	05 37 51.35	-69 09 46.75	5.89	85.6	13.54	-0.08	C ST92 1-78, Brey 74a, BAT99-093, 2MASS J05375133–6909467
181	I	05 37 51.39	-69 12 40.83	8.04	117.0	16.24	0.15	W
182	B	05 37 51.43	-69 05 30.19	4.58	66.6	15.19	0.61	W 2MASS J05375142–6905301
183	H	05 37 51.50	-69 11 25.57	7.04	102.3	16.51	0.38	W
184	B	05 37 51.83	-69 04 24.83	4.80	69.8	15.38	-0.09	C
185	B	05 37 51.92	-69 09 20.88	5.58	81.2	14.45	0.07	W ST92 1-80, 2MASS J05375194–6909208
186	C	05 37 52.04	-69 04 39.88	4.70	68.3	15.79	0.11	W
187	I	05 37 52.19	-69 11 31.37	7.07	102.9	15.81	0.22	W ST92 1-81
188	F	05 37 52.41	-69 10 51.32	6.56	95.3	16.82	0.30	W
189	D	05 37 52.86	-69 09 45.87	5.77	84.0	16.31	0.10	W ST92 1-82
190	G	05 37 53.30	-69 12 57.34	8.18	118.9	14.67	-0.04	C 2MASS J05375329–6912573
191	C	05 37 53.42	-69 10 23.53	6.16	89.6	15.74	0.12	W ST92 1-84
192	A	05 37 53.65	-69 10 12.41	6.02	87.5	16.23	-0.01	W ST92 1-85
193	D	05 37 54.20	-69 08 41.49	5.05	73.4	16.10	1.58	W ST92 1-86, 2MASS J05375419–6908414
194	C	05 37 54.20	-69 05 46.18	4.31	62.6	16.08	0.12	W
195	D	05 37 54.22	-69 05 17.89	4.36	63.4	16.86	0.06	W

continued on next page

**Table 5.** *continued*

Star [VFTS]	Field	$\alpha$ (2000)	$\delta$ (2000)	$r_d$ [']	$V$	$B - V$	Ref.	Aliases (& comments)
				[pc]				
196	E	05 37 54.27	-69 01 44.64	6.08	88.4	15.58	0.05	W
197	A	05 37 54.44	-69 09 41.62	5.62	81.7	13.86	-0.06	C ST92 1-87, 2MASS J05375443-6909415
198	A	05 37 54.64	-69 09 03.36	5.21	75.8	14.02	2.04	C ST92 1-88, 2MASS J05375464-6909032
199	I	05 37 54.78	-69 00 24.99	7.05	102.6	16.91	-0.01	W
200	B	05 37 54.95	-69 10 12.62	5.93	86.3	14.83	0.09	W ST92 1-89, 2MASS J05375495-6910124
201	F	05 37 55.00	-69 11 32.94	6.94	100.9	16.43	0.16	W
202	G	05 37 55.01	-69 08 55.12	5.11	74.3	16.16	0.13	W ST92 1-90
203	B	05 37 55.01	-69 04 00.52	4.69	68.2	16.77	-0.02	W
204	H	05 37 55.04	-69 07 02.20	4.34	63.1	16.13	0.31	W
205	A	05 37 55.39	-69 10 20.89	6.00	87.3	15.90	0.00	W ST92 1-91
206	H	05 37 55.43	-68 57 06.99	9.86	143.5	14.99	0.15	W Some cross-contamination; 2MASS J05375543-6857069
207	B	05 37 56.08	-69 10 39.05	6.18	89.9	16.22	0.09	W ST92 1-92
208	A	05 37 56.23	-69 11 50.90	7.11	103.4	14.65	0.33	W ST92 1-93, 2MASS J05375622-6911507
209	E	05 37 56.58	-69 03 48.68	4.66	67.7	16.33	-0.06	W
210	E	05 37 56.97	-69 08 21.25	4.66	67.8	15.60	0.00	W ST92 1-94
211	G	05 37 57.34	-68 58 41.89	8.38	121.8	16.56	-0.12	W
212	D	05 37 57.88	-69 08 48.83	4.84	70.4	15.18	0.02	W ST92 1-95
213	B	05 37 57.96	-69 09 54.11	5.53	80.4	15.50	0.04	W ST92 1-96, 2MASS J05375795-6909540
214	G	05 37 58.01	-69 13 09.59	8.14	118.4	15.84	0.27	W
215	E	05 37 58.03	-69 02 23.54	5.39	78.3	16.58	-0.03	W
216	A	05 37 59.06	-69 11 56.83	7.05	102.6	14.41	0.25	W ST92 1-97, 2MASS J05375905-6911566
217	A	05 37 59.49	-69 09 01.76	4.85	70.5	13.79	-0.11	C ST92 1-98
218	H	05 37 59.71	-69 11 14.29	6.44	93.6	15.63	0.38	W ST92 1-99, 2MASS J05375972-6911142
219	D	05 37 59.80	-69 03 35.50	4.52	65.8	16.93	0.04	W
220	C	05 38 00.40	-69 08 27.90	4.46	64.8	16.66	0.03	W
221	E	05 38 00.43	-69 03 45.80	4.38	63.8	16.27	-0.08	W
222	C	05 38 00.57	-69 09 41.64	5.22	75.9	14.86	1.85	C ST92 1-100, 2MASS J05380057-6909415
223	D	05 38 00.61	-69 08 41.93	4.57	66.5	14.77	-0.05	W ST92 1-101
224	D	05 38 00.83	-69 03 59.80	4.24	61.6	16.02	0.11	W
225	H	05 38 00.96	-68 57 23.28	9.42	136.9	15.07	-0.01	W Some cross-contamination
226	G	05 38 01.00	-69 14 21.74	9.10	132.3	15.92	-0.03	W
227	B	05 38 01.31	-69 03 13.91	4.62	67.2	16.51	-0.09	W
228	E	05 38 01.70	-69 01 34.87	5.76	83.7	16.46	-0.04	W
229	E	05 38 02.94	-69 02 19.17	5.13	74.6	16.48	0.00	W
230	B	05 38 04.43	-69 07 57.96	3.89	56.6	16.59	0.44	W 2MASS J05380443-6907579
231	C	05 38 04.71	-69 08 53.03	4.40	63.9	16.18	0.11	W ST92 1-103
232	A	05 38 04.76	-69 09 05.50	4.53	65.9	14.52	0.50	W ST92 1-104, 2MASS J05380477-6909055
233	E	05 38 04.82	-69 11 22.50	6.29	91.5	16.40	0.23	W
234	C	05 38 06.29	-69 06 53.03	3.33	48.4	16.22	0.11	W
235	F	05 38 06.36	-69 05 14.35	3.31	48.2	15.48	-0.06	W
236	C	05 38 06.61	-69 03 45.25	3.93	57.2	13.80	1.88	W 2MASS J05380659-6903452
237	G	05 38 06.63	-69 14 06.96	8.68	126.2	15.93	0.06	W
238	F	05 38 06.67	-69 03 59.28	3.79	55.2	16.84	-0.01	C
239	D	05 38 06.72	-69 09 32.50	4.72	68.7	16.41	0.02	W
240	C	05 38 06.75	-69 06 08.76	3.18	46.2	15.85	0.01	C Extended/blended in WFI image
241	B	05 38 07.09	-69 04 14.77	3.63	52.8	16.65	-0.03	W
242	D	05 38 07.83	-69 00 57.10	5.96	86.6	16.82	0.04	W
243	C	05 38 08.40	-69 09 19.04	4.46	64.8	15.26	0.21	W 2MASS J05380840-6909190
244	E	05 38 08.42	-69 05 44.56	3.04	44.3	14.04	-0.10	C 2MASS J05380840-6905446
245	B	05 38 08.78	-69 03 45.19	3.78	54.9	16.82	1.69	W 2MASS J05380879-6903451
246	C	05 38 08.86	-69 10 40.04	5.50	80.0	16.83	0.45	W
247	C	05 38 08.90	-69 08 16.97	3.73	54.3	16.88	0.02	W
248	D	05 38 09.32	-69 10 14.33	5.12	74.5	16.49	0.00	W

continued on next page

**Table 5.** *continued*

Star [VFTS]	Field	$\alpha$ (2000)	$\delta$ (2000)	$r_d$ [']	$V$	$B - V$	Ref.	Aliases (& comments)
				[pc]				
249	B	05 38 09.57	-69 06 54.10	3.05	44.3	15.52	-0.03	W
250	B	05 38 10.23	-69 08 56.46	4.07	59.2	15.74	0.02	W
251	E	05 38 10.23	-69 05 04.73	3.03	44.0	15.62	-0.05	W
252	B	05 38 10.37	-69 02 30.65	4.55	66.1	15.46	-0.13	W
253	I	05 38 10.38	-69 14 33.74	8.98	130.6	15.18	0.04	W
254	C	05 38 10.41	-69 05 17.67	2.95	42.9	16.90	0.03	W
255	B	05 38 11.05	-69 07 19.70	3.07	44.7	16.68	0.02	W
256	B	05 38 11.30	-69 04 49.27	3.03	44.1	15.02	-0.10	W
257	G	05 38 11.40	-69 14 24.65	8.81	128.1	16.70	-0.04	W
258	E	05 38 11.58	-69 11 42.47	6.29	91.5	16.34	0.10	W
259	C	05 38 12.03	-69 06 34.30	2.76	40.1	13.65	0.21	C 2MASS J05381202-6906342
260	G	05 38 12.26	-69 13 40.49	8.09	117.6	16.63	1.42	W
261	D	05 38 12.34	-69 00 57.35	5.75	83.7	12.33	0.03	C 2MASS J05381233-6900573
262	H	05 38 12.37	-69 13 37.82	8.04	116.9	15.80	0.50	W
263	B	05 38 12.56	-69 03 51.87	3.44	50.1	16.80	0.05	W
264	D	05 38 12.88	-69 01 39.51	5.12	74.4	16.79	1.50	W Some cross-contamination ; 2MASS J05381287-6901394
265	A	05 38 12.94	-69 05 14.79	2.75	39.9	16.05	0.18	W
266	D	05 38 13.30	-69 11 19.04	5.87	85.4	15.38	0.12	W
267	A	05 38 13.97	-69 07 47.85	3.08	44.8	13.49	-0.05	C 2MASS J05381396-6907477
268	B	05 38 14.69	-69 03 32.23	3.52	51.2	16.65	0.11	W
269	A	05 38 14.89	-69 03 48.51	3.32	48.3	12.90	0.05	C R132, WB97-1, 2MASS J05381489-6903485
270	F	05 38 15.14	-69 04 01.18	3.17	46.0	14.35	-0.07	C WB97-2
271	G	05 38 15.38	-69 04 03.57	3.12	45.4	12.84	0.22	C Mk B2, WB97-3, 2MASS J05381536-6904035
272	D	05 38 15.59	-69 04 02.22	3.12	45.4	16.00	-0.01	C GC00-Be5; blended in the PSF wing of VFTS 271/WB97-3
273	E	05 38 15.62	-69 12 12.21	6.60	96.0	16.74	0.03	W
274	D	05 38 15.87	-69 09 31.62	4.21	61.2	16.94	-0.01	W
275	C	05 38 16.00	-69 10 11.39	4.76	69.3	14.22	2.28	C 2MASS J05381601-6910112
276	B	05 38 16.00	-69 03 54.72	3.18	46.2	15.84	-0.13	C GC00-Be2
277	C	05 38 16.11	-69 09 16.81	3.99	58.1	15.04	0.01	W 2MASS J05381611-6909168
278	I	05 38 16.21	-69 04 04.01	3.06	44.5	16.82	-0.07	C
279	F	05 38 16.44	-69 03 51.15	3.19	46.4	16.73	0.05	W GC00-Be8
280	F	05 38 16.54	-69 04 53.23	2.58	37.5	15.40	0.00	W
281	C	05 38 16.68	-69 04 14.09	2.92	42.5	13.99	2.40	C WB97-4, 2MASS J05381667-6904140
282	C	05 38 16.84	-69 03 57.17	3.10	45.0	16.11	-0.06	C GC00-Be7
283	I	05 38 17.09	-69 03 50.71	3.15	45.9	15.31	-0.01	C WB97-6, GC00-Be4
284	B	05 38 17.26	-69 09 11.16	3.86	56.1	16.84	-0.02	W
285	A	05 38 17.34	-69 05 42.14	2.26	32.9	15.63	-0.06	W
286	D	05 38 17.35	-69 04 47.92	2.56	37.2	15.83	-0.08	W
287	G	05 38 17.35	-69 03 56.48	3.07	44.7	16.58	-0.08	C GC00-Be9
288	A	05 38 17.59	-69 07 24.31	2.59	37.7	16.58	0.13	W
289	E	05 38 17.64	-69 04 12.03	2.88	41.9	13.96	1.76	W WB97-7, 2MASS J05381763-6904119
290	C	05 38 17.72	-69 05 45.88	2.22	32.3	15.67	0.04	W
291	F	05 38 17.73	-69 03 38.66	3.26	47.4	14.85	0.12	W WB97-8, 2MASS J05381772-6903386
292	E	05 38 17.78	-69 03 55.90	3.05	44.3	16.47	-0.14	C
293	H	05 38 18.00	-69 04 09.77	2.88	41.9	14.95	-0.04	C WB97-9, GC00-Be1
294	D	05 38 18.23	-69 04 02.47	2.94	42.8	13.19	0.13	C Mk B1, WB97-10
295	H	05 38 18.25	-68 57 26.27	8.88	129.1	16.33	-0.07	W
296	C	05 38 18.28	-69 11 06.46	5.50	80.0	15.45	-0.01	W
297	B	05 38 18.42	-69 03 51.70	3.06	44.5	16.64	0.04	W
298	C	05 38 18.49	-69 09 20.55	3.92	57.1	16.68	0.24	W
299	E	05 38 18.52	-69 12 28.11	6.76	98.4	16.36	-0.05	W
300	C	05 38 18.57	-69 01 51.92	4.69	68.2	16.41	-0.03	W Some cross-contamination
301	H	05 38 18.84	-69 03 59.64	2.94	42.7	—	—	GC00-Be3; companion (GC00-Be6) at ~1.''0

continued on next page

**Table 5.** *continued*

Star [VFTS]	Field	$\alpha$ (2000)	$\delta$ (2000)	$r_d$ [']	$V$	$B - V$	Ref.	Aliases (& comments)
				[pc]				
302	D	05 38 19.00	-69 11 12.83	5.57	81.0	15.53	0.32	W 2MASS J05381900-6911128
303	B	05 38 19.05	-69 06 34.55	2.15	31.2	15.39	0.00	C 2MASS J05381905-6906346
304	A	05 38 19.10	-69 04 58.11	2.34	34.0	15.94	-0.08	W
305	G	05 38 19.22	-68 57 37.48	8.67	126.2	16.59	-0.10	W
306	D	05 38 19.24	-69 06 00.54	2.06	30.0	14.08	0.03	W Mk 80, 2MASS J05381925-6906005
307	B	05 38 19.30	-68 57 15.75	9.02	131.2	13.56	-0.06	C Sk-68° 136, 2MASS J05381928-6857156
308	A	05 38 19.40	-69 04 03.10	2.86	41.6	15.88	-0.01	W
309	F	05 38 19.75	-69 04 10.41	2.76	40.1	16.19	0.00	W
310	C	05 38 19.83	-69 03 52.39	2.96	43.1	16.91	0.03	W
311	A	05 38 19.84	-69 07 10.17	2.30	33.5	16.20	1.90	W 2MASS J05381985-6907102
312	F	05 38 20.19	-68 59 20.34	7.00	101.7	16.90	1.59	W 2MASS J05382020-6859202
313	A	05 38 20.37	-69 06 22.76	1.99	29.0	16.32	0.07	W
314	E	05 38 20.41	-69 03 10.37	3.48	50.6	16.06	0.03	W
315	H	05 38 20.61	-69 15 37.79	9.78	142.2	14.81	0.03	W 2MASS J05382060-6915378
316	C	05 38 20.87	-69 06 17.24	1.93	28.1	15.97	0.08	W Some cross-contamination
317	A	05 38 20.91	-69 03 50.00	2.93	42.6	13.84	0.48	C Mk B3, WB97-11, 2MASS J05382092-6903500
318	H	05 38 20.93	-69 12 00.15	6.25	91.0	16.56	-0.07	W
319	E	05 38 20.98	-69 12 21.27	6.59	95.8	16.42	1.73	W 2MASS J05382099-6912212
320	D	05 38 21.17	-69 06 17.00	1.91	27.7	16.11	0.23	W Some cross-contamination
321	B	05 38 21.32	-69 07 51.20	2.61	37.9	16.89	-0.03	W P93-0003
322	D	05 38 21.62	-69 03 14.43	3.36	48.9	16.76	0.17	W P93-0006
323	D	05 38 21.77	-69 10 42.95	5.02	73.0	15.46	0.41	W 2MASS J05382176-6910429
324	H	05 38 21.89	-69 12 48.05	7.00	101.7	15.53	-0.13	W
325	F	05 38 21.96	-69 05 59.99	1.82	26.5	16.84	-0.03	W P93-0009
326	A	05 38 22.26	-69 08 07.90	2.75	40.0	16.53	-0.06	W P93-0014
327	D	05 38 22.27	-69 07 50.85	2.54	37.0	15.33	0.01	W P93-0015
328	I	05 38 22.33	-69 13 15.25	7.42	108.0	15.90	-0.11	W
329	C	05 38 22.42	-69 05 21.30	1.91	27.8	15.55	0.00	W P93-0019
330	C	05 38 22.70	-69 09 41.84	4.05	58.9	16.14	0.18	W
331	G	05 38 23.28	-69 12 54.07	7.06	102.7	16.71	-0.06	W
332	A	05 38 23.30	-69 07 16.07	2.09	30.5	14.07	0.08	W Mk 70, P93-0032, 2MASS J05382331-6907161
333	B	05 38 23.67	-69 05 03.66	1.94	28.2	12.49	-0.06	P R133, P93-0042, 2MASS J05382371-6905036
334	G	05 38 24.02	-69 05 23.99	1.76	25.6	16.26	-0.06	W P93-0050
335	B	05 38 24.29	-69 06 28.12	1.67	24.3	16.29	0.18	W P93-0053
336	D	05 38 25.58	-69 06 09.25	1.50	21.9	15.92	0.00	W P93-0075
337	C	05 38 25.60	-69 06 04.31	1.50	21.8	16.72	0.14	W P93-0076
338	D	05 38 26.19	-69 03 38.77	2.80	40.8	16.82	0.48	W P93-0084, 2MASS J05382620-6903389
339	B	05 38 26.21	-69 05 01.79	1.77	25.7	15.45	-0.08	W P93-0083
340	A	05 38 26.56	-69 05 31.59	1.51	21.9	16.89	0.24	P P93-0088
341	D	05 38 26.69	-69 08 52.70	3.16	45.9	14.02	2.46	P P93-0090, 2MASS J05382670-6908527
342	A	05 38 26.86	-69 04 17.82	2.23	32.5	16.94	-0.04	W P93-0097
343	C	05 38 27.04	-69 04 46.63	1.87	27.2	16.45	0.04	W Some cross-contamination; P93-0099
344	H	05 38 27.22	-68 57 43.25	8.44	122.7	16.58	1.54	W 2MASS J05382723-6857432
345	C	05 38 27.41	-69 08 09.41	2.50	36.3	15.57	-0.03	W P93-0103
346	A	05 38 27.75	-69 06 06.70	1.31	19.0	16.30	0.07	W P93-0113
347	G	05 38 27.79	-69 05 27.20	1.43	20.8	16.68	0.01	W P93-0116
348	A	05 38 27.81	-69 03 36.57	2.76	40.2	16.27	0.04	W P93-0118
349	C	05 38 27.99	-69 04 09.36	2.29	33.3	16.50	-0.03	W P93-0125
350	C	05 38 28.05	-69 06 29.05	1.35	19.6	14.95	0.12	W P93-0124, 2MASS J05382805-6906290
351	A	05 38 28.39	-69 06 40.89	1.40	20.4	15.98	0.08	W P93-0136
352	C	05 38 28.45	-69 11 19.17	5.42	78.8	14.38	-0.10	W 2MASS J05382845-6911191
353	C	05 38 28.53	-69 07 51.20	2.19	31.8	16.60	0.13	W P93-0138
354	F	05 38 28.55	-69 04 32.52	1.95	28.3	15.91	0.00	W P93-0141

continued on next page

**Table 5.** *continued*

Star [VFTS]	Field	$\alpha$ (2000)	$\delta$ (2000)	$r_d$ [']	$V$	$B - V$	Ref.	Aliases (& comments)
				[pc]				
355	H	05 38 29.15	-68 57 39.35	8.48	123.3	14.12	-0.19	C 2MASS J05382913-6857393
356	C	05 38 29.20	-69 09 13.79	3.39	49.3	15.87	0.16	W P93-0153
357	F	05 38 29.34	-68 59 20.17	6.81	99.1	16.57	1.47	W 2MASS J05382934-6859202
358	F	05 38 29.37	-69 08 50.45	3.02	44.0	16.87	0.00	W P93-0158
359	D	05 38 29.39	-69 05 59.19	1.16	16.9	16.30	0.03	S S99-290
360	E	05 38 29.45	-69 05 21.29	1.35	19.6	14.80	0.19	S P93-0169, S99-107
361	B	05 38 29.52	-69 06 20.59	1.18	17.2	15.82	0.02	S P93-0171, S99-216
362	H	05 38 29.54	-69 05 30.88	1.26	18.4	16.98	0.44	P P93-0176 (offset by 0'37 and within nebulosity)
363	B	05 38 30.01	-69 05 05.31	1.46	21.3	14.88	-0.07	S Mk 60, P93-0195, S99-098, 2MASS J05383000-6905053
364	E	05 38 30.07	-69 08 27.60	2.65	38.5	16.82	0.03	W P93-0193
365	H	05 38 30.09	-68 59 31.27	6.62	96.3	16.24	-0.02	W
366	E	05 38 30.11	-69 04 44.55	1.70	24.8	16.83	-0.02	W P93-0202
367	A	05 38 30.27	-69 03 52.75	2.42	35.3	15.92	-0.04	W P93-0207
368	D	05 38 30.43	-69 05 29.58	1.20	17.5	16.68	0.01	S S99-377
369	A	05 38 30.61	-69 08 24.44	2.58	37.6	16.66	0.15	W P93-0214
370	D	05 38 30.74	-69 08 27.13	2.62	38.1	15.74	-0.05	W P93-0222
371	A	05 38 31.04	-69 04 27.08	1.89	27.5	15.47	-0.03	W P93-0240
372	G	05 38 31.16	-69 14 01.83	8.04	117.0	16.80	1.00	W 2MASS J05383117-6914018
373	E	05 38 31.26	-69 05 53.03	1.01	14.6	15.25	0.09	S P93-0246, S99-141
374	C	05 38 31.28	-69 05 56.96	1.00	14.5	16.36	0.19	S Some cross-contamination; S99-326
375	C	05 38 31.65	-69 05 27.06	1.13	16.4	16.20	0.02	S S99-275
376	D	05 38 31.66	-69 05 48.99	0.98	14.3	16.33	0.04	S P93-0260, S99-297
377	B	05 38 31.78	-69 05 56.73	0.95	13.8	16.83	0.11	S S99-418
378	F	05 38 31.88	-69 05 32.78	1.06	15.5	16.98	0.26	P P93-0271
379	E	05 38 31.99	-69 11 44.66	5.77	83.9	16.92	1.71	W 2MASS J05383199-6911445
380	D	05 38 32.00	-69 02 52.51	3.31	48.1	16.18	0.04	W
381	G	05 38 32.12	-69 04 31.83	1.77	25.8	16.11	0.07	P P93-0280
382	C	05 38 32.28	-69 05 44.57	0.95	13.8	15.88	0.14	S S99-226
383	C	05 38 32.31	-69 07 32.22	1.74	25.3	16.10	0.20	W P93-0284
384	D	05 38 32.32	-69 07 35.91	1.79	26.1	16.72	0.49	W P93-0287
385	E	05 38 32.32	-69 05 23.87	1.11	16.1	14.65	0.00	S P93-0288, S99-084
386	H	05 38 32.54	-69 04 32.02	1.75	25.5	14.75	0.20	P Mk 58(e), P93-0294
387	G	05 38 32.63	-68 57 14.08	8.86	128.8	15.58	0.10	W
388	D	05 38 32.63	-69 03 55.93	2.29	33.3	16.42	0.06	P P93-0305
389	F	05 38 32.67	-69 04 32.60	1.74	25.3	14.17	-0.16	P Mk 58(w), P93-0304
390	C	05 38 32.78	-69 03 19.51	2.85	41.5	15.49	0.14	P P93-0316
391	D	05 38 32.80	-69 05 24.92	1.06	15.5	16.32	-0.02	S S99-287
392	E	05 38 32.83	-69 05 44.60	0.91	13.2	16.10	0.13	S S99-268
393	B	05 38 33.02	-69 05 13.10	1.18	17.1	15.26	-0.06	S P93-0324, S99-131
394	E	05 38 33.02	-69 02 43.09	3.43	49.9	16.93	-0.03	W
395	A	05 38 33.20	-69 04 51.36	1.45	21.0	16.95	-0.18	S S99-393
396	C	05 38 33.27	-69 10 24.00	4.43	64.4	16.32	0.11	W
397	A	05 38 33.34	-69 04 17.05	1.94	28.2	16.68	0.01	W P93-0338
398	D	05 38 33.38	-69 04 38.39	1.62	23.6	14.40	-0.03	P Mk 59, P93-0341
399	D	05 38 33.41	-69 11 59.05	5.99	87.1	15.83	0.08	W
400	C	05 38 33.55	-69 05 21.75	1.04	15.2	16.03	-0.04	S P93-0348, S99-227
401	H	05 38 33.59	-68 56 05.83	9.98	145.2	15.48	0.17	W 2MASS J05383359-6856056
402	C	05 38 33.62	-69 04 50.58	1.44	20.9	13.48	-0.85	S R135, S99-012, Brey 80, BAT99-095, 2MASS J05383362-6904503
403	I	05 38 33.82	-69 04 36.17	1.64	23.8	17.12	0.19	P P93-0364 (offset by 0'34 and within nebulosity)
404	B	05 38 33.82	-69 09 57.11	3.98	57.9	14.14	0.02	C 2MASS J05383381-6909569
405	F	05 38 33.84	-69 05 51.80	0.78	11.4	16.74	0.13	S S99-401
406	C	05 38 33.96	-69 04 21.17	1.85	27.0	14.30	0.01	P Some cross-contamination; Mk 55, P93-0370, 2MASS J05383397-6904211
407	F	05 38 34.46	-69 06 14.49	0.73	10.7	16.97	0.08	S S99-466

continued on next page

**Table 5.** *continued*

Star [VFTS]	Field	$\alpha$ (2000)	$\delta$ (2000)	$r_d$ [']	$V$	$B - V$	Ref.	Aliases (& comments)
				[pc]				
408	D	05 38 34.46	-69 01 39.67	4.44	64.6	16.32	0.02	W P93-9011
409	C	05 38 34.58	-69 06 52.76	1.08	15.8	15.75	0.59	S P93-0404, S99-228
410	E	05 38 34.61	-69 06 05.90	0.70	10.1	16.03	0.76	S P93-0409, S99-288
411	B	05 38 34.79	-69 05 00.54	1.24	18.0	16.93	-0.09	S S99-409
412	F	05 38 34.90	-69 04 53.88	1.33	19.3	16.49	0.44	S S99-319
413	F	05 38 34.90	-68 58 45.40	7.32	106.5	16.48	0.02	W
414	D	05 38 35.24	-69 05 12.14	1.06	15.4	16.89	0.03	S S99-430
415	A	05 38 35.48	-69 04 57.70	1.25	18.2	15.48	-0.10	S P93-0466, S99-150
416	U	05 38 35.59	-69 06 06.58	0.61	8.9	14.67	0.10	S S99-093
417	A	05 38 35.68	-69 06 17.40	0.65	9.4	15.51	0.34	S S99-204
418	A	05 38 35.73	-69 08 19.71	2.36	34.3	16.12	0.21	W P93-0473
419	E	05 38 35.92	-69 05 34.90	0.74	10.8	15.40	0.09	S P93-0485, S99-158
420	B+U	05 38 35.96	-69 06 09.16	0.58	8.5	13.02	0.25	S Mk 54, P93-0488, S99-016
421	E	05 38 35.99	-69 04 20.65	1.80	26.1	16.42	-0.04	W
422	I	05 38 36.02	-69 06 16.85	0.61	8.9	15.14	0.24	S S99-140
423	G+U	05 38 36.07	-69 06 46.49	0.92	13.4	13.51	0.43	S Mk 52, P93-0493, S99-048, 2MASS J05383606-6906466
424	A+U	05 38 36.15	-69 05 57.87	0.56	8.2	11.74	0.33	S R138, S99-004, 2MASS J05383613-6905578
425	I	05 38 36.21	-69 06 05.77	0.55	8.0	16.50	0.06	S S99-331
426	G	05 38 36.31	-69 04 48.69	1.35	19.6	17.04	0.06	P P93-0511
427	D	05 38 36.42	-69 06 57.51	1.05	15.3	13.76	0.26	S Mk 53, S99-051, Brey 81, BAT99-096, 2MASS J05383641-6906573
428	E	05 38 36.50	-69 03 51.13	2.26	32.8	16.19	0.01	W P93-0525
429	E	05 38 36.85	-69 04 58.30	1.18	17.2	14.69	-0.11	S Mk 57, P93-0541, S99-079
430	D	05 38 36.87	-69 06 46.08	0.87	12.7	15.11	0.64	S P93-0538, S99-181, 2MASS J05383685-6906461
431	I	05 38 36.97	-69 05 07.84	1.04	15.1	12.05	0.11	S R137, P93-0548, S99-005, 2MASS J05383697-6905077
432	C	05 38 37.04	-69 06 50.69	0.93	13.5	15.65	0.25	S P93-0547, S99-214
433	B	05 38 37.09	-69 05 48.84	0.53	7.7	16.87	0.05	P P93-0560
434	F	05 38 37.22	-69 04 25.98	1.68	24.4	16.13	0.16	P P93-0572
435	E	05 38 37.22	-69 07 05.69	1.14	16.6	16.86	0.53	P P93-0566
436	C	05 38 37.36	-69 05 21.23	0.83	12.0	15.92	-0.05	S S99-209
437	B	05 38 37.37	-69 08 42.89	2.70	39.3	16.68	1.72	W P93-0574, 2MASS J05383738-6908428
438	E	05 38 37.55	-69 04 37.57	1.49	21.6	16.99	0.07	P P93-0591
439	H	05 38 37.66	-69 06 52.70	0.93	13.5	16.76	1.55	P P93-0594
440	H+U	05 38 37.74	-69 05 21.00	0.81	11.8	13.66	0.02	S Mk 47, P93-0607, S99-029, 2MASS J05383771-6905209
441	C	05 38 37.81	-69 03 28.93	2.60	37.8	15.07	-0.07	W P93-0613
442	G	05 38 37.89	-69 03 36.76	2.47	35.9	16.66	0.08	P P93-0616
443	A	05 38 37.99	-69 06 15.23	0.44	6.4	15.71	0.18	S P93-0615, S99-208
444	D	05 38 38.02	-69 05 08.58	0.99	14.3	16.13	-0.09	S S99-233
445	A+U	05 38 38.04	-69 05 43.22	0.51	7.4	14.75	0.10	S P93-0621, S99-097
446	B	05 38 38.26	-69 06 17.29	0.44	6.4	15.47	0.35	S S99-194
447	F	05 38 38.32	-69 02 27.49	3.61	52.5	15.79	-0.15	C
448	B	05 38 38.34	-69 06 44.96	0.79	11.5	16.85	0.33	P P93-0632
449	G	05 38 38.36	-69 05 08.07	0.98	14.3	16.91	0.03	S S99-428
450	F+U	05 38 38.49	-69 06 21.90	0.47	6.8	13.60	0.20	S Mk 50, P93-0643, S99-034, J05383848-6906218
451	C	05 38 38.52	-69 06 29.92	0.57	8.3	16.25	0.37	S Some cross-contamination; S99-346
452	E	05 38 38.73	-69 12 32.76	6.51	94.6	16.44	-0.04	W
453	E	05 38 38.75	-69 04 12.36	1.87	27.2	15.31	-0.03	W P93-0668
454	C	05 38 38.76	-69 11 20.30	5.30	77.1	16.37	1.54	W 2MASS J05383877-6911201
455	I+U	05 38 38.78	-69 06 13.15	0.36	5.3	14.84	0.15	S P93-0661, S99-108
456	B	05 38 38.83	-69 05 25.52	0.70	10.2	15.46	0.13	S S99-172
457	E+U	05 38 38.85	-69 06 49.46	0.84	12.2	13.74	0.49	S Mk 51, P93-0666, S99-050, BAT99-097
458	C	05 38 38.87	-69 08 14.61	2.22	32.3	12.67	0.60	P Mk B, P93-0662, 2MASS J05383886-6908144
459	I	05 38 38.94	-69 03 12.10	2.86	41.6	16.39	0.01	W P93-0684
460	C	05 38 39.00	-69 06 58.90	0.98	14.3	15.86	0.44	S P93-0674, S99-278

continued on next page

**Table 5.** *continued*

Star [VFTS]	Field	$\alpha$ (2000)	$\delta$ (2000)	$r_d$ [']	$V$	$B - V$	Ref.	Aliases (& comments)
				[pc]				
461	C	05 38 39.15	-69 05 05.75	1.00	14.5	16.83	-0.58	S S99-303
462	F	05 38 39.16	-69 01 40.77	4.38	63.7	16.27	-0.52	W P93-9013
463	I	05 38 39.25	-69 06 01.13	0.28	4.1	16.92	-0.03	S S99-422
464	F	05 38 39.28	-69 05 52.69	0.33	4.7	16.80	-0.02	P P93-0702
465	D	05 38 39.28	-69 06 38.93	0.66	9.6	16.38	0.54	S P93-0700, S99-365
466	A	05 38 39.28	-69 07 52.96	1.86	27.0	15.60	0.37	W P93-0696
467	H	05 38 39.32	-69 15 35.02	9.54	138.7	16.91	0.38	W
468	F	05 38 39.38	-69 06 06.39	0.27	4.0	14.59	0.04	S Mk 36, P93-0706, S99-086
469	H	05 38 39.40	-69 03 07.67	2.93	42.7	16.09	0.00	W Some cross-contamination; P93-0714
470	F	05 38 39.49	-69 04 38.64	1.43	20.8	15.46	-0.08	W P93-0716
471	I	05 38 39.49	-69 02 30.84	3.54	51.5	16.36	-0.10	W
472	E	05 38 39.55	-69 07 05.34	1.07	15.6	16.39	0.26	W P93-0712
473	F	05 38 39.58	-69 04 56.73	1.13	16.5	16.85	-0.02	S S99-402
474	C	05 38 39.70	-69 09 27.80	3.42	49.8	16.67	0.07	W
475	D	05 38 39.73	-69 07 56.07	1.90	27.6	16.43	0.37	W P93-0722
476	B	05 38 39.75	-69 05 39.21	0.46	6.7	15.67	0.21	S S99-206
477	I	05 38 39.75	-69 05 50.55	0.31	4.5	16.95	0.20	S S99-455
478	G	05 38 39.82	-69 07 10.91	1.16	16.8	16.72	0.32	W P93-0738
479	B	05 38 39.82	-69 03 41.10	2.37	34.5	15.90	0.14	W P93-0747
480	D	05 38 40.15	-69 05 13.41	0.85	12.3	16.94	0.43	S S99-340
481	C	05 38 40.17	-69 01 12.29	4.85	70.5	14.16	-0.04	P P93-9017, 2MASS J05384016–6901122
482	U	05 38 40.23	-69 05 59.76	0.20	2.9	12.85	0.12	S Brey 78, Mk 39, P93-0767, S99-014
483	D	05 38 40.24	-69 05 30.78	0.57	8.3	16.38	0.12	S S99-309
484	G	05 38 40.37	-69 05 43.72	0.37	5.3	15.07	0.14	S S99-124
485	E	05 38 40.58	-69 05 11.28	0.88	12.7	16.90	-0.05	S S99-412
486	G	05 38 40.60	-69 04 56.03	1.13	16.4	15.48	0.28	S S99-164
487	G	05 38 40.71	-69 05 25.98	0.63	9.2	16.88	0.12	S S99-441 (1.''05 from S99-080/Mk 28)
488	D	05 38 40.72	-69 08 24.90	2.37	34.5	15.87	0.26	W P93-0791
489	D	05 38 40.75	-69 01 48.87	4.24	61.6	16.54	-0.07	W P93-9018
490	D	05 38 40.82	-69 10 09.00	4.10	59.7	16.44	1.64	W 2MASS J05384084–6910088
491	F	05 38 40.85	-69 06 57.50	0.92	13.4	15.62	0.29	S P93-0803, S99-213
492	D	05 38 41.04	-69 04 24.83	1.64	23.8	14.16	-0.11	P Mk 21, P93-0830
493	I	05 38 41.04	-69 06 16.71	0.26	3.8	16.74	0.33	S S99-432
494	D	05 38 41.04	-69 06 59.90	0.96	13.9	16.73	0.42	P P93-0822
495	E	05 38 41.10	-69 01 46.02	4.28	62.3	15.85	0.02	P P93-9019
496	A	05 38 41.11	-69 06 51.50	0.82	11.9	16.66	0.22	S S99-399
497	C+U	05 38 41.13	-69 05 13.14	0.84	12.2	14.66	-0.06	S R140d [M87], S99-081
498	B	05 38 41.19	-69 06 35.17	0.55	8.0	16.45	0.19	S S99-347
499	F	05 38 41.19	-69 04 06.31	1.95	28.3	16.77	0.06	P Some cross-contamination; P93-0848
500	A	05 38 41.20	-69 02 58.28	3.08	44.8	14.19	-0.08	C 2MASS J05384122–6902583
501	H	05 38 41.23	-69 04 14.22	1.81	26.4	15.74	0.08	P P93-0849
502	H	05 38 41.28	-69 05 32.33	0.52	7.6	13.76	0.07	S Mk 27(W), P93-0850, S99-038
503	F	05 38 41.38	-69 05 32.54	0.51	7.5	14.87	0.00	S Mk 27(E), S99-100
504	D	05 38 41.39	-69 03 00.89	3.03	44.1	16.27	0.61	P P93-0861
505	A	05 38 41.49	-69 05 34.52	0.48	7.0	16.24	-0.02	S S99-265
506	F	05 38 41.55	-69 05 19.39	0.73	10.6	13.31	0.02	S Mk 25, P93-0871, S99-019, 2MASS J05384154–6905193
507	H	05 38 41.60	-69 05 13.39	0.83	12.0	12.12	0.06	S Brey 87, R140N [Mk], R140a [M87], S99-006, BAT99-101 + 102
508	G	05 38 41.60	-69 07 02.40	0.99	14.5	15.98	0.17	P P93-0872
509	G	05 38 41.62	-69 05 15.09	0.80	11.6	12.66	-0.05	S Brey 87, R140S [Mk], R140b [M87], S99-008, BAT99-103
510	H	05 38 41.68	-69 06 18.48	0.27	3.9	16.28	0.27	S S99-305 (blended with S99-154)
511	E	05 38 41.73	-69 06 28.06	0.42	6.2	15.28	0.12	S P93-0884, S99-143
512	G	05 38 41.75	-69 06 24.94	0.37	5.4	14.28	0.20	S P93-0885, S99-068
513	C	05 38 41.81	-69 05 31.91	0.52	7.6	16.20	0.06	S S99-266

continued on next page

**Table 5.** *continued*

Star [VFTS]	Field	$\alpha$ (2000)	$\delta$ (2000)	$r_d$ [']	$V$	$B - V$	Ref.	Aliases (& comments)
				[pc]				
514	C	05 38 41.85	-69 01 58.84	4.07	59.2	15.84	-0.13	W P93-9021
515	B	05 38 41.86	-69 05 32.40	0.51	7.4	16.94	0.08	S S99-434
516	D	05 38 41.88	-69 09 22.94	3.33	48.5	16.61	0.03	W
517	H	05 38 41.92	-69 04 38.75	1.40	20.4	14.72	-0.08	P Mk 29, P93-0909
518	C	05 38 41.94	-69 06 29.62	0.45	6.5	15.11	0.27	S P93-0901, S99-138
519	I+U	05 38 41.94	-69 05 13.00	0.83	12.1	14.11	0.03	S R140c [M87], S99-055
520	E	05 38 41.99	-69 06 53.46	0.84	12.3	16.69	0.08	S S99-397
521	B	05 38 41.99	-69 07 04.95	1.03	15.0	15.34	0.17	P P93-0905
522	I	05 38 42.10	-69 05 45.41	0.29	4.3	15.22	0.08	S S99-134
523	A	05 38 42.12	-69 04 32.93	1.50	21.8	17.05	0.01	P P93-0909
524	B	05 38 42.18	-69 08 04.19	2.02	29.4	16.14	1.33	W P93-0920, 2MASS J05384218-6908040
525	F+U	05 38 42.22	-69 06 25.49	0.38	5.5	13.76	0.16	S Mk 38, P93-0930, S99-045
526	D	05 38 42.23	-69 08 32.32	2.49	36.2	14.92	0.54	W P93-0925, 2MASS J05384223-6908322
527	F	05 38 42.35	-69 04 58.18	1.08	15.7	11.94	0.10	S R139, Brey 86, P93-0952, S99-002 , BAT99-107, 2MASS J05384235-6904580
528	C	05 38 42.36	-69 04 24.72	1.64	23.8	15.58	0.00	P P93-0956
529	D	05 38 42.37	-69 04 43.15	1.33	19.3	15.94	0.07	P P93-0955
530	B	05 38 42.40	-69 03 04.21	2.98	43.3	16.28	-0.02	P P93-0965
531	B	05 38 42.64	-69 04 13.43	1.82	26.5	14.50	-0.11	W Mk 22W, P93-0983
532	A+U	05 38 42.67	-69 06 35.77	0.55	8.0	14.76	0.20	S P93-0974, S99-104, 2MASS J05384265-6906357
533	F	05 38 42.75	-69 05 42.47	0.34	5.0	11.82	0.29	S R142, P93-0987, S99-003, 2MASS J05384274-6905424
534	I	05 38 42.80	-69 15 40.29	9.62	140.0	15.66	0.21	W 2MASS J05384281-6915401
535	I	05 38 42.80	-69 04 31.50	1.52	22.2	16.53	0.34	P P93-0995
536	I	05 38 42.82	-69 06 32.43	0.49	7.2	16.21	0.23	S S99-295
537	A	05 38 43.02	-69 03 44.78	2.30	33.5	15.99	0.07	W Some cross-contamination; P93-1022
538	A	05 38 43.07	-69 04 13.07	1.83	26.6	13.99	-0.03	P Mk 22, P93-1024, 2MASS J05384302-6904131
539	H	05 38 43.08	-69 07 02.07	0.99	14.4	16.14	0.14	P P93-1012
540	G	05 38 43.08	-69 06 36.88	0.57	8.3	16.55	0.23	S S99-372
541	D	05 38 43.09	-69 01 32.59	4.51	65.5	13.12	0.13	P P93-9024, 2MASS J05384307-6901324
542	G+U	05 38 43.10	-69 05 46.76	0.28	4.0	13.47	0.09	S Mk 30, P93-1018, S99-024, BAT99-113; also observed in Field A5 of the IFU data
543	A	05 38 43.20	-69 05 27.46	0.60	8.7	15.41	0.02	S P93-1031, S99-152
544	G	05 38 43.20	-69 15 04.75	9.03	131.4	16.90	1.49	W 2MASS J05384322-6915046
545	U	05 38 43.21	-69 06 14.37	0.20	3.0	13.40	0.12	S Mk 35, P93-1029, S99-023; also observed in Field A3 of the IFU data
546	G	05 38 43.37	-69 04 46.39	1.28	18.6	15.36	0.04	W P93-1052
547	I	05 38 43.54	-69 01 58.79	4.07	59.2	16.79	0.03	W P93-9026
548	E	05 38 43.56	-69 05 29.31	0.57	8.3	16.13	-0.02	S S99-240
549	A	05 38 43.58	-69 07 51.89	1.82	26.5	16.51	0.35	W P93-1063
550	A	05 38 43.60	-69 04 42.46	1.35	19.6	15.25	0.09	P P93-1077
551	G	05 38 43.66	-69 06 18.86	0.29	4.2	16.82	0.13	S S99-416
552	H	05 38 43.69	-69 06 16.57	0.26	3.7	16.16	0.31	S S99-299
553	D	05 38 43.73	-69 06 27.18	0.42	6.1	17.00	0.06	S S99-450
554	H	05 38 43.79	-69 05 38.70	0.42	6.1	16.61	0.04	S S99-343
555	D	05 38 43.89	-69 03 16.30	2.78	40.4	15.88	0.08	W P93-1109
556	H	05 38 44.00	-69 04 48.25	1.25	18.2	16.88	0.04	S S99-417
557	E	05 38 44.06	-69 04 59.49	1.07	15.5	16.57	0.12	S S99-354
558	D	05 38 44.24	-69 00 27.58	5.59	81.3	16.69	0.01	P P93-9028
559	C	05 38 44.29	-69 07 16.57	1.24	18.0	16.49	0.22	P P93-1133
560	I	05 38 44.35	-69 06 40.73	0.65	9.5	16.59	0.05	S P93-1139, S99-350
561	B	05 38 44.37	-69 05 14.34	0.83	12.0	15.46	0.07	S P93-1145, S99-168
562	U	05 38 44.41	-69 05 36.13	0.48	7.0	13.66	0.09	S Mk 26, P93-1150, S99-032
563	A	05 38 44.54	-69 06 28.73	0.47	6.9	15.91	0.19	S P93-1154, S99-237
564	H	05 38 44.56	-69 05 12.31	0.87	12.6	16.02	0.17	S S99-253
565	A	05 38 44.56	-69 04 55.09	1.15	16.7	16.55	0.05	S S99-332
566	I	05 38 44.56	-69 04 51.28	1.21	17.6	14.05	0.06	S Mk 23, P93-1163, S99-042

continued on next page

**Table 5.** *continued*

Star [VFTS]	Field	$\alpha$ (2000)	$\delta$ (2000)	$r_d$ [']	$V$	$B - V$	Ref.	Aliases (& comments)
				[pc]				
567	C	05 38 44.61	-69 07 56.61	1.91	27.7	16.29	0.24	W P93-1155
568	I	05 38 44.66	-69 04 24.88	1.65	23.9	16.79	0.15	P P93-1172
569	E	05 38 44.67	-69 05 13.90	0.84	12.2	16.09	0.07	S P93-1170, S99-259
570	E	05 38 44.70	-69 05 45.13	0.36	5.2	15.42	0.31	S S99-179 (blended with S99-161); also observed in Field A5 of the IFU data
571	D	05 38 44.70	-69 05 41.01	0.42	6.1	16.92	0.18	S S99-454
572	A	05 38 44.72	-69 08 57.12	2.91	42.3	16.38	0.15	W P93-1160
573	D	05 38 44.77	-69 06 57.55	0.94	13.6	16.94	0.03	S S99-440
574	H	05 38 44.82	-68 57 34.57	8.48	123.3	15.89	-0.12	W
575	I	05 38 44.91	-69 05 33.10	0.55	7.9	15.11	0.02	S P93-1191, S99-128
576	H	05 38 44.94	-69 15 11.45	9.15	133.0	15.67	0.78	W 2MASS J05384495-6915113
577	E	05 38 44.94	-69 07 04.59	1.05	15.3	16.64	0.40	P P93-1189
578	B	05 38 44.96	-69 08 06.72	2.08	30.2	14.52	0.40	W P93-1184, 2MASS J05384496-6908066
579	C	05 38 44.97	-69 05 07.69	0.95	13.8	15.51	0.00	S In 'Knot 1' [WB87]; P93-1201, S99-171
580	B	05 38 45.03	-69 03 19.32	2.74	39.8	16.62	0.05	W P93-1217
581	G	05 38 45.07	-69 04 15.57	1.80	26.3	16.07	0.18	W P93-1218, 2MASS J05384509-6904157
582	C	05 38 45.19	-69 05 37.43	0.49	7.2	16.83	0.16	S S99-414
583	C	05 38 45.22	-69 05 48.39	0.35	5.1	14.93	0.06	S S99-106
584	C	05 38 45.25	-69 06 54.84	0.90	13.1	16.95	0.05	S S99-443
585	H	05 38 45.28	-69 05 46.47	0.38	5.5	13.65	0.12	S P93-1231, S99-031; also observed in Field A5 of the IFU data
586	B	05 38 45.38	-69 02 51.36	3.20	46.6	15.04	-0.12	C 2MASS J05384539-6902514
587	D	05 38 45.38	-69 05 24.44	0.69	10.1	16.38	0.00	S S99-293
588	G	05 38 45.40	-69 05 39.76	0.47	6.8	16.53	0.14	S S99-356
589	A	05 38 45.59	-69 07 34.86	1.56	22.7	15.83	0.15	P P93-1247
590	F+U	05 38 45.59	-69 05 47.73	0.38	5.5	12.49	0.22	S R141, P93-1253, S99-009
591	B	05 38 45.69	-69 06 22.45	0.44	6.4	12.55	0.23	S Mk 12, P93-1257, S99-011
592	D	05 38 45.69	-69 06 15.33	0.36	5.2	16.40	0.14	S S99-318
593	C	05 38 45.70	-69 09 40.13	3.63	52.8	16.84	0.09	W
594	G	05 38 45.76	-69 05 13.29	0.88	12.8	16.16	0.07	S S99-267
595	E	05 38 45.87	-69 02 43.37	3.34	48.6	16.48	1.63	W 2MASS J05384588-6902433
596	C	05 38 46.07	-69 06 15.51	0.39	5.7	15.23	0.03	S S99-137
597	B	05 38 46.07	-69 06 56.19	0.95	13.8	15.56	0.03	S P93-1288, S99-175
598	E	05 38 46.13	-69 06 23.51	0.48	7.0	16.94	0.34	S S99-475
599	G+U	05 38 46.19	-69 06 17.33	0.42	6.0	13.80	0.08	S P93-1311, S99-040
600	E	05 38 46.24	-69 10 14.74	4.21	61.3	16.40	-0.04	W
601	E	05 38 46.29	-69 05 59.25	0.35	5.1	14.69	0.09	S Mk 14N, P93-1317, S99-091, 2MASS J05384628-6905592
602	C	05 38 46.34	-69 04 33.50	1.53	22.3	16.71	0.09	W P93-1326
603	G	05 38 46.52	-69 04 27.98	1.62	23.6	13.99	0.04	W Mk 10, P93-1341
604	A+U	05 38 46.58	-69 05 37.07	0.57	8.3	14.94	0.04	S P93-1340, S99-110
605	D	05 38 46.70	-69 02 40.54	3.39	49.4	16.85	-0.13	W
606	I	05 38 46.71	-69 05 38.78	0.56	8.1	16.60	0.06	S S99-357
607	A	05 38 46.76	-69 05 48.75	0.46	6.6	16.34	0.08	S S99-294
608	H	05 38 46.79	-69 06 03.03	0.39	5.7	14.22	0.16	S Mk 14, P93-1350, S99-064, 2MASS J05384677-6906030
609	B	05 38 46.87	-69 05 20.07	0.82	11.9	16.76	-0.01	S S99-384
610	D	05 38 46.89	-69 06 26.61	0.56	8.2	16.73	0.17	S P93-1354, S99-408
611	C	05 38 46.90	-69 05 58.71	0.41	5.9	16.16	0.13	S S99-270
612	C	05 38 47.15	-69 06 35.81	0.69	10.1	16.53	0.20	S S99-362
613	B	05 38 47.17	-69 05 54.40	0.45	6.5	15.78	0.16	S P93-1369, S99-219
614	H	05 38 47.20	-69 06 20.01	0.52	7.5	16.07	0.69	S S99-313, 2MASS J05384718-6906198
615	A	05 38 47.33	-69 06 17.70	0.50	7.3	15.89	0.02	S S99-218
616	I	05 38 47.46	-69 07 13.41	1.26	18.3	16.48	0.09	W P93-1389
617	A	05 38 47.49	-69 00 25.21	5.65	82.1	13.11	-0.12	P HDE 269926, R146, Sk-69° 245, Brey 88, BAT99-117, P93-9033, 2MASS J05384751-6900252
618	F	05 38 47.59	-69 07 05.91	1.15	16.7	16.70	0.38	P P93-1395
619	B	05 38 47.72	-69 06 44.96	0.85	12.3	15.98	0.12	S P93-1401, S99-234

continued on next page

**Table 5.** *continued*

Star [VFTS]	Field	$\alpha$ (2000)	$\delta$ (2000)	$r_d$ [']	$V$	$B - V$	Ref.	Aliases (& comments)
				[pc]				
620	B	05 38 47.92	-69 05 32.89	0.70	10.2	16.61	0.03	S P93-1416, S99-345
621	H	05 38 48.08	-69 04 42.24	1.44	20.9	15.39	0.27	P In 'Knot 2' [WB87]; P93-1429
622	B	05 38 48.12	-69 06 12.27	0.53	7.8	16.56	0.05	S S99-333
623	C	05 38 48.13	-69 07 41.56	1.72	25.0	16.10	0.14	W P93-1419
624	A	05 38 48.13	-69 06 04.80	0.51	7.5	16.98	0.11	S S99-453
625	B	05 38 48.17	-69 08 34.11	2.57	37.4	16.91	0.11	W P93-1418
626	D	05 38 48.19	-69 08 10.87	2.19	31.9	14.90	0.26	W P93-1423
627	E	05 38 48.39	-68 59 49.84	6.24	90.8	15.38	-0.15	W P93-9034
628	D	05 38 48.44	-69 06 36.41	0.78	11.3	16.64	0.09	S S99-378
629	G	05 38 48.51	-69 05 40.32	0.66	9.6	16.78	0.07	S S99-404
630	C	05 38 48.65	-69 04 58.89	1.20	17.5	16.21	0.17	S P93-1455, S99-279
631	A	05 38 48.87	-69 08 28.06	2.49	36.2	16.00	0.14	W P93-1459
632	C	05 38 48.89	-69 08 55.25	2.93	42.6	15.97	0.12	W P93-1460
633	E	05 38 48.95	-69 08 12.41	2.24	32.5	16.50	0.19	W P93-1464
634	A	05 38 49.01	-69 04 10.60	1.96	28.5	16.50	0.31	P P93-1473
635	I	05 38 49.05	-69 06 19.56	0.66	9.5	15.52	0.07	S P93-1468, S99-174
636	B	05 38 49.19	-69 10 04.47	4.07	59.2	16.53	0.06	W
637	C	05 38 49.40	-69 06 15.28	0.66	9.6	16.61	0.04	S S99-359
638	C	05 38 49.50	-69 02 30.27	3.60	52.4	15.63	-0.14	W
639	C	05 38 49.63	-69 09 24.09	3.41	49.7	15.41	-0.01	W
640	A	05 38 49.66	-69 08 54.81	2.94	42.7	16.82	0.16	W P93-1489
641	U	05 38 49.72	-69 06 43.00	0.93	13.6	13.09	0.16	S Mk 11, P93-1500, S99-015, 2MASS J05384974-6906430
642	F	05 38 49.89	-69 10 42.86	4.71	68.6	16.03	0.38	W 2MASS J05384990-6910428
643	A	05 38 49.97	-69 07 05.34	1.24	18.0	16.41	0.13	P Some cross-contamination; P93-1508
644	A	05 38 50.03	-69 06 52.00	1.06	15.5	16.62	0.15	S S99-391
645	D	05 38 50.20	-69 07 45.19	1.84	26.8	16.29	0.16	W P93-1519
646	F	05 38 50.27	-69 06 04.36	0.70	10.2	14.94	0.14	S P93-1527, S99-119, 2MASS J05385025-6906043
647	B	05 38 50.33	-69 05 02.76	1.23	17.9	16.29	0.10	S S99-285
648	A+U	05 38 50.41	-69 05 38.19	0.83	12.0	14.16	0.08	S Mk 08, P93-1531, S99-058, 2MASS J05385039-6905381
649	B	05 38 50.62	-69 05 54.56	0.75	10.9	16.07	0.05	S S99-239
650	I	05 38 50.69	-68 57 55.47	8.16	118.6	16.98	-0.10	W
651	D+U	05 38 51.04	-69 05 54.70	0.78	11.4	14.70	0.08	S Mk 07, P93-1553, S99-094, 2MASS J05385100-6905547
652	B+U	05 38 51.05	-69 06 20.42	0.83	12.0	13.88	0.20	S Mk 05, P93-1552, S99-054, 2MASS J05385103-6906203
653	D	05 38 51.09	-69 06 48.77	1.09	15.8	16.63	0.22	S P93-1554, S99-403
654	D	05 38 51.17	-69 05 41.82	0.86	12.5	15.71	0.05	S P93-1560, S99-200
655	I	05 38 51.19	-69 06 41.29	1.01	14.7	15.13	2.13	S S99-148, 2MASS J05385119-6906411
656	C+U	05 38 51.21	-69 05 59.28	0.79	11.5	14.24	0.06	S Mk 06, P93-1563, S99-061
657	A	05 38 51.31	-69 04 08.48	2.07	30.1	15.45	0.44	P P93-1573, 2MASS J05385131-6904084
658	H	05 38 51.70	-69 15 41.36	9.68	140.7	16.17	0.68	W 2MASS J05385171-6915412
659	E	05 38 51.77	-69 06 01.16	0.84	12.2	15.96	0.04	S P93-1584, S99-229
660	E	05 38 51.82	-69 05 46.86	0.88	12.8	15.92	0.03	S P93-1586, S99-224
661	E	05 38 52.05	-69 05 33.84	0.99	14.4	15.13	0.08	S P93-1594, S99-125
662	B	05 38 52.55	-69 02 20.30	3.82	55.5	16.12	0.08	W
663	F	05 38 52.71	-69 10 14.80	4.30	62.5	16.52	0.23	W
664	H	05 38 52.73	-69 06 43.25	1.14	16.6	14.25	0.14	S Mk 04, P93-1607, S99-065, 2MASS J05385272-6906431
665	B	05 38 52.74	-69 07 28.71	1.70	24.8	16.43	0.11	W P93-1604
666	B	05 38 52.79	-69 01 38.05	4.51	65.6	16.42	-0.08	W P93-9036
667	A	05 38 52.84	-69 06 12.06	0.94	13.7	15.03	0.07	S Some cross-contamination; P93-1614, S99-118
668	H	05 38 52.86	-69 07 36.01	1.81	26.3	16.60	0.10	W P93-1611
669	A	05 38 52.97	-69 07 45.33	1.95	28.4	14.18	0.27	P P93-1619, 2MASS J05385298-6907452
670	E	05 38 53.05	-69 08 24.82	2.55	37.1	16.02	0.15	W P93-1621
671	D	05 38 53.21	-69 02 40.89	3.50	50.9	16.43	-0.11	W
672	C	05 38 54.09	-69 08 07.66	2.33	33.8	14.59	0.23	W P93-1661, 2MASS J05385410-6908076

continued on next page

**Table 5.** *continued*

Star [VFTS]	Field	$\alpha$ (2000)	$\delta$ (2000)	$r_d$ [']	$V$	$B - V$	Ref.	Aliases (& comments)
				[pc]				
673	G	05 38 54.12	-69 06 53.00	1.34	19.5	16.98	0.03	W P93-1664
674	D	05 38 54.36	-69 11 10.17	5.23	76.1	15.97	0.50	W 2MASS J05385436-6911101
675	F	05 38 54.43	-69 08 00.46	2.23	32.5	14.48	0.28	W P93-1674, 2MASS J05385443-6908003
676	D	05 38 54.62	-69 04 54.79	1.57	22.9	16.52	0.07	W P93-1686
677	B	05 38 54.73	-69 03 48.85	2.49	36.2	16.68	0.40	P P93-1696
678	B	05 38 54.82	-69 07 50.24	2.10	30.6	16.95	0.41	W P93-1689
679	A	05 38 54.85	-69 03 50.22	2.47	36.0	16.73	0.25	P P93-1698
680	D	05 38 55.10	-69 03 31.90	2.76	40.1	16.62	0.61	W P93-1712, 2MASS J05385508-6903319
681	F	05 38 55.22	-69 05 56.70	1.15	16.7	16.55	0.06	W P93-1714
682	B	05 38 55.51	-69 04 26.72	1.98	28.9	16.08	0.58	W P93-1732, 2MASS J05385552-6904267
683	G	05 38 55.54	-68 58 56.09	7.21	104.9	16.33	-0.10	W
684	B	05 38 55.55	-69 08 28.28	2.69	39.2	16.91	0.13	W P93-1722
685	B	05 38 55.56	-69 09 37.80	3.77	54.8	16.64	0.21	W
686	B	05 38 55.63	-69 07 23.77	1.79	26.1	14.99	0.17	W P93-1729, 2MASS J05385562-6907237
687	F	05 38 55.83	-69 08 22.38	2.62	38.0	14.29	0.28	P P93-1737, 2MASS J05385584-6908223
688	G	05 38 56.05	-69 05 54.09	1.23	17.8	15.60	0.11	W P93-1756
689	A	05 38 56.38	-69 08 22.62	2.64	38.4	16.51	0.08	P Some cross-contamination; P93-1763
690	D	05 38 56.62	-69 07 19.65	1.80	26.2	16.46	0.09	W P93-1772
691	D	05 38 56.80	-69 08 41.00	2.93	42.6	14.88	0.32	W P93-1775
692	A	05 38 56.92	-69 06 39.00	1.43	20.8	16.17	0.05	P Some cross-contamination; P93-1786
693	C	05 38 57.02	-69 00 57.16	5.26	76.5	16.61	1.32	W P93-9039, 2MASS J05385705-6900571
694	G	05 38 57.04	-68 58 06.70	8.04	117.0	16.87	1.75	W
695	A	05 38 57.07	-69 06 05.70	1.31	19.1	12.04	-0.01	P HDE 269928, R145, Sk-69° 248, Brey 90, P93-1788, BAT99-119, 2MASS J05385706-6906055
696	A	05 38 57.17	-68 56 53.20	9.26	134.6	12.73	-0.02	C Sk-68° 140, 2MASS J05385718-6856530
697	A	05 38 57.28	-69 03 41.68	2.70	39.3	16.55	0.18	W P93-1799
698	B	05 38 57.31	-69 07 09.70	1.73	25.2	13.68	0.44	P Mk 02, P93-1797, 2MASS J05385731-6907096
699	B	05 38 57.48	-69 03 48.43	2.61	38.0	16.19	-0.05	W P93-1805
700	F	05 38 57.85	-68 59 16.74	6.91	100.5	16.77	1.68	W 2MASS J05385786-6859167
701	A	05 38 58.17	-69 04 58.09	1.77	25.8	16.60	0.26	P P93-1820
702	C	05 38 58.38	-69 04 35.12	2.04	29.7	16.31	0.33	W P93-1829
703	H	05 38 58.56	-69 07 52.49	2.33	33.8	16.91	0.30	W P93-1828
704	D	05 38 58.70	-69 02 44.74	3.61	52.5	16.76	-0.07	C
705	C	05 38 58.71	-69 06 47.10	1.63	23.7	16.43	0.07	W P93-1834
706	B	05 38 58.76	-69 05 23.93	1.60	23.2	15.77	0.14	W P93-1838
707	D	05 38 58.90	-69 06 42.15	1.61	23.4	15.59	0.07	W P93-1840
708	B	05 38 59.00	-69 02 44.49	3.62	52.7	16.80	1.42	C
709	F	05 38 59.01	-69 00 20.41	5.90	85.8	16.58	-0.07	W P93-9041
710	C	05 38 59.13	-69 06 24.30	1.53	22.3	16.14	-0.02	W P93-1849
711	E	05 38 59.28	-69 08 12.27	2.63	38.3	16.48	0.31	W P93-1850
712	E	05 38 59.44	-69 05 49.64	1.54	22.3	16.13	0.21	W P93-1859
713	A	05 38 59.90	-69 08 14.69	2.69	39.2	16.68	0.25	W P93-1868
714	B	05 38 59.93	-69 05 41.92	1.60	23.3	15.57	0.33	W P93-1875
715	C	05 39 00.01	-69 01 39.76	4.66	67.8	16.64	-0.10	W P93-9043
716	C	05 39 00.38	-69 03 30.50	3.00	43.7	15.91	0.06	W P93-1890
717	E	05 39 00.75	-69 07 12.89	2.01	29.2	15.69	0.19	W P93-1892
718	I	05 39 00.89	-68 57 29.65	8.71	126.7	15.99	-0.06	W
719	B	05 39 00.91	-69 06 29.16	1.71	24.9	17.00	0.08	W P93-1898
720	F	05 39 01.05	-68 59 05.78	7.15	104.0	16.74	-0.06	W
721	G	05 39 02.18	-69 14 29.38	8.62	125.4	15.75	1.03	W 2MASS J05390219-6914292
722	G	05 39 02.78	-68 57 07.82	9.10	132.4	15.04	-0.13	W
723	A	05 39 02.85	-69 05 26.35	1.92	28.0	16.19	0.16	W P93-1955
724	I	05 39 02.95	-69 15 00.08	9.14	132.9	16.80	0.43	W
725	A	05 39 03.22	-69 08 18.23	2.92	42.5	15.84	0.11	W P93-1961

continued on next page

**Table 5.** *continued*

Star [VFTS]	Field	$\alpha$ (2000)	$\delta$ (2000)	$r_d$ [']	$V$	$B - V$	Ref.	Aliases (& comments)
				[pc]				
726	B	05 39 03.30	-69 09 31.92	3.95	57.5	16.40	0.03	W
727	E	05 39 03.32	-69 10 39.68	4.98	72.4	16.74	0.18	W
728	A	05 39 03.42	-69 06 34.63	1.95	28.3	15.61	0.07	W
729	A	05 39 03.60	-69 07 16.82	2.26	32.8	14.97	0.25	W
730	E	05 39 03.61	-69 00 18.98	6.04	87.8	15.41	-0.10	W
731	B	05 39 03.75	-69 03 46.51	2.97	43.1	16.34	0.34	W
732	C	05 39 04.76	-69 04 09.80	2.74	39.9	13.03	0.19	P
733	B	05 39 04.86	-69 05 40.41	2.04	29.7	14.28	0.12	P
734	A	05 39 04.92	-69 05 35.33	2.06	30.0	16.31	0.15	W
735	I	05 39 05.02	-69 13 29.72	7.72	112.2	16.30	0.43	C
736	A	05 39 05.29	-69 04 16.06	2.71	39.4	15.85	0.05	W
737	A	05 39 05.38	-69 04 31.09	2.56	37.2	15.70	0.13	W
738	I	05 39 05.41	-68 57 37.29	8.67	126.1	14.55	0.02	W
739	A	05 39 05.94	-69 16 26.80	10.61	154.3	12.26	0.31	Z
740	I	05 39 06.02	-69 15 41.69	9.87	143.6	16.50	0.35	W
741	D	05 39 06.03	-69 09 58.45	4.46	64.8	16.97	0.29	W
742	I	05 39 06.41	-68 56 58.70	9.32	135.5	16.93	-0.02	W
743	E	05 39 06.91	-69 00 16.42	6.17	89.8	15.04	-0.17	C
744	C	05 39 07.13	-69 01 52.77	4.72	68.6	15.63	1.71	W
745	B	05 39 07.31	-69 02 36.45	4.10	59.6	16.59	0.28	W
746	A	05 39 07.33	-69 07 45.90	2.81	40.9	15.38	0.12	W
747	B	05 39 07.62	-69 06 24.96	2.28	33.2	15.28	0.12	W
748	A	05 39 07.94	-69 06 02.63	2.28	33.1	16.78	0.16	W
749	E	05 39 08.16	-69 05 55.90	2.30	33.5	16.76	0.13	W
750	D	05 39 08.35	-69 00 57.46	5.59	81.3	15.43	-0.11	W
751	D	05 39 08.98	-69 01 29.18	5.14	74.8	16.32	0.15	W
752	G	05 39 09.12	-68 57 47.26	8.60	125.1	16.48	-0.12	W
753	E	05 39 09.14	-69 12 10.37	6.57	95.6	16.46	0.42	W
754	C	05 39 10.06	-69 06 21.45	2.49	36.2	16.55	0.26	W
755	A	05 39 10.91	-69 06 13.67	2.55	37.1	15.04	0.14	W
756	H	05 39 10.94	-68 56 46.75	9.61	139.8	14.59	0.06	W
757	B	05 39 11.13	-69 02 59.02	4.00	58.1	16.78	0.26	W
758	A	05 39 11.32	-69 02 01.62	4.78	69.5	13.02	0.00	C
759	G	05 39 12.38	-68 58 44.91	7.77	113.1	16.76	1.54	W
760	E	05 39 12.50	-69 02 09.56	4.73	68.7	14.12	0.49	C
761	I	05 39 12.72	-68 58 47.33	7.75	112.7	15.35	-0.13	W
762	B	05 39 13.28	-69 09 27.47	4.38	63.8	16.46	0.22	W
763	B	05 39 13.44	-69 09 10.58	4.18	60.8	16.03	0.87	W
764	A	05 39 14.53	-69 16 42.50	11.04	160.5	12.26	0.09	Z
765	B	05 39 14.63	-69 05 03.55	3.04	44.2	16.47	1.70	W
766	F	05 39 15.19	-68 58 51.50	7.76	112.9	15.34	-0.07	W
767	H	05 39 15.26	-68 59 54.01	6.81	99.1	16.79	1.43	W
768	D	05 39 16.22	-69 01 20.28	5.59	81.4	16.10	0.20	W
769	B	05 39 16.71	-69 07 03.00	3.22	46.8	15.83	0.08	P
770	D	05 39 16.75	-69 03 27.59	4.01	58.3	15.79	0.08	W
771	B	05 39 17.39	-69 06 09.85	3.12	45.4	15.66	0.16	W
772	G	05 39 17.80	-68 57 33.69	9.06	131.7	16.89	-0.01	W
773	B	05 39 18.07	-69 05 16.54	3.27	47.6	16.69	1.46	P
774	C	05 39 18.69	-69 07 47.14	3.67	53.4	16.89	0.49	W
775	G	05 39 18.88	-69 14 19.46	8.89	129.3	16.85	0.29	W
776	F	05 39 19.52	-68 59 20.86	7.47	108.7	—	—	2MASS J05391953–6859208
777	D	05 39 19.88	-69 01 12.78	5.88	85.5	15.30	0.38	W
778	D	05 39 20.77	-69 02 11.81	5.15	74.9	16.64	0.14	C

continued on next page

**Table 5.** *continued*

Star [VFTS]	Field	$\alpha$ (2000)	$\delta$ (2000)	$r_d$ [']	$V$	$B - V$	Ref.	Aliases (& comments)
				[pc]				
779	C	05 39 21.53	-69 03 18.36	4.44	64.6	15.46	0.19	W 2MASS J05392153-6903184
780	I	05 39 21.66	-68 57 01.58	9.68	140.8	16.73	-0.11	W
781	H	05 39 22.44	-69 15 18.43	9.92	144.3	15.66	0.32	W 2MASS J05392246-6915185
782	E	05 39 23.81	-69 10 54.48	6.10	88.8	15.47	0.36	W 2MASS J05392379-6910544
783	G	05 39 23.94	-69 13 56.36	8.72	126.8	16.68	1.76	W 2MASS J05392396-6913563
784	F	05 39 24.22	-69 06 11.72	3.73	54.3	16.83	0.19	W P93-2151
785	G	05 39 24.46	-68 59 58.60	7.14	103.8	16.88	1.86	W 2MASS J05392447-6859585
786	G	05 39 24.72	-69 12 39.54	7.61	110.7	16.53	0.27	W 2MASS J05392472-6912394
787	E	05 39 24.79	-69 05 51.53	3.79	55.1	16.53	0.15	W P93-2157
788	D	05 39 25.10	-69 01 30.72	5.92	86.2	16.15	0.09	W
789	F	05 39 25.67	-69 12 45.44	7.74	112.6	16.88	0.21	W
790	B	05 39 25.95	-69 06 29.08	3.91	56.9	16.64	0.77	W P93-2168, 2MASS J05392595-6906291
791	C	05 39 26.35	-69 05 23.57	3.97	57.8	16.36	1.52	W P93-2170, 2MASS J05392634-6905235
792	H	05 39 28.08	-68 56 58.89	9.94	144.6	15.96	-0.06	W
793	I	05 39 28.18	-69 05 50.49	4.09	59.5	13.58	1.19	P P93-2186, 2MASS J05392816-6905504
794	G	05 39 29.15	-68 58 05.03	8.99	130.8	15.80	0.04	W
795	F	05 39 29.46	-69 09 22.86	5.36	78.0	16.35	0.41	W
796	G	05 39 30.09	-68 58 57.71	8.27	120.2	16.89	0.00	W
797	H	05 39 30.65	-69 09 26.32	5.48	79.7	14.68	0.05	W 2MASS J05393061-6909262
798	I	05 39 30.88	-69 13 17.69	8.44	122.7	16.71	0.44	W
799	C	05 39 31.13	-69 04 36.80	4.58	66.6	16.86	0.10	P P93-2210
800	A	05 39 31.45	-69 12 11.41	7.54	109.7	15.89	0.24	C
801	F	05 39 31.65	-68 59 47.39	7.65	111.2	15.94	-0.07	W
802	F	05 39 32.57	-69 00 02.47	7.49	109.0	14.14	-0.19	C BI 258, 2MASS J05393258-6900024
803	C	05 39 33.63	-69 08 55.03	5.40	78.5	16.63	1.58	W 2MASS J05393363-6908549
804	E	05 39 33.76	-69 01 01.96	6.79	98.8	17.03	0.05	W
805	I	05 39 34.42	-69 00 19.31	7.37	107.2	16.47	1.65	C 2MASS J05393443-6900193
806	H	05 39 34.87	-68 59 48.60	7.80	113.4	14.06	-0.17	C BI 259, 2MASS J05393489-6859486
807	I	05 39 35.14	-69 10 30.73	6.49	94.3	16.37	0.56	W
808	C	05 39 35.22	-69 04 00.55	5.13	74.7	16.80	1.35	W P93-2238, 2MASS J05393522-6904004
809	E	05 39 35.77	-69 03 06.77	5.59	81.3	16.76	1.38	W 2MASS J05393576-6903067
810	D	05 39 35.81	-69 07 08.11	4.89	71.1	16.36	0.07	W P93-2242
811	G	05 39 35.85	-68 59 02.76	8.47	123.2	16.56	-0.08	W
812	D	05 39 36.12	-69 04 59.08	4.91	71.4	14.81	0.05	W P93-2246, 2MASS J05393611-6904591
813	H	05 39 36.20	-68 57 29.60	9.81	142.7	16.54	-0.06	W
814	G	05 39 36.40	-69 01 07.79	6.88	100.1	16.81	0.05	W Some cross-contamination
815	A	05 39 36.49	-69 12 00.32	7.67	111.5	16.68	0.19	W
816	E	05 39 36.53	-69 08 48.91	5.56	80.9	16.35	1.55	W 2MASS J05393653-6908488
817	E	05 39 37.21	-69 04 04.39	5.27	76.7	15.53	0.17	W P93-2252
818	E	05 39 37.79	-69 05 00.97	5.05	73.4	16.60	1.94	W P93-2257, 2MASS J05393779-6905009
819	G	05 39 37.83	-69 13 32.99	8.98	130.7	16.79	0.40	W
820	C	05 39 37.92	-69 11 46.09	7.57	110.0	12.73	0.55	C 2MASS J05393793-6911462
821	I	05 39 38.43	-68 58 36.04	8.97	130.5	16.03	-0.14	W
822	E	05 39 38.49	-69 09 00.50	5.81	84.5	15.60	0.37	W 2MASS J05393847-6909004
823	E	05 39 39.06	-69 11 51.61	7.70	112.0	16.06	0.17	C
824	D	05 39 39.17	-69 11 55.29	7.75	112.8	16.36	0.36	C
825	A	05 39 39.21	-69 11 41.72	7.59	110.4	16.20	0.33	W
826	H	05 39 39.25	-69 11 45.95	7.64	111.2	14.85	0.17	C
827	I	05 39 39.27	-69 11 44.20	7.62	110.9	15.34	0.31	W
828	B	05 39 39.41	-69 11 52.05	7.73	112.4	14.52	2.20	W
829	G	05 39 39.64	-69 12 01.33	7.86	114.3	15.13	0.41	W
830	D	05 39 39.74	-69 04 30.29	5.34	77.7	15.39	-0.03	W P93-2270
831	F	05 39 39.87	-69 12 04.34	7.91	115.0	13.04	0.29	C

continued on next page

**Table 5.** *continued*

Star [VFTS]	Field	$\alpha$ (2000)	$\delta$ (2000)	$r_d$ [']	$V$	$B - V$	Ref.	Aliases (& comments)
				[pc]				
832	A	05 39 39.96	-69 11 55.54	7.80	113.5	16.50	0.37	W
833	F	05 39 40.15	-69 09 02.23	5.96	86.6	16.96	0.22	W
834	C	05 39 40.32	-69 11 43.84	7.68	111.7	15.19	0.33	W
835	G	05 39 40.84	-69 11 52.41	7.82	113.7	—	—	—
836	F	05 39 40.94	-69 11 53.62	7.84	114.0	15.71	0.18	C
837	I	05 39 41.25	-68 59 37.94	8.29	120.6	16.07	-0.09	W
838	F	05 39 41.76	-69 09 32.44	6.34	92.3	15.81	0.28	W
839	A	05 39 41.78	-69 11 31.01	7.61	110.7	14.64	2.16	W 2MASS J05394177-6911309
840	D	05 39 42.17	-69 11 48.87	7.85	114.2	16.74	0.24	W
841	I	05 39 42.24	-69 13 28.43	9.14	133.0	15.83	0.89	W 2MASS J05394225-6913284
842	B	05 39 42.69	-69 11 51.39	7.92	115.1	16.29	0.33	W 2MASS J05394267-6911512
843	G	05 39 43.37	-69 01 22.34	7.17	104.3	15.88	-0.05	W
844	F	05 39 43.63	-69 10 39.68	7.15	104.0	16.41	1.59	W 2MASS J05394362-6910396
845	C	05 39 43.79	-69 05 49.67	5.48	79.7	15.30	0.15	W P93-2305, 2MASS J05394378-6905496
846	I	05 39 44.62	-69 14 19.46	9.96	144.9	16.78	0.11	W
847	E	05 39 45.58	-69 04 26.23	5.86	85.2	15.48	-0.06	W P93-2313
848	A	05 39 45.67	-69 12 08.26	8.30	120.8	15.54	0.25	W 2MASS J05394565-6912082
849	I	05 39 47.36	-68 59 21.99	8.84	128.6	15.14	-0.08	W
850	I	05 39 51.16	-69 11 53.59	8.47	123.2	16.15	0.18	W
851	F	05 39 51.52	-69 02 22.63	7.18	104.4	15.83	-0.09	W
852	F	05 39 52.39	-69 09 41.26	7.23	105.1	14.30	1.41	C 2MASS J05395239-6909412
853	E	05 39 52.51	-69 07 38.68	6.45	93.9	16.78	0.33	W
854	I	05 39 52.64	-69 00 19.83	8.48	123.4	16.28	0.10	W
855	I	05 39 53.55	-69 11 31.07	8.38	121.9	15.34	0.27	W 2MASS J05395353-6911311
856	I	05 39 53.67	-69 10 34.68	7.81	113.5	16.47	0.72	W 2MASS J05395367-6910347
857	I	05 39 53.73	-69 11 02.26	8.09	117.6	16.26	0.17	W
858	G	05 39 53.80	-69 03 01.82	7.05	102.5	14.72	0.37	W Some cross-contamination; 2MASS J05395380-6903018
859	F	05 39 54.59	-69 06 40.15	6.47	94.1	15.66	0.03	W
860	H	05 39 55.12	-69 11 22.14	8.39	122.0	16.67	0.13	W
861	G	05 39 55.42	-69 02 26.67	7.44	108.3	16.23	1.41	W 2MASS J05395542-6902266
862	I	05 39 56.08	-69 12 05.04	8.92	129.8	16.64	0.79	W 2MASS J05395607-6912050
863	E	05 39 56.62	-69 07 42.88	6.83	99.3	15.29	0.52	W 2MASS J05395662-6907429
864	H	05 39 56.81	-69 01 23.06	8.11	118.0	16.64	-0.05	W
865	I	05 39 58.19	-69 00 20.71	8.84	128.6	16.69	1.32	W 2MASS J05395820-6900206
866	I	05 40 00.41	-69 01 16.27	8.44	122.8	16.24	-0.12	W
867	I	05 40 01.34	-69 07 59.55	7.30	106.2	14.63	0.13	W BI 261, 2MASS J05400134-6907595
868	I	05 40 04.29	-69 11 02.94	8.85	128.7	16.65	0.27	W
869	G	05 40 05.54	-69 02 44.99	8.12	118.0	16.76	0.05	W
870	I	05 40 06.32	-69 00 01.13	9.61	139.8	15.32	0.55	W 2MASS J05400633-6900010
871	H	05 40 07.33	-69 10 42.70	8.90	129.4	15.82	0.67	W 2MASS J05400733-6910427
872	I	05 40 07.62	-69 03 23.99	8.05	117.1	16.09	-0.07	W
873	F	05 40 07.66	-69 06 43.97	7.64	111.1	15.07	0.21	W 2MASS J05400767-6906439
874	I	05 40 10.33	-69 03 04.95	8.38	122.0	15.37	0.02	W
875	I	05 40 11.76	-69 00 37.85	9.64	140.2	16.46	-0.02	W
876	H	05 40 12.48	-69 03 58.13	8.30	120.7	16.30	0.00	W
877	H	05 40 12.81	-69 09 10.30	8.65	125.8	16.36	0.18	W
878	G	05 40 12.85	-69 08 13.53	8.36	121.5	16.39	1.37	W 2MASS J05401285-6908135
879	H	05 40 13.69	-69 05 09.79	8.19	119.1	16.73	0.11	W
880	H	05 40 14.75	-69 01 04.43	9.62	140.0	16.66	0.06	C
881	H	05 40 17.25	-69 06 27.10	8.47	123.2	15.66	-0.06	W
882	I	05 40 17.96	-69 04 17.00	8.70	126.6	15.96	-0.10	W
883	I	05 40 18.03	-69 08 36.06	8.90	129.5	16.49	0.13	W
884	H	05 40 19.96	-69 01 23.88	9.87	143.5	16.37	1.71	C 2MASS J05401997-6901238

continued on next page

**Table 5.** *continued*

Star [VFTS]	Field	$\alpha$ (2000)	$\delta$ (2000)	$r_d$ [']	$V$	$B - V$	Ref.	Aliases (& comments)
				[pc]				
885	I	05 40 20.28	-69 03 11.99	9.18	133.6	15.90	0.01	W
886	H	05 40 21.19	-69 03 29.59	9.17	133.4	16.82	-0.04	W
887	H	05 40 21.54	-69 04 23.70	9.00	130.8	14.96	-0.06	W
888	H	05 40 22.62	-69 04 06.07	9.15	133.1	16.18	-0.07	W
889	I	05 40 23.67	-69 05 14.35	9.07	131.9	16.56	0.37	W
890	I	05 40 24.86	-69 09 44.14	9.85	143.3	16.13	0.02	W
891	H	05 40 25.73	-69 06 30.78	9.23	134.2	16.48	0.07	W
892	I	05 40 25.99	-69 07 58.18	9.44	137.3	15.69	0.05	W
893	I	05 40 33.31	-69 05 37.53	9.90	144.0	15.82	0.62	W 2MASS J05403332-6905375
1001	A2	05 38 40.555	-69 05 57.12	0.19	2.8	12.75	0.09	S R134, S99-013
1002	A2	05 38 40.646	-69 06 05.73	0.16	2.4	16.40	0.14	S S99-312
1003	A2	05 38 40.779	-69 06 03.37	0.14	2.1	16.10	0.23	S S99-283
1004	A2	05 38 40.848	-69 06 04.51	0.14	2.0	15.38	0.39	S S99-193
1005	A2	05 38 40.977	-69 06 08.33	0.16	2.3	16.48	0.12	S S99-330
1006	A4	05 38 41.066	-69 06 15.16	0.24	3.4	16.11	1.06	S S99-257
1007	A2	05 38 41.077	-69 06 01.74	0.12	1.7	14.68	0.17	S S99-095
1008	A2	05 38 41.108	-69 05 58.33	0.14	2.0	14.63	1.15	S S99-163
1009	A2	05 38 41.163	-69 06 02.83	0.11	1.6	15.44	0.04	S S99-165
1010	A4	05 38 41.268	-69 06 16.94	0.25	3.7	15.53	0.21	S S99-189
1011	A4	05 38 41.355	-69 06 13.96	0.21	3.0	15.35	0.35	S S99-177
1012	A2	05 38 41.386	-69 06 02.49	0.09	1.3	16.06	0.14	S S99-249
1013	A4	05 38 41.417	-69 06 09.34	0.14	2.0	16.36	0.32	S S99-339
1014	A2	05 38 41.515	-69 06 00.83	0.09	1.2	13.67	0.61	S S99-056
1015	A2	05 38 41.650	-69 06 03.17	0.07	1.0	15.38	0.42	S S99-187
1016	A4	05 38 41.766	-69 06 18.98	0.27	4.0	15.30	0.20	S S99-154; S99-305 (= VFTS 510) is in adj. spaxel
1017	A4	05 38 41.874	-69 06 14.29	0.20	2.8	14.50	0.27	S S99-088
1018	A4	05 38 41.887	-69 06 12.45	0.17	2.4	14.34	0.28	S S99-077
1019	A1	05 38 42.016	-69 06 07.51	0.08	1.2	14.34	0.22	S S99-070
1020	A4	05 38 42.023	-69 06 16.75	0.23	3.4	15.51	0.15	S S99-178
1021	A4	05 38 42.068	-69 06 14.19	0.19	2.8	13.31	0.21	S S99-025
1022	A3+4	05 38 42.407	-69 06 15.01	0.20	2.9	13.44	0.25	S Mk 37, S99-028
1023	A3	05 38 42.631	-69 06 10.91	0.14	2.0	15.26	0.15	S S99-142
1024	A1	05 38 42.685	-69 06 07.03	0.07	1.1	15.20	0.30	S S99-147
1025	A1	05 38 42.935	-69 06 04.98	0.06	0.9	<i>Blend of S99-027 &amp; 063</i>		
1026	A3	05 38 43.083	-69 06 11.26	0.15	2.2	<i>Blend of S99-076 &amp; 191</i>		
1027	A5	05 38 43.210	-69 05 42.46	0.35	5.1	14.74	0.00	S S99-085
1028	A3	05 38 43.274	-69 06 16.45	0.24	3.5	13.82	0.04	S Mk 35S, S99-037
1029	A5	05 38 43.351	-69 05 47.47	0.27	3.9	14.68	0.03	S S99-087
1030	A5	05 38 43.427	-69 05 41.95	0.36	5.3	16.45	0.10	S S99-335
1031	A5	05 38 43.695	-69 05 47.81	0.28	4.0	13.89	0.00	S S99-039
1032	A5	05 38 44.076	-69 05 44.77	0.34	4.9	14.67	0.29	S S99-078
1033	A5	05 38 44.175	-69 05 42.07	0.38	5.6	14.53	0.32	S S99-074
1034	A5	05 38 44.203	-69 05 46.96	0.31	4.5	13.36	0.12	S Mk 32, S99-021
1035	A5	05 38 44.321	-69 05 45.05	0.34	5.0	15.53	0.09	S S99-169
1036	A5	05 38 44.820	-69 05 43.62	0.39	5.6	16.41	0.12	S S99-308
1037	A5	05 38 45.095	-69 05 42.81	0.41	6.0	16.51	0.14	S S99-334

**Table 6.** Near-IR photometry from the InfraRed Survey Facility (IRSF) Magellanic Clouds catalogue (Kato et al. 2007) for targets observed by the VLT-FLAMES Tarantula Survey (VFTS). IRSF photometry is not available for six Medusa targets: VFTS 151, 503, 275, 620, 823, and 828; nor for six ARGUS sources: VFTS 1012, 1014, 1015, 1019, 1024, and 1025.

Star [VFTS]	IRSF identification	<i>J</i>	$\sigma J$	<i>H</i>	$\sigma H$	<i>K<sub>s</sub></i>	$\sigma K_s$	qflag
001	05365338–6908183	16.92	0.03	16.71	0.07	16.68	0.13	122
002	05365466–6911383	13.23	0.04	—	—	—	—	500
003	05365519–6911376	11.39	0.02	11.26	0.01	11.21	0.02	115
004	05365845–6906472	16.57	0.02	16.54	0.02	16.58	0.09	111
005	05370174–6908162	16.29	0.02	16.29	0.02	16.25	0.07	111
006	05370250–6906436	13.38	0.01	12.54	0.01	12.28	0.01	111
007	05370294–6902041	16.93	0.03	16.96	0.05	16.98	0.13	114
008	05370310–6908225	16.77	0.02	16.73	0.03	16.75	0.10	111
009	05370427–6908056	15.93	0.02	16.11	0.04	15.79	0.06	111
010	05370471–6908566	16.92	0.02	16.90	0.03	16.94	0.12	114
011	05370495–6904586	13.72	0.01	13.03	0.01	12.88	0.01	111
012	05370564–6909123	15.53	0.01	15.46	0.01	15.45	0.03	111
013	05370629–6904413	16.33	0.02	16.31	0.02	16.33	0.08	111
014	05370750–6905068	15.16	0.02	15.15	0.01	15.16	0.03	111
015	05370855–6905100	16.19	0.01	16.18	0.02	16.24	0.07	111
016	05370888–6907203	13.39	0.01	13.37	0.01	13.35	0.01	111
017	05371142–6905042	15.03	0.02	15.03	0.01	15.05	0.03	111
018	05371146–6910309	16.24	0.02	16.19	0.02	16.12	0.05	111
019	05371148–6907381	15.47	0.01	15.22	0.01	14.97	0.02	111
020	05371409–6904028	16.75	0.02	16.78	0.03	16.76	0.10	111
021	05371437–6906325	15.41	0.01	15.38	0.01	15.36	0.03	111
022	05371502–6908430	14.47	0.04	14.30	0.04	13.81	0.05	255
023	05371608–6908529	11.78	0.02	10.84	0.02	—	—	553
024	05371668–6908504	15.02	0.02	14.80	0.02	14.66	0.02	111
025	05371696–6907545	16.10	0.02	16.06	0.02	16.01	0.05	111
026	05371705–6906599	13.82	0.02	13.04	0.01	12.82	0.01	111
027	05371736–6907481	14.59	0.02	14.55	0.01	14.55	0.02	111
028	05371786–6909462	12.58	0.02	12.41	0.01	12.26	0.01	511
029	05371829–6903046	17.02	0.03	17.02	0.05	17.29	0.19	114
030	05371879–6902131	15.82	0.02	15.57	0.02	15.37	0.04	111
031	05372047–6859522	16.57	0.02	16.57	0.03	16.57	0.11	111
032	05372050–6901378	14.27	0.02	13.51	0.01	13.36	0.02	111
033	05372204–6907552	16.09	0.02	16.10	0.02	16.06	0.05	111
034	05372231–6907161	15.94	0.02	15.87	0.02	15.79	0.04	111
035	05372276–6912098	16.48	0.02	16.36	0.03	16.33	0.06	111
036	05372361–6904298	16.36	0.02	16.35	0.03	16.29	0.07	111
037	05372394–6912212	15.98	0.02	15.96	0.02	15.93	0.05	111
038	05372433–6907172	16.44	0.02	16.41	0.03	16.43	0.08	111
039	05372465–6909529	12.57	0.02	12.15	0.01	11.63	0.01	511
040	05372474–6908277	16.67	0.02	16.69	0.03	16.67	0.09	111
041	05372487–6904158	16.61	0.02	16.56	0.03	16.61	0.13	111
042	05372512–6907426	14.75	0.02	14.77	0.01	14.82	0.02	111
043	05372584–6907285	16.34	0.03	16.48	0.04	16.41	0.09	111
044	05372606–6907294	16.51	0.02	16.48	0.03	16.53	0.09	111
045	05372618–6908566	14.40	0.02	14.24	0.01	14.15	0.01	111
046	05372618–6909530	14.26	0.02	14.19	0.01	14.16	0.02	111
047	05372654–6910406	15.56	0.02	15.32	0.02	15.17	0.03	111
048	05372655–6907018	16.40	0.02	16.34	0.02	16.40	0.07	111
049	05372690–6903442	15.76	0.02	15.71	0.02	15.62	0.04	111
050	05372742–6910401	16.30	0.04	16.24	0.05	16.25	0.09	111
051	05372783–6908029	14.39	0.02	14.09	0.01	13.70	0.01	111
052	05372886–6907065	14.49	0.02	14.48	0.01	14.45	0.02	111
053	05372892–6906529	15.26	0.05	15.06	0.02	15.03	0.03	111
054	05372907–6913039	16.09	0.02	15.98	0.02	15.98	0.05	111
055	05372906–6903446	14.86	0.02	14.74	0.02	14.62	0.02	111
056	05372911–6908414	15.05	0.02	14.87	0.02	14.72	0.02	111
057	05372985–6911110	14.01	0.02	13.23	0.01	13.05	0.01	111
058	05373010–6909509	15.17	0.02	15.13	0.02	15.11	0.02	111
059	05373040–6910005	15.90	0.02	15.81	0.02	15.79	0.04	111
060	05373062–6909129	14.56	0.02	14.29	0.01	14.11	0.01	111
061	05373074–6905175	14.88	0.02	14.80	0.02	14.78	0.02	111
062	05373081–6903219	15.89	0.02	15.79	0.02	15.75	0.05	111
063	05373088–6911485	13.90	0.02	13.83	0.01	13.82	0.02	111
064	05373092–6911070	13.49	0.02	13.29	0.01	13.19	0.02	111
065	05373262–6906407	15.86	0.02	15.85	0.02	15.76	0.04	111
066	05373309–6904347	15.20	0.02	15.14	0.02	15.09	0.02	111
067	05373334–6902476	16.43	0.02	16.33	0.03	16.32	0.07	111
068	05373351–6907141	12.43	0.02	11.66	0.01	11.37	0.01	111
069	05373376–6908132	12.82	0.02	12.67	0.01	12.56	0.01	111

continued on next page

**Table 6.** *continued*

Star [VFTS]	IRSF identification	<i>J</i>	$\sigma J$	<i>H</i>	$\sigma H$	<i>K<sub>s</sub></i>	$\sigma K_s$	qflag
070	05373389–6908583	16.20	0.02	16.08	0.02	16.02	0.05	111
071	05373421–6906393	16.67	0.02	16.72	0.03	16.73	0.11	111
072	05373446–6901102	13.81	0.02	13.78	0.01	13.81	0.01	511
073	05373446–6909094	15.25	0.02	15.10	0.02	15.00	0.02	111
074	05373454–6910102	16.06	0.02	16.02	0.02	15.92	0.04	111
075	05373468–6907133	16.97	0.03	16.91	0.04	16.75	0.10	111
076	05373480–6908013	14.72	0.02	14.60	0.02	14.56	0.02	111
077	05373514–6909412	16.27	0.02	16.20	0.02	16.14	0.06	111
078	05373543–6907571	16.23	0.02	16.12	0.02	16.02	0.06	111
079	05373571–6908403	15.09	0.02	14.58	0.01	14.05	0.01	111
080	05373574–6908075	15.61	0.02	15.50	0.02	15.43	0.03	111
081	05373598–6912298	10.29	0.02	—	—	—	—	533
082	05373608–6906450	13.55	0.02	13.51	0.01	13.51	0.01	111
083	05373633–6905012	15.77	0.02	15.71	0.02	15.69	0.04	111
084	05373649–6909593	16.36	0.02	16.29	0.02	16.18	0.05	111
085	05373651–6901413	16.79	0.03	16.80	0.04	16.87	0.14	114
086	05373654–6910325	13.69	0.02	13.55	0.01	13.46	0.01	111
087	05373666–6907319	13.77	0.02	13.79	0.01	13.81	0.01	111
088	05373681–6906332	14.43	0.02	14.30	0.01	14.12	0.02	111
089	05373687–6908228	15.55	0.02	15.44	0.02	15.38	0.03	111
090	05373713–6910181	15.30	0.01	15.23	0.02	15.17	0.02	111
091	05373752–6908206	15.46	0.03	15.32	0.03	15.25	0.05	511
092	05373768–6858556	13.67	0.02	12.80	0.01	12.57	0.01	111
093	05373780–6905456	14.92	0.02	14.88	0.02	14.85	0.02	111
094	05373795–6910148	13.49	0.01	13.38	0.01	13.28	0.01	111
095	05373851–6906045	16.16	0.02	16.21	0.02	16.13	0.06	111
096	05373852–6910199	13.93	0.04	13.54	0.05	13.59	0.04	155
097	05373874–6910276	15.84	0.01	15.75	0.02	15.65	0.03	111
098	05373878–6908087	14.69	0.02	14.60	0.02	14.57	0.02	111
099	05373880–6858318	17.06	0.03	17.08	0.05	17.32	0.19	114
100	05373890–6910082	16.09	0.01	16.01	0.02	15.94	0.04	111
101	05373919–6908409	15.42	0.02	15.20	0.02	14.92	0.02	111
102	05373922–6909510	14.59	0.02	14.33	0.01	13.95	0.02	111
103	05373924–6911344	14.84	0.01	14.58	0.01	14.41	0.02	111
104	05373989–6905468	16.28	0.02	16.30	0.03	16.31	0.07	111
105	05374016–6910461	14.74	0.03	14.46	0.04	14.36	0.04	111
106	05374020–6904121	16.46	0.02	16.41	0.02	16.34	0.07	111
107	05374040–6905541	16.67	0.02	16.70	0.03	16.68	0.09	111
108	05374049–6907577	12.82	0.02	12.53	0.01	12.18	0.01	111
109	05374075–6908012	15.99	0.02	15.87	0.02	15.87	0.05	111
110	05374085–6910483	14.94	0.02	14.80	0.02	14.68	0.02	111
111	05374086–6900042	14.56	0.02	14.55	0.01	14.59	0.02	111
112	05374087–6904415	16.34	0.02	16.32	0.03	16.37	0.07	111
113	05374090–6908443	16.27	0.02	16.20	0.02	16.12	0.06	111
114	05374111–6910378	15.33	0.01	15.21	0.01	15.09	0.02	111
115	05374141–6906105	13.97	0.02	13.33	0.01	13.14	0.01	111
116	05374145–6909192	15.89	0.02	15.76	0.02	15.71	0.04	111
117	05374145–6910469	15.92	0.02	15.78	0.02	15.66	0.04	111
118	05374160–6908087	15.75	0.02	15.67	0.02	15.64	0.04	111
119	05374172–6907282	16.27	0.02	16.26	0.02	16.18	0.06	111
120	05374196–6908334	14.66	0.02	14.62	0.02	14.54	0.02	511
121	05374223–6907144	15.97	0.02	15.94	0.02	15.88	0.06	111
122	05374226–6909415	15.99	0.02	15.92	0.03	15.77	0.05	111
123	05374244–6912215	15.61	0.01	15.58	0.01	15.55	0.03	111
124	05374260–6909192	16.20	0.02	16.13	0.02	16.10	0.06	111
125	05374294–6910350	15.25	0.02	14.83	0.01	14.49	0.02	111
126	05374294–6901053	17.12	0.03	17.20	0.05	—	—	110
127	05374336–6910458	16.50	0.03	16.43	0.04	16.35	0.07	111
128	05374339–6909590	16.23	0.02	16.24	0.02	16.22	0.05	111
129	05374365–6910151	12.58	0.01	11.69	0.01	11.33	0.01	115
130	05374367–6910504	15.65	0.01	15.42	0.01	15.27	0.02	111
131	05374374–6910222	16.55	0.02	16.54	0.03	16.56	0.07	111
132	05374394–6909390	15.90	0.02	15.93	0.02	15.85	0.04	111
133	05374396–6906344	15.85	0.02	15.82	0.03	15.84	0.06	111
134	05374407–6905270	16.93	0.02	16.95	0.04	17.01	0.13	114
135	05374420–6906373	16.09	0.02	16.02	0.02	15.91	0.06	111
136	05374464–6914257	14.37	0.01	14.21	0.01	13.56	0.01	111
137	05374472–6909182	16.69	0.02	16.68	0.03	16.73	0.10	111
138	05374504–6902296	15.92	0.02	15.93	0.02	16.03	0.06	111
139	05374521–6858487	14.13	0.02	13.34	0.01	13.15	0.01	111
140	05374524–6910136	15.48	0.02	15.37	0.01	15.29	0.02	111
141	05374574–6909133	15.21	0.02	15.18	0.02	15.21	0.03	111
142	05374589–6910220	15.67	0.01	15.57	0.01	15.44	0.03	111

*continued on next page*

**Table 6.** *continued*

Star [VFTS]	IRSF identification	<i>J</i>	$\sigma J$	<i>H</i>	$\sigma H$	<i>K<sub>s</sub></i>	$\sigma K_s$	qflag
143	05374590-6911093	14.68	0.01	14.54	0.01	14.43	0.02	111
144	05374611-6909142	16.43	0.07	16.34	0.09	16.40	0.11	222
145	05374611-6909088	13.46	0.03	13.50	0.02	13.38	0.03	211
146	05374609-6906349	15.82	0.02	15.72	0.02	15.69	0.04	111
147	05374618-6909105	13.09	0.04	12.91	0.02	12.70	0.04	515
148	05374628-6900062	16.39	0.02	16.42	0.03	16.27	0.07	111
149	05374631-6908207	16.11	0.02	16.01	0.02	16.00	0.06	111
150	05374638-6909120	14.51	0.05	14.16	0.08	14.87	0.08	221
152	05374669-6906196	14.66	0.02	14.47	0.01	14.30	0.02	111
153	05374670-6909112	14.86	0.10	14.73	0.04	14.57	0.08	212
154	05374708-6909076	14.60	0.02	14.55	0.02	14.54	0.02	111
155	05374718-6913135	16.80	0.02	16.84	0.04	16.66	0.07	111
156	05374720-6909030	14.99	0.02	14.68	0.01	14.35	0.02	111
157	05374724-6858492	17.08	0.03	17.12	0.05	17.29	0.19	114
158	05374742-6904127	14.59	0.02	14.39	0.01	14.11	0.01	111
159	05374767-6900351	15.79	0.02	15.82	0.02	15.80	0.05	111
160	05374780-6909148	13.88	0.02	13.85	0.01	13.82	0.01	111
161	05374790-6910410	16.17	0.01	16.15	0.03	16.04	0.04	111
162	05374805-6909598	16.58	0.02	16.61	0.03	16.63	0.08	111
163	05374806-6909263	14.90	0.02	14.67	0.01	14.53	0.02	111
164	05374820-6909315	15.33	0.02	15.10	0.02	14.79	0.02	111
165	05374833-6909152	13.41	0.02	13.35	0.01	13.31	0.01	111
166	05374838-6902376	16.54	0.03	16.28	0.04	16.02	0.07	111
167	05374880-6909158	15.85	0.02	15.83	0.02	15.84	0.04	111
168	05374951-6912331	15.46	0.01	15.44	0.01	15.46	0.03	111
169	05374991-6910279	14.07	0.01	13.99	0.01	13.90	0.01	111
170	05375000-6907421	15.64	0.02	15.59	0.02	15.56	0.04	111
171	05375001-6909599	13.90	0.02	13.87	0.01	13.85	0.01	111
172	05375012-6910015	16.33	0.02	16.21	0.03	16.21	0.05	111
173	05375039-6908544	15.49	0.02	15.31	0.02	15.22	0.03	111
174	05375066-6908484	15.07	0.02	14.97	0.02	14.96	0.03	111
175	05375078-6911355	14.88	0.01	14.71	0.01	14.57	0.02	111
176	05375095-6911002	14.50	0.01	14.49	0.01	14.45	0.02	111
177	05375102-6906106	14.12	0.02	14.01	0.01	13.95	0.01	111
178	05375104-6909339	12.84	0.02	12.83	0.01	12.81	0.01	511
179	05375116-6909374	17.02	0.02	17.03	0.05	17.03	0.11	111
180	05375134-6909467	13.40	0.02	13.38	0.01	13.32	0.01	111
181	05375139-6912408	15.97	0.01	15.92	0.02	15.91	0.04	111
182	05375142-6905302	13.98	0.02	13.70	0.01	13.60	0.01	111
183	05375150-6911255	15.54	0.01	15.33	0.01	15.20	0.02	111
184	05375182-6904248	15.29	0.02	15.28	0.02	15.28	0.03	111
185	05375194-6909208	14.29	0.02	14.26	0.02	14.23	0.01	111
186	05375203-6904398	15.63	0.02	15.60	0.02	15.60	0.04	111
187	05375218-6911313	15.32	0.01	15.24	0.01	15.19	0.02	111
188	05375240-6910512	15.97	0.02	15.80	0.02	15.67	0.03	111
189	05375284-6909458	16.03	0.01	16.03	0.02	15.95	0.04	111
190	05375330-6912573	14.67	0.01	14.65	0.01	14.66	0.02	111
191	05375341-6910234	15.49	0.01	15.49	0.01	15.45	0.03	111
192	05375364-6910123	16.46	0.03	16.47	0.03	16.51	0.07	111
193	05375420-6908414	13.18	0.02	12.44	0.01	12.18	0.01	111
194	05375419-6905462	15.75	0.02	15.64	0.02	15.44	0.03	111
195	05375422-6905179	16.81	0.02	16.77	0.03	16.76	0.10	111
196	05375427-6901446	15.04	0.02	14.91	0.01	14.80	0.02	111
197	05375446-6909415	13.84	0.02	13.86	0.02	13.85	0.01	111
198	05375465-6909033	10.26	0.02	9.32	0.03	—	—	553
199	05375478-6900249	17.17	0.03	17.19	0.05	17.07	0.13	114
200	05375495-6910125	14.50	0.01	14.35	0.01	14.12	0.01	111
201	05375499-6911329	16.15	0.01	16.12	0.02	16.05	0.05	111
202	05375502-6908550	15.92	0.02	15.85	0.02	15.81	0.05	111
203	05375549-6904005	16.92	0.02	16.98	0.03	17.05	0.13	114
204	05375503-6907022	15.32	0.02	15.16	0.02	15.01	0.02	111
205	05375539-6910208	15.90	0.01	15.88	0.02	15.93	0.04	111
206	05375543-6857069	14.87	0.02	14.80	0.01	14.73	0.02	111
207	05375608-6910389	16.08	0.02	16.01	0.02	16.02	0.04	111
208	05375622-6911508	13.95	0.01	13.82	0.01	13.73	0.01	111
209	05375659-6903486	16.49	0.02	16.48	0.02	16.50	0.08	111
210	05375697-6908212	15.69	0.02	15.68	0.02	15.66	0.04	111
211	05375732-6858421	17.04	0.06	17.00	0.10	16.51	0.14	112
212	05375789-6908488	15.25	0.02	15.24	0.02	15.24	0.03	111
213	05375796-6909540	15.47	0.02	15.48	0.02	15.40	0.03	111
214	05375802-6913095	15.41	0.01	15.33	0.01	15.30	0.03	111
215	05375805-6902235	16.69	0.02	16.65	0.03	16.62	0.10	111
216	05375906-6911568	13.93	0.01	13.83	0.01	13.78	0.01	111

*continued on next page*

**Table 6.** *continued*

Star [VFTS]	IRSF identification	<i>J</i>	$\sigma J$	<i>H</i>	$\sigma H$	<i>K<sub>s</sub></i>	$\sigma K_s$	qflag
217	05375949–6909017	13.86	0.02	13.87	0.01	13.87	0.01	111
218	05375971–6911142	14.87	0.01	14.75	0.01	14.68	0.02	111
219	05375980–6903354	16.94	0.02	16.93	0.04	16.87	0.11	111
220	05380040–6908278	16.76	0.03	16.72	0.03	16.73	0.10	111
221	05380041–6903458	16.54	0.02	16.62	0.03	16.56	0.08	111
222	05380057–6909415	11.48	0.01	10.55	0.02	—	—	153
223	05380061–6908419	14.94	0.02	14.93	0.01	14.93	0.02	111
224	05380082–6903597	15.51	0.02	15.36	0.02	15.08	0.02	111
225	05380096–6857232	15.12	0.02	15.19	0.02	15.16	0.04	111
226	05380101–6914217	16.14	0.01	16.18	0.02	16.20	0.05	111
227	05380130–6903138	16.45	0.04	16.52	0.03	16.49	0.09	111
228	05380169–6901349	16.67	0.02	16.63	0.03	16.63	0.10	111
229	05380296–6902192	16.48	0.03	16.45	0.03	16.40	0.08	111
230	05380442–6907579	15.32	0.02	15.05	0.02	14.85	0.02	111
231	05380471–6908529	15.89	0.02	15.84	0.02	15.76	0.05	111
232	05380477–6909055	13.36	0.02	13.16	0.01	12.99	0.01	111
233	05380481–6911224	15.76	0.02	15.57	0.02	15.41	0.03	111
234	05380629–6906530	15.82	0.02	15.75	0.02	15.67	0.04	111
235	05380635–6905143	15.64	0.02	15.64	0.02	15.68	0.04	111
236	05380660–6903452	10.53	0.02	9.62	0.03	—	—	553
237	05380664–6914070	15.75	0.01	15.63	0.02	15.53	0.03	111
238	05380668–6903593	16.66	0.02	16.73	0.03	16.89	0.12	114
239	05380673–6909324	16.30	0.02	16.30	0.02	16.24	0.07	111
240	05380676–6906088	16.17	0.05	15.61	0.04	15.58	0.06	111
241	05380708–6904147	16.65	0.02	16.65	0.03	16.78	0.11	114
242	05380783–6900570	16.75	0.02	16.77	0.03	16.75	0.11	114
243	05380841–6909190	14.73	0.02	14.62	0.01	14.55	0.02	111
244	05380841–6905446	14.00	0.02	13.98	0.01	13.97	0.01	111
245	05380880–6903451	13.53	0.02	12.67	0.01	12.41	0.01	511
246	05380886–6910399	15.99	0.02	15.86	0.02	15.76	0.03	111
247	05380890–6908169	16.89	0.02	16.97	0.04	17.01	0.13	114
248	05380931–6910142	16.43	0.01	16.43	0.03	16.41	0.06	111
249	05380956–6906540	15.67	0.02	15.69	0.02	15.69	0.04	111
250	05381024–6908564	15.71	0.02	15.70	0.02	15.69	0.04	111
251	05381023–6905047	15.69	0.02	15.69	0.02	15.71	0.05	111
252	05381038–6902307	15.80	0.02	15.83	0.02	15.87	0.06	111
253	05381039–6914337	15.02	0.01	14.98	0.02	14.98	0.02	111
254	05381042–6905177	16.66	0.02	16.60	0.03	16.45	0.08	111
255	05381105–6907196	16.10	0.02	15.97	0.03	15.88	0.05	111
256	05381131–6904492	15.20	0.02	15.22	0.02	15.24	0.03	111
257	05381141–6914246	16.81	0.02	16.86	0.04	16.80	0.09	111
258	05381157–6911424	16.21	0.02	16.17	0.02	16.17	0.05	111
259	05381202–6906342	12.85	0.02	12.73	0.01	12.61	0.01	111
260	05381227–6913404	14.04	0.01	13.36	0.01	13.21	0.01	111
261	05381234–6900574	12.13	0.02	12.06	0.01	12.02	0.01	551
262	05381238–6913378	14.54	0.01	14.25	0.01	14.12	0.01	111
263	05381255–6903518	16.41	0.02	16.26	0.02	16.00	0.06	111
264	05381288–6901394	13.98	0.02	13.20	0.01	13.01	0.01	111
265	05381293–6905147	15.52	0.02	15.44	0.02	15.33	0.03	111
266	05381329–6911189	15.26	0.02	15.25	0.01	15.21	0.02	111
267	05381396–6907478	13.34	0.02	13.29	0.01	13.28	0.01	111
268	05381468–6903321	16.17	0.02	16.02	0.02	15.69	0.05	111
269	05381490–6903485	12.50	0.02	12.45	0.02	12.40	0.01	551
270	05381512–6904011	14.24	0.02	14.26	0.02	14.26	0.02	111
271	05381537–6904036	11.93	0.02	11.77	0.01	11.67	0.01	511
272	05381560–6904022	15.31	0.04	15.24	0.04	14.98	0.03	211
273	05381561–6912121	16.68	0.02	16.63	0.03	16.66	0.07	111
274	05381587–6909315	17.02	0.02	17.11	0.04	17.18	0.15	114
276	05381601–6903547	15.67	0.03	15.77	0.03	15.66	0.06	111
277	05381610–6909167	15.01	0.02	15.02	0.02	14.99	0.02	111
278	05381619–6904038	—	—	16.24	0.08	—	—	020
279	05381643–6903511	16.31	0.02	16.08	0.04	15.87	0.05	111
280	05381655–6904532	15.32	0.02	15.30	0.02	15.32	0.03	111
281	05381668–6904140	9.85	0.03	—	—	—	—	500
282	05381682–6903571	15.68	0.05	—	—	—	—	200
283	05381707–6903507	14.72	0.03	14.59	0.03	14.40	0.03	551
284	05381724–6909110	16.88	0.02	16.89	0.03	16.70	0.10	111
285	05381733–6905421	15.66	0.02	15.66	0.02	15.66	0.04	111
286	05381734–6904479	16.02	0.02	16.06	0.02	16.14	0.05	111
287	05381731–6903566	16.04	0.06	—	—	—	—	100
288	05381759–6907242	16.21	0.02	16.01	0.02	15.96	0.06	111
289	05381763–6904119	10.82	0.02	9.98	0.02	—	—	150
290	05381771–6905458	15.66	0.02	15.63	0.02	15.64	0.04	111

*continued on next page*

**Table 6.** *continued*

Star [VFTS]	IRSF identification	<i>J</i>	$\sigma J$	<i>H</i>	$\sigma H$	<i>K<sub>s</sub></i>	$\sigma K_s$	qflag
291	05381772–6903386	14.33	0.02	14.19	0.02	14.03	0.01	111
292	05381773–6903557	16.22	0.07	—	—	—	—	100
293	05381799–6904097	13.95	0.02	13.82	0.02	13.65	0.02	111
294	05381830–6904023	12.49	0.02	12.40	0.02	12.33	0.01	555
295	05381824–6857262	16.46	0.02	16.48	0.03	16.42	0.08	111
296	05381827–6911064	15.40	0.01	15.39	0.01	15.36	0.02	111
297	05381841–6903517	16.44	0.02	16.40	0.03	16.32	0.06	111
298	05381849–6909204	15.81	0.02	15.62	0.02	15.28	0.03	111
299	05381852–6912280	16.48	0.02	16.46	0.03	16.49	0.06	111
300	05381858–6901519	16.42	0.02	16.34	0.03	16.29	0.09	111
301	05381885–6903597	15.26	0.02	15.09	0.05	14.83	0.04	111
302	05381900–6911127	14.54	0.01	14.35	0.01	14.21	0.01	111
303	05381905–6906346	15.18	0.02	15.13	0.02	15.16	0.03	111
304	05381911–6904582	16.14	0.02	16.17	0.02	16.31	0.07	111
305	05381921–6857374	16.88	0.02	17.00	0.04	16.90	0.11	114
306	05381925–6906006	13.82	0.02	13.74	0.01	13.71	0.01	111
307	05381930–6857157	13.54	0.02	13.51	0.01	13.46	0.01	111
308	05381941–6904031	15.86	0.02	15.85	0.02	15.89	0.04	111
309	05381975–6904105	16.15	0.02	16.13	0.03	16.11	0.05	111
310	05381984–6903524	16.55	0.03	16.48	0.03	16.38	0.08	111
311	05381986–6907102	13.03	0.02	12.34	0.01	12.02	0.01	111
312	05382020–6859203	13.77	0.02	12.96	0.01	12.73	0.01	111
313	05382038–6906228	16.23	0.02	16.22	0.02	16.24	0.07	111
314	05382043–6903103	16.08	0.03	16.07	0.02	16.07	0.06	111
315	05382061–6915378	14.76	0.01	14.74	0.01	14.68	0.02	111
316	05382087–6906172	15.83	0.02	15.76	0.03	15.78	0.06	111
317	05382092–6903500	12.16	0.02	11.84	0.01	11.63	0.01	511
318	05382093–6912001	16.86	0.02	16.92	0.04	16.93	0.10	111
319	05382099–6912212	13.07	0.01	12.23	0.01	11.95	0.01	111
320	05382118–6906170	15.19	0.02	14.98	0.02	14.64	0.02	111
321	05382134–6907513	16.97	0.02	16.96	0.04	16.96	0.14	114
322	05382164–6903145	16.07	0.03	15.82	0.02	15.54	0.04	111
323	05382177–6910429	14.26	0.01	14.07	0.01	13.91	0.01	111
324	05382189–6912480	15.87	0.01	15.92	0.02	15.93	0.04	111
325	05382197–6906001	16.80	0.03	16.82	0.04	16.87	0.11	111
326	05382228–6908079	16.69	0.02	16.83	0.03	16.80	0.11	111
327	05382227–6907509	15.15	0.02	15.14	0.02	15.12	0.03	111
328	05382234–6913152	16.14	0.02	16.17	0.02	16.20	0.05	111
329	05382243–6905213	15.57	0.02	15.55	0.02	15.55	0.04	111
330	05382270–6909418	15.58	0.01	15.42	0.02	15.23	0.02	111
331	05382329–6912540	16.88	0.02	16.80	0.04	16.86	0.09	111
332	05382331–6907161	13.98	0.02	13.94	0.01	13.94	0.01	111
333	05382371–6905036	12.61	0.02	12.62	0.01	12.64	0.01	111
334	05382403–6905240	16.44	0.02	16.43	0.03	16.51	0.08	111
335	05382430–6906282	15.83	0.02	15.72	0.02	15.60	0.04	111
336	05382559–6906093	15.84	0.02	15.83	0.02	15.69	0.06	111
337	05382561–6906044	16.19	0.02	16.06	0.02	15.85	0.05	111
338	05382620–6903388	14.93	0.02	14.51	0.02	14.02	0.01	111
339	05382622–6905019	15.67	0.02	15.67	0.02	15.63	0.04	111
340	05382657–6905317	16.41	0.02	16.38	0.02	16.33	0.07	111
341	05382670–6908526	9.68	0.03	—	—	—	—	533
342	05382688–6904178	16.94	0.02	16.95	0.03	16.87	0.09	111
343	05382704–6904468	16.25	0.03	16.16	0.04	16.14	0.06	111
344	05382723–6857432	13.72	0.02	12.93	0.01	12.72	0.01	111
345	05382741–6908094	15.48	0.02	15.47	0.03	15.37	0.04	111
346	05382777–6906067	15.97	0.03	16.00	0.03	15.78	0.07	511
347	05382781–6905273	16.68	0.02	16.67	0.03	16.82	0.13	114
348	05382782–6903366	16.18	0.03	16.21	0.03	16.15	0.06	111
349	05382800–6904094	16.66	0.02	16.71	0.03	16.73	0.10	111
350	05382806–6906290	14.46	0.03	14.42	0.02	14.38	0.03	511
351	05382840–6906409	15.83	0.02	15.87	0.02	15.93	0.06	111
352	05382846–6911192	14.32	0.01	14.31	0.01	14.31	0.01	111
353	05382855–6907512	16.31	0.02	16.23	0.02	16.13	0.06	111
354	05382855–6904325	15.89	0.02	15.90	0.02	15.90	0.05	111
355	05382915–6857393	14.40	0.02	14.40	0.01	14.45	0.02	111
356	05382921–6909138	15.32	0.02	15.27	0.02	15.15	0.03	111
357	05382935–6859202	13.90	0.02	13.11	0.01	12.94	0.01	111
358	05382938–6908504	17.07	0.04	17.09	0.06	17.35	0.21	114
359	05382935–6905592	15.86	0.04	15.59	0.04	15.59	0.07	151
360	05382943–6905212	14.05	0.02	13.89	0.01	13.68	0.01	111
361	05382949–6906206	14.96	0.02	14.82	0.01	14.74	0.02	111
362	05382958–6905310	16.04	0.06	16.23	0.08	15.83	0.12	222
363	05382999–6905052	14.55	0.02	14.54	0.02	14.52	0.03	511

*continued on next page*

**Table 6.** *continued*

Star [VFTS]	IRSF identification	<i>J</i>	$\sigma J$	<i>H</i>	$\sigma H$	<i>K<sub>s</sub></i>	$\sigma K_s$	qflag
364	05383007–6908275	16.79	0.02	16.82	0.05	16.81	0.11	111
365	05383010–6859313	16.20	0.02	16.18	0.02	16.16	0.06	111
366	05383012–6904446	17.00	0.04	17.03	0.05	16.83	0.12	114
367	05383027–6903527	15.97	0.02	16.00	0.02	15.99	0.05	111
368	05383038–6905295	16.62	0.04	16.25	0.06	16.82	0.15	114
369	05383062–6908244	16.14	0.02	16.02	0.02	15.90	0.05	111
370	05383076–6908271	15.95	0.02	15.97	0.03	16.11	0.07	111
371	05383105–6904272	15.54	0.02	15.56	0.02	15.57	0.03	111
372	05383117–6914018	14.87	0.01	14.40	0.01	14.26	0.02	111
373	05383123–6905530	14.89	0.02	14.83	0.02	14.88	0.02	511
374	05383126–6905570	15.99	0.03	15.91	0.03	15.77	0.06	111
375	05383163–6905270	16.42	0.07	16.35	0.07	16.70	0.25	555
376	05383162–6905490	15.86	0.04	15.75	0.05	15.80	0.07	221
377	05383175–6905567	16.42	0.10	16.15	0.05	16.73	0.13	114
378	05383187–6905329	17.15	0.07	17.06	0.08	15.93	0.12	512
379	05383200–6911446	13.57	0.01	12.72	0.01	12.46	0.01	111
380	05383202–6902525	15.88	0.02	15.77	0.02	15.78	0.05	111
381	05383213–6904319	16.10	0.03	16.16	0.04	16.24	0.07	111
382	05383225–6905446	14.96	0.04	15.02	0.03	14.73	0.06	212
383	05383232–6907322	15.55	0.02	15.49	0.02	15.45	0.04	111
384	05383233–6907359	15.37	0.02	15.07	0.01	14.97	0.03	111
385	05383231–6905239	14.50	0.02	14.47	0.02	14.42	0.02	111
386	05383254–6904320	14.67	0.04	14.83	0.05	14.67	0.10	111
387	05383262–6857140	15.00	0.01	14.80	0.02	14.57	0.03	111
388	05383263–6903559	16.48	0.02	16.51	0.03	16.43	0.08	111
389	05383266–6904325	14.30	0.06	14.24	0.07	14.39	0.07	551
390	05383281–6903195	15.13	0.01	14.92	0.02	14.89	0.04	111
391	05383277–6905250	16.22	0.03	16.23	0.03	16.03	0.06	111
392	05383282–6905446	15.49	0.02	15.33	0.02	15.22	0.03	111
393	05383301–6905131	14.67	0.06	15.00	0.04	14.67	0.05	211
394	05383303–6902429	16.61	0.03	16.61	0.04	16.56	0.11	111
395	05383320–6904513	16.92	0.03	17.09	0.06	17.11	0.15	114
396	05383328–6910239	16.03	0.02	16.01	0.02	15.93	0.05	111
397	05383336–6904171	16.49	0.03	16.60	0.04	16.48	0.10	112
398	05383338–6904384	14.34	0.03	14.40	0.02	14.41	0.02	511
399	05383341–6911590	15.40	0.01	15.30	0.01	15.22	0.02	111
400	05383353–6905218	16.45	0.11	15.83	0.02	16.37	0.19	515
401	05383360–6856057	14.76	0.02	14.58	0.02	14.31	0.02	111
402	05383362–6904505	11.99	0.02	11.77	0.01	11.47	0.01	111
403	05383383–6904364	16.45	0.06	16.41	0.08	16.95	0.16	224
404	05383383–6909571	13.77	0.02	13.70	0.01	13.69	0.01	111
405	05383383–6905519	15.79	0.05	15.77	0.04	15.72	0.08	212
406	05383397–6904212	14.15	0.02	14.15	0.01	14.13	0.02	111
407	05383445–6906145	15.36	0.10	15.44	0.08	14.86	0.14	222
408	05383448–6901397	15.96	0.02	15.82	0.03	15.58	0.05	111
409	05383457–6906527	14.86	0.03	14.78	0.02	14.68	0.03	511
410	05383459–6906057	14.75	0.07	14.20	0.05	13.85	0.07	525
411	05383478–6905004	16.00	0.10	16.26	0.08	15.97	0.13	222
412	05383490–6904539	15.78	0.06	15.85	0.08	—	—	220
413	05383490–6858454	16.79	0.02	16.89	0.04	16.76	0.13	114
414	05383523–6905120	16.28	0.04	16.27	0.04	16.06	0.07	111
415	05383548–6904576	16.10	0.13	16.07	0.13	16.26	0.23	555
416	05383556–6906067	14.18	0.02	14.06	0.02	14.00	0.03	111
417	05383566–6906175	14.28	0.03	14.17	0.02	14.02	0.02	511
418	05383574–6908197	15.44	0.02	15.35	0.02	15.27	0.03	111
419	05383589–6905349	14.96	0.03	14.87	0.03	14.63	0.06	511
420	05383594–6906092	12.32	0.02	12.17	0.01	12.05	0.01	111
421	05383599–6904206	16.54	0.05	16.52	0.05	16.77	0.16	514
422	05383600–6906169	14.15	0.02	14.03	0.01	13.89	0.02	111
423	05383605–6906465	12.51	0.02	12.29	0.01	12.12	0.01	111
424	05383611–6905579	10.84	0.02	10.61	0.02	—	—	153
425	05383618–6906057	16.20	0.04	16.16	0.06	16.26	0.13	111
426	05383630–6904488	16.17	0.08	16.31	0.08	16.55	0.12	221
427	05383641–6906575	12.22	0.02	11.92	0.01	11.62	0.01	111
428	05383650–6903511	16.07	0.02	16.04	0.02	16.03	0.06	111
429	05383686–6904583	14.68	0.02	14.66	0.02	14.71	0.02	111
430	05383686–6906461	13.48	0.02	13.16	0.01	12.99	0.02	115
431	05383696–6905078	11.59	0.02	11.51	0.01	11.44	0.01	115
432	05383703–6906507	14.90	0.03	14.76	0.02	14.71	0.05	111
433	05383708–6905489	16.12	0.08	16.34	0.07	15.86	0.11	212
434	05383723–6904258	15.19	0.10	15.61	0.09	15.17	0.12	222
435	05383724–6907056	15.50	0.08	15.44	0.08	15.14	0.08	221
436	05383736–6905212	15.51	0.07	15.57	0.05	15.51	0.08	211

*continued on next page*

**Table 6.** *continued*

Star [VFTS]	IRSF identification	<i>J</i>	$\sigma J$	<i>H</i>	$\sigma H$	<i>K<sub>s</sub></i>	$\sigma K_s$	qflag
437	05383739–6908429	13.41	0.02	12.58	0.01	12.35	0.01	111
438	05383756–6904376	15.29	0.11	—	—	—	—	200
439	05383768–6906527	14.20	0.02	13.38	0.02	13.21	0.02	111
440	05383772–6905210	13.33	0.02	13.31	0.01	13.28	0.02	511
441	05383782–6903290	15.09	0.03	15.10	0.03	15.05	0.04	511
442	05383790–6903367	16.25	0.05	16.36	0.05	16.22	0.10	212
443	05383798–6906153	14.90	0.02	14.79	0.02	14.63	0.03	111
444	05383798–6905089	15.98	0.05	15.98	0.06	15.80	0.11	511
445	05383803–6905433	14.18	0.02	14.08	0.01	14.03	0.02	111
446	05383825–6906174	14.43	0.03	14.10	0.02	13.88	0.03	551
447	05383834–6902275	15.96	0.03	15.85	0.03	15.85	0.08	111
448	05383835–6906449	16.00	0.06	15.91	0.05	15.59	0.09	211
449	05383835–6905083	16.65	0.06	—	—	—	—	100
450	05383848–6906220	13.08	0.02	12.91	0.01	12.89	0.03	115
451	05383850–6906300	14.20	0.07	14.12	0.04	13.61	0.07	252
452	05383871–6912326	16.44	0.03	16.38	0.06	16.42	0.10	111
453	05383876–6904124	15.28	0.03	15.34	0.02	15.26	0.04	511
454	05383877–6911203	13.46	0.01	12.75	0.01	12.51	0.01	111
455	05383875–6906132	14.51	0.02	14.45	0.02	14.30	0.03	111
456	05383882–6905256	14.86	0.03	14.73	0.02	14.50	0.03	111
457	05383884–6906495	12.78	0.02	12.58	0.01	12.38	0.01	111
458	05383887–6908145	11.24	0.02	10.95	0.02	10.79	0.02	155
459	05383897–6903121	16.41	0.02	16.38	0.03	16.43	0.10	111
460	05383899–6906589	14.73	0.02	14.51	0.02	14.42	0.02	111
461	05383916–6905057	16.13	0.04	16.21	0.04	16.27	0.08	511
462	05383918–6901408	16.58	0.02	16.60	0.04	16.60	0.11	111
463	05383923–6906013	16.40	0.05	16.05	0.06	15.79	0.07	111
464	05383928–6905527	14.55	0.06	14.26	0.04	13.63	0.05	211
465	05383928–6906390	14.55	0.03	14.22	0.02	13.93	0.03	511
466	05383929–6907529	14.61	0.02	14.44	0.02	14.38	0.02	111
467	05383933–6915350	16.00	0.02	15.80	0.02	15.47	0.03	111
468	05383937–6906064	13.80	0.03	13.64	0.03	13.61	0.03	151
469	05383943–6903076	15.91	0.02	15.84	0.02	15.78	0.06	111
470	05383950–6904386	15.46	0.03	15.52	0.02	15.46	0.05	511
471	05383950–6902308	16.60	0.02	16.58	0.03	16.70	0.12	114
472	05383956–6907053	15.80	0.02	15.69	0.02	15.62	0.05	111
473	05383957–6904569	16.85	0.04	16.82	0.06	16.79	0.17	114
474	05383971–6909277	16.58	0.02	16.54	0.03	16.50	0.08	111
475	05383974–6907560	15.38	0.02	15.23	0.02	15.13	0.03	111
476	05383974–6905393	14.73	0.02	14.49	0.02	14.40	0.03	511
477	05383971–6905506	—	—	15.42	0.06	15.08	0.09	022
478	05383983–6907109	15.96	0.02	15.82	0.02	15.78	0.06	111
479	05383983–6903411	15.40	0.03	15.31	0.02	15.26	0.04	111
480	05384018–6905135	17.05	0.06	17.09	0.10	16.63	0.11	151
481	05384019–6901123	14.09	0.01	14.06	0.01	14.08	0.03	511
482	05384022–6905599	12.39	0.02	12.24	0.02	12.16	0.01	551
483	05384025–6905311	15.36	0.05	15.79	0.07	15.44	0.08	211
484	05384036–6905438	14.47	0.02	14.37	0.01	14.28	0.02	111
485	05384056–6905114	—	—	—	—	17.09	0.18	004
486	05384061–6904560	14.94	0.04	14.66	0.02	14.52	0.05	511
487	05384068–6905260	—	—	15.69	0.09	15.37	0.12	021
488	05384073–6908249	15.14	0.02	14.99	0.02	14.93	0.02	111
489	05384076–6901489	16.48	0.02	16.45	0.03	16.52	0.10	111
490	05384083–6910090	13.51	0.01	12.71	0.01	12.49	0.01	111
491	05384085–6906575	14.86	0.02	14.69	0.02	14.62	0.03	111
492	05384104–6904249	14.17	0.03	14.25	0.02	14.33	0.02	511
493	05384103–6906168	15.74	0.03	15.46	0.03	15.37	0.05	111
494	05384106–6906599	15.83	0.02	15.64	0.02	15.55	0.04	111
495	05384110–6901460	15.78	0.04	15.84	0.03	15.90	0.08	211
496	05384110–6906516	16.08	0.04	15.87	0.03	15.91	0.08	511
497	05384113–6905132	14.63	0.03	14.66	0.03	14.65	0.05	151
498	05384117–6906352	15.65	0.07	15.62	0.04	15.13	0.09	512
499	05384119–6904063	16.99	0.03	17.31	0.08	—	—	110
500	05384123–6902582	13.80	0.02	13.73	0.01	13.68	0.03	511
501	05384124–6904142	15.67	0.03	15.71	0.02	15.70	0.04	111
502	05384129–6905325	13.21	0.04	13.14	0.02	13.11	0.02	555
504	05384141–6903008	16.04	0.03	15.95	0.04	15.94	0.12	111
505	05384152–6905346	15.92	0.05	16.09	0.07	16.11	0.13	111
506	05384155–6905194	12.99	0.02	12.97	0.02	12.96	0.01	111
507	05384160–6905134	11.67	0.02	11.46	0.01	11.18	0.02	115
508	05384162–6907024	15.57	0.02	15.33	0.04	15.48	0.05	151
509	05384162–6905152	12.33	0.02	12.16	0.01	11.95	0.01	111
510	05384168–6906185	15.37	0.12	—	—	—	—	100

*continued on next page*

**Table 6.** *continued*

Star [VFTS]	IRSF identification	<i>J</i>	$\sigma J$	<i>H</i>	$\sigma H$	<i>K<sub>s</sub></i>	$\sigma K_s$	qflag
511	05384172–6906282	14.91	0.02	14.79	0.02	14.81	0.04	111
512	05384174–6906250	13.69	0.02	13.55	0.01	13.49	0.01	111
513	05384180–6905321	15.47	0.11	15.23	0.03	15.33	0.14	111
514	05384188–6901588	16.12	0.02	16.16	0.03	16.25	0.08	111
515	05384186–6905327	—	—	—	—	16.19	0.16	002
516	05384189–6909229	16.61	0.02	16.63	0.03	16.59	0.09	111
517	05384193–6904388	14.74	0.02	14.73	0.02	14.70	0.02	111
518	05384194–6906297	14.38	0.02	14.24	0.02	14.20	0.03	111
519	05384194–6905131	13.98	0.03	13.91	0.02	13.91	0.04	111
520	05384199–6906535	16.52	0.03	16.51	0.06	16.80	0.19	114
521	05384201–6907049	14.83	0.07	14.86	0.08	14.79	0.08	222
522	05384208–6905455	14.95	0.03	14.69	0.02	14.74	0.02	111
523	05384211–6904329	16.34	0.08	16.29	0.05	16.09	0.09	211
524	05384219–6908042	13.73	0.02	13.04	0.01	12.88	0.01	111
525	05384221–6906256	13.38	0.02	13.26	0.01	13.21	0.01	111
526	05384224–6908323	13.57	0.02	13.31	0.01	13.15	0.01	111
527	05384235–6904581	11.52	0.02	11.42	0.01	11.31	0.01	115
528	05384237–6904248	15.30	0.06	15.55	0.03	14.98	0.11	212
529	05384238–6904432	15.78	0.02	15.76	0.03	15.70	0.05	111
530	05384243–6903042	16.27	0.06	15.80	0.04	15.72	0.06	111
531	05384265–6904135	14.56	0.02	14.57	0.02	14.48	0.03	511
532	05384266–6906359	14.24	0.02	14.12	0.02	14.08	0.02	111
533	05384274–6905426	11.15	0.02	11.00	0.02	10.95	0.02	155
534	05384281–6915403	15.15	0.01	15.06	0.01	14.98	0.02	111
535	05384281–6904313	15.97	0.09	16.24	0.11	15.95	0.13	222
536	05384280–6906325	15.52	0.02	15.38	0.03	15.33	0.04	111
537	05384303–6903448	15.37	0.02	15.24	0.02	15.13	0.03	111
538	05384308–6904131	13.89	0.02	13.84	0.02	13.77	0.02	111
539	05384310–6907020	15.23	0.10	15.59	0.06	15.05	0.09	212
540	05384308–6906370	16.02	0.02	15.88	0.02	15.91	0.06	111
541	05384309–6901325	12.83	0.02	12.74	0.01	12.70	0.02	511
542	05384309–6905469	13.13	0.02	12.99	0.02	12.93	0.02	111
543	05384318–6905274	15.50	0.06	15.43	0.05	15.74	0.13	515
544	05384321–6915047	14.17	0.01	13.41	0.01	13.24	0.01	111
545	05384320–6906145	12.93	0.02	12.83	0.02	12.75	0.02	111
546	05384338–6904464	15.09	0.02	15.00	0.02	14.99	0.04	111
547	05384356–6901589	16.59	0.02	16.50	0.03	16.37	0.08	111
548	05384357–6905293	16.25	0.08	16.05	0.04	16.17	0.12	515
549	05384359–6907518	15.64	0.02	15.49	0.02	15.43	0.03	111
550	05384362–6904425	15.00	0.04	15.02	0.02	14.89	0.03	511
551	05384365–6906186	16.39	0.07	—	—	—	—	200
552	05384368–6906168	15.80	0.05	15.57	0.09	15.57	0.10	522
553	05384372–6906272	16.68	0.03	16.62	0.04	16.45	0.08	111
554	05384376–6905389	17.06	0.11	—	—	17.12	0.24	504
555	05384392–6903163	15.51	0.02	15.37	0.02	15.29	0.04	111
556	05384402–6904482	16.78	0.04	16.91	0.08	—	—	150
557	05384408–6904595	14.89	0.10	15.24	0.05	14.96	0.07	211
558	05384425–6900275	16.22	0.02	16.17	0.02	16.09	0.07	111
559	05384429–6907166	16.12	0.04	16.22	0.05	16.07	0.14	511
560	05384434–6906408	16.30	0.03	16.29	0.03	16.27	0.07	111
561	05384436–6905144	14.77	0.05	14.77	0.04	14.26	0.10	212
562	05384441–6905362	13.29	0.02	13.18	0.01	13.13	0.02	111
563	05384453–6906288	15.54	0.02	15.40	0.02	15.37	0.04	111
564	05384458–6905123	15.01	0.08	14.95	0.09	14.29	0.13	222
565	05384456–6904551	15.59	0.10	15.75	0.08	15.17	0.13	222
566	05384457–6904512	13.72	0.03	13.73	0.02	13.65	0.02	511
567	05384461–6907566	15.57	0.02	15.44	0.02	15.36	0.03	111
568	05384465–6904249	16.39	0.02	16.39	0.04	16.27	0.07	111
569	05384470–6905139	15.27	0.08	15.06	0.09	14.86	0.09	222
570	05384466–6905452	14.08	0.03	13.85	0.03	13.55	0.03	151
571	05384468–6905411	16.09	0.05	—	—	—	—	100
572	05384473–6908571	16.07	0.02	16.03	0.02	16.01	0.05	111
573	05384478–6906577	15.90	0.07	16.27	0.12	15.64	0.12	212
574	05384482–6857346	16.24	0.02	16.23	0.03	16.26	0.07	111
575	05384490–6905331	15.21	0.04	15.16	0.04	15.18	0.07	511
576	05384495–6915114	13.63	0.01	13.27	0.01	13.04	0.01	111
577	05384494–6907046	15.57	0.03	15.39	0.03	15.38	0.04	511
578	05384497–6908067	13.41	0.02	13.19	0.01	13.05	0.01	111
579	05384493–6905078	14.39	0.07	14.17	0.06	13.65	0.07	222
580	05384506–6903193	16.40	0.03	16.21	0.02	16.28	0.09	111
581	05384508–6904156	15.10	0.02	14.92	0.02	14.67	0.03	111
582	05384519–6905375	16.58	0.05	—	—	16.41	0.13	101
583	05384521–6905485	14.68	0.02	14.78	0.03	14.62	0.03	111

*continued on next page*

**Table 6.** *continued*

Star [VFTS]	IRSF identification	<i>J</i>	$\sigma J$	<i>H</i>	$\sigma H$	<i>K<sub>s</sub></i>	$\sigma K_s$	qflag
584	05384524–6906549	16.12	0.06	16.19	0.05	15.91	0.11	212
585	05384527–6905466	13.45	0.02	13.43	0.02	13.36	0.01	111
586	05384540–6902514	14.96	0.02	14.91	0.01	14.88	0.03	511
587	05384538–6905245	16.10	0.04	16.23	0.04	15.94	0.09	512
588	05384538–6905399	16.31	0.04	16.84	0.15	16.34	0.09	151
589	05384559–6907348	15.62	0.04	15.71	0.02	15.65	0.05	211
590	05384558–6905478	12.03	0.02	11.92	0.01	11.84	0.01	111
591	05384569–6906225	11.76	0.02	11.62	0.01	11.53	0.01	111
592	05384568–6906154	16.06	0.02	15.99	0.03	15.79	0.06	111
593	05384571–6909401	16.59	0.02	16.62	0.04	16.55	0.08	111
594	05384578–6905133	15.02	0.11	15.95	0.04	14.97	0.12	212
595	05384590–6902434	13.38	0.02	12.57	0.01	12.35	0.02	511
596	05384606–6906156	14.67	0.02	14.60	0.02	14.53	0.02	111
597	05384606–6906563	15.46	0.02	15.46	0.02	15.36	0.05	111
598	05384616–6906236	15.70	0.07	15.73	0.06	15.57	0.07	211
599	05384618–6906174	13.49	0.02	13.42	0.01	13.38	0.01	111
600	05384625–6910148	16.55	0.02	16.57	0.03	16.61	0.08	111
601	05384628–6905594	14.33	0.02	14.24	0.02	14.23	0.02	111
602	05384636–6904335	16.72	0.07	16.61	0.08	16.89	0.23	554
603	05384653–6904280	13.49	0.02	13.40	0.01	13.29	0.02	111
604	05384658–6905371	14.80	0.02	14.71	0.02	14.71	0.03	111
605	05384671–6902405	16.74	0.03	16.80	0.04	16.74	0.14	114
606	05384671–6905388	16.57	0.04	16.46	0.05	16.66	0.12	111
607	05384674–6905489	16.04	0.04	16.01	0.04	15.96	0.07	511
608	05384679–6906031	13.70	0.02	13.62	0.01	13.58	0.02	111
609	05384686–6905199	15.55	0.10	15.54	0.10	15.20	0.13	222
610	05384688–6906267	16.38	0.06	16.20	0.08	—	—	110
611	05384689–6905588	15.94	0.02	15.85	0.03	15.89	0.06	111
612	05384715–6906359	15.81	0.04	15.83	0.02	15.67	0.07	511
613	05384716–6905545	15.38	0.02	15.38	0.02	15.19	0.03	111
614	05384720–6906202	14.70	0.02	14.34	0.02	14.25	0.02	111
615	05384733–6906178	15.64	0.02	15.60	0.02	15.59	0.04	111
616	05384746–6907134	16.04	0.04	16.06	0.03	15.95	0.06	511
617	05384752–6900252	12.89	0.01	12.79	0.01	12.67	0.02	511
618	05384758–6907059	16.32	0.05	16.40	0.06	16.00	0.12	212
619	05384772–6906450	15.71	0.02	15.65	0.02	15.54	0.03	111
621	05384808–6904422	14.15	0.05	13.88	0.05	13.53	0.06	222
622	05384811–6906123	16.55	0.02	16.37	0.03	16.33	0.07	111
623	05384814–6907415	15.79	0.02	15.68	0.02	15.66	0.04	111
624	05384812–6906049	16.62	0.02	16.70	0.04	16.56	0.09	111
625	05384818–6908341	16.68	0.02	16.63	0.03	16.60	0.08	111
626	05384820–6908108	14.23	0.02	14.10	0.01	14.05	0.01	111
627	05384840–6859499	15.70	0.02	15.73	0.02	15.80	0.06	111
628	05384845–6906364	15.98	0.04	15.97	0.05	15.85	0.07	111
629	05384851–6905403	16.06	0.03	15.73	0.05	15.44	0.06	111
630	05384863–6904591	15.56	0.08	15.92	0.05	15.47	0.15	212
631	05384888–6908281	15.76	0.02	15.66	0.02	15.66	0.04	111
632	05384890–6908552	15.86	0.02	15.82	0.02	15.84	0.05	111
633	05384895–6908124	16.05	0.02	15.97	0.02	15.86	0.05	111
634	05384901–6904106	14.91	0.06	14.79	0.05	14.31	0.07	251
635	05384904–6906196	15.47	0.02	15.44	0.02	15.45	0.04	111
636	05384920–6910045	16.52	0.02	16.55	0.03	16.61	0.07	111
637	05384939–6906153	16.62	0.03	16.57	0.05	16.62	0.10	111
638	05384952–6902303	15.94	0.02	15.99	0.02	15.98	0.06	111
639	05384964–6909240	15.50	0.02	15.49	0.02	15.55	0.03	111
640	05384967–6908548	16.58	0.02	16.54	0.03	16.49	0.09	111
641	05384973–6906430	12.63	0.02	12.58	0.02	12.48	0.02	555
642	05384990–6910428	15.20	0.01	15.04	0.01	15.03	0.03	111
643	05384997–6907053	16.33	0.03	16.25	0.03	16.17	0.07	111
644	05385002–6906522	15.18	0.03	14.65	0.02	14.39	0.03	511
645	05385021–6907452	15.91	0.02	15.80	0.02	15.82	0.05	111
646	05385027–6906044	14.59	0.02	14.49	0.01	14.45	0.02	111
647	05385036–6905026	14.59	0.12	14.83	0.11	14.29	0.14	222
648	05385040–6905382	14.00	0.02	13.95	0.01	13.92	0.01	111
649	05385062–6905546	15.93	0.02	15.88	0.02	15.86	0.05	111
650	05385068–6857555	17.17	0.03	17.14	0.05	17.34	0.20	114
651	05385103–6905548	14.52	0.02	14.45	0.01	14.46	0.02	111
652	05385104–6906204	13.40	0.02	13.28	0.01	13.22	0.01	111
653	05385108–6906487	15.46	0.08	15.54	0.07	15.27	0.09	222
654	05385116–6905419	15.54	0.02	15.43	0.02	15.39	0.03	111
655	05385120–6906411	11.53	0.02	10.65	0.02	—	—	153
656	05385120–6905593	14.14	0.02	14.10	0.01	14.09	0.02	111
657	05385132–6904085	14.19	0.02	13.96	0.02	13.73	0.02	511

*continued on next page*

**Table 6.** *continued*

Star [VFTS]	IRSF identification	<i>J</i>	$\sigma J$	<i>H</i>	$\sigma H$	<i>K<sub>s</sub></i>	$\sigma K_s$	qflag
658	05385171–6915413	14.32	0.02	13.96	0.01	13.80	0.01	111
659	05385176–6906012	15.91	0.02	15.86	0.02	15.85	0.04	111
660	05385180–6905469	15.78	0.02	15.65	0.02	15.66	0.05	111
661	05385205–6905338	15.15	0.02	15.12	0.02	15.12	0.03	111
662	05385257–6902203	15.93	0.02	15.85	0.02	15.77	0.05	111
663	05385271–6910148	15.98	0.02	15.88	0.02	15.92	0.04	111
664	05385272–6906432	13.88	0.02	13.78	0.01	13.74	0.02	111
665	05385274–6907287	16.19	0.02	16.08	0.03	16.13	0.07	111
666	05385281–6901381	16.65	0.02	16.71	0.04	16.75	0.12	114
667	05385283–6906121	14.86	0.02	14.83	0.01	14.82	0.02	111
668	05385287–6907360	16.37	0.02	16.27	0.03	16.33	0.08	111
669	05385297–6907453	13.75	0.02	13.64	0.01	13.58	0.01	111
670	05385306–6908248	15.70	0.02	15.58	0.02	15.62	0.04	111
671	05385324–6902408	17.06	0.15	16.54	0.03	16.52	0.10	111
672	05385410–6908077	13.94	0.02	13.79	0.01	13.68	0.01	111
673	05385413–6906530	16.93	0.03	16.91	0.05	17.11	0.19	114
674	05385437–6911101	14.48	0.02	14.24	0.02	14.10	0.02	111
675	05385443–6908004	13.76	0.02	13.59	0.02	13.54	0.02	111
676	05385462–6904550	15.87	0.06	15.70	0.07	15.28	0.15	222
677	05385474–6903489	15.59	0.05	15.17	0.07	14.96	0.07	151
678	05385483–6907502	16.07	0.03	15.87	0.03	15.79	0.05	111
679	05385485–6903501	15.98	0.05	15.88	0.05	15.77	0.09	211
680	05385511–6903319	15.37	0.02	15.05	0.01	15.01	0.02	111
681	05385522–6905566	16.45	0.02	16.43	0.03	16.38	0.07	111
682	05385552–6904267	13.53	0.02	12.96	0.01	12.48	0.01	111
683	05385555–6858561	16.51	0.02	16.50	0.04	16.55	0.10	111
684	05385556–6908283	16.64	0.02	16.51	0.03	16.52	0.09	111
685	05385557–6909378	15.80	0.02	15.64	0.02	15.37	0.03	111
686	05385564–6907238	14.56	0.02	14.45	0.01	14.42	0.02	111
687	05385583–6908224	13.84	0.02	13.73	0.01	13.69	0.01	111
688	05385606–6905541	15.34	0.02	15.28	0.02	15.28	0.04	111
689	05385638–6908227	15.83	0.02	15.63	0.02	15.37	0.03	111
690	05385663–6907197	16.21	0.02	16.13	0.03	16.14	0.06	111
691	05385681–6908410	13.90	0.02	13.69	0.01	13.59	0.01	111
692	05385692–6906389	16.09	0.05	16.15	0.03	16.02	0.09	211
693	05385705–6900572	13.98	0.01	13.24	0.01	13.06	0.02	511
694	05385705–6858067	13.36	0.01	12.47	0.01	12.23	0.02	151
695	05385707–6906056	11.31	0.02	11.13	0.01	10.99	0.02	155
696	05385716–6856531	12.50	0.01	12.45	0.01	12.40	0.02	551
697	05385729–6903417	15.30	0.02	15.08	0.02	14.78	0.02	111
698	05385732–6907097	12.34	0.02	11.89	0.01	11.43	0.01	111
699	05385747–6903484	16.28	0.03	16.27	0.04	16.32	0.09	111
700	05385786–6859168	13.61	0.01	12.75	0.01	12.52	0.02	111
701	05385815–6904581	16.15	0.05	15.81	0.08	15.52	0.12	522
702	05385839–6904351	15.35	0.02	15.12	0.02	14.91	0.03	111
703	05385856–6907525	16.17	0.02	16.10	0.02	16.16	0.07	111
704	05385873–6902448	16.29	0.04	16.32	0.04	16.05	0.10	111
705	05385872–6906471	16.20	0.02	16.16	0.02	16.17	0.06	111
706	05385877–6905239	15.60	0.04	15.49	0.03	15.61	0.10	515
707	05385891–6906421	15.42	0.02	15.35	0.02	15.33	0.03	111
708	05385903–6902445	14.20	0.02	13.52	0.01	13.33	0.02	111
709	05385903–6900205	16.81	0.02	16.74	0.04	16.72	0.11	114
710	05385914–6906243	16.15	0.02	16.15	0.03	16.21	0.06	111
711	05385928–6908123	15.65	0.02	15.49	0.02	15.43	0.03	111
712	05385945–6905496	15.71	0.02	15.61	0.02	15.56	0.04	111
713	05385990–6908147	16.32	0.02	16.19	0.02	16.12	0.05	111
714	05385994–6905419	14.81	0.02	14.71	0.02	14.65	0.02	111
715	05390004–6901398	16.89	0.02	16.87	0.04	16.89	0.14	114
716	05390039–6903305	15.57	0.02	15.51	0.02	15.45	0.03	111
717	05390075–6907129	15.12	0.02	15.02	0.02	14.98	0.03	111
718	05390089–6857297	16.04	0.01	16.03	0.03	16.04	0.06	111
719	05390092–6906292	17.05	0.05	16.97	0.06	17.02	0.18	114
720	05390105–6859058	16.79	0.02	16.77	0.05	16.60	0.10	111
721	05390220–6914293	12.82	0.02	12.34	0.01	12.03	0.02	111
722	05390278–6857078	15.33	0.01	15.40	0.02	15.39	0.04	111
723	05390287–6905263	15.66	0.03	15.54	0.04	15.40	0.07	511
724	05390295–6915000	15.71	0.02	15.54	0.02	15.40	0.03	111
725	05390323–6908183	15.59	0.02	15.57	0.02	15.56	0.04	111
726	05390331–6909319	16.26	0.02	16.25	0.02	16.17	0.06	111
727	05390333–6910397	16.07	0.02	15.98	0.02	15.93	0.04	111
728	05390343–6906346	15.50	0.02	15.45	0.02	15.42	0.04	111
729	05390360–6907169	14.37	0.02	14.26	0.01	14.18	0.02	111
730	05390364–6900191	15.53	0.02	15.49	0.03	15.50	0.05	111

*continued on next page*

**Table 6.** *continued*

Star [VFTS]	IRSF identification	<i>J</i>	$\sigma J$	<i>H</i>	$\sigma H$	<i>K<sub>s</sub></i>	$\sigma K_s$	qflag
731	05390378–6903465	14.86	0.02	14.38	0.02	13.54	0.01	111
732	05390477–6904098	12.35	0.02	12.19	0.01	12.08	0.01	511
733	05390487–6905404	13.90	0.02	13.82	0.01	13.74	0.02	111
734	05390493–6905353	15.84	0.03	15.66	0.03	15.61	0.05	111
735	05390503–6913297	15.44	0.03	15.02	0.03	—	—	110
736	05390530–6904161	15.51	0.02	15.50	0.02	15.41	0.03	111
737	05390539–6904311	15.20	0.02	15.18	0.02	15.10	0.03	111
738	05390542–6857373	14.19	0.01	14.04	0.01	13.78	0.02	111
739	05390593–6916267	11.13	0.02	10.93	0.03	10.85	0.02	555
740	05390603–6915416	15.66	0.01	15.53	0.02	15.43	0.03	111
741	05390605–6909585	16.24	0.02	16.15	0.02	16.07	0.04	111
742	05390640–6856586	16.89	0.03	16.87	0.06	17.14	0.16	114
743	05390692–6900165	15.33	0.01	15.39	0.02	15.41	0.04	111
744	05390715–6901528	11.64	0.02	10.73	0.01	—	—	553
745	05390733–6902365	16.10	0.16	15.48	0.02	15.30	0.04	111
746	05390733–6907460	15.01	0.02	14.94	0.02	14.88	0.02	111
747	05390763–6906249	14.87	0.02	14.76	0.01	14.65	0.02	111
748	05390795–6906026	16.41	0.02	16.40	0.03	16.39	0.08	111
749	05390816–6905558	16.24	0.03	16.04	0.05	16.02	0.08	111
750	05390836–6900575	15.70	0.01	15.71	0.02	15.68	0.06	111
751	05390900–6901292	15.62	0.02	15.48	0.04	15.31	0.04	111
752	05390913–6857473	16.71	0.02	16.81	0.04	16.76	0.11	114
753	05390915–6912104	15.49	0.01	15.36	0.02	15.26	0.02	111
754	05391006–6906214	15.83	0.02	15.71	0.02	15.63	0.04	111
755	05391092–6906137	14.62	0.02	14.52	0.01	14.49	0.02	111
756	05391093–6856468	14.07	0.01	13.93	0.01	13.67	0.02	111
757	05391116–6902590	16.29	0.02	16.24	0.02	16.12	0.07	111
758	05391132–6902015	12.27	0.02	12.06	0.01	11.78	0.02	511
759	05391239–6858449	13.73	0.01	12.93	0.01	12.67	0.02	111
760	05391252–6902096	12.82	0.02	12.57	0.01	12.44	0.02	511
761	05391271–6858473	15.51	0.01	15.47	0.02	15.51	0.05	111
762	05391328–6909275	15.95	0.02	15.87	0.02	15.82	0.04	111
763	05391344–6909106	14.28	0.02	13.77	0.01	13.67	0.01	111
764	05391453–6916424	12.34	0.01	12.32	0.01	12.32	0.01	111
765	05391464–6905035	12.39	0.02	11.52	0.01	11.26	0.01	111
766	05391520–6858515	15.14	0.01	15.01	0.01	14.76	0.03	111
767	05391527–6859541	14.03	0.01	13.29	0.01	13.08	0.02	111
768	05391623–6901203	15.29	0.02	15.16	0.02	15.02	0.04	111
769	05391669–6907031	15.37	0.02	15.30	0.02	15.31	0.03	111
770	05391675–6903276	15.48	0.02	15.46	0.02	15.44	0.03	111
771	05391739–6906098	15.17	0.02	15.08	0.02	15.04	0.03	111
772	05391780–6857337	16.82	0.02	16.79	0.04	16.87	0.14	114
773	05391808–6905165	14.17	0.02	13.48	0.01	13.31	0.01	111
774	05391868–6907473	15.48	0.02	15.28	0.02	15.17	0.03	111
775	05391888–6914194	16.13	0.01	16.01	0.02	16.04	0.04	111
776	05391953–6859209	13.15	0.01	12.33	0.01	12.00	0.02	111
777	05391990–6901128	14.05	0.01	13.83	0.01	13.68	0.02	511
778	05392077–6902118	15.98	0.04	15.77	0.03	15.64	0.06	511
779	05392155–6903184	15.01	0.02	14.78	0.01	14.71	0.03	111
780	05392164–6857016	16.94	0.02	17.02	0.05	16.96	0.14	114
781	05392244–6915184	14.86	0.01	14.67	0.02	14.43	0.02	111
782	05392381–6910545	14.58	0.02	14.44	0.01	14.35	0.02	111
783	05392395–6913564	13.25	0.01	12.38	0.01	12.14	0.02	111
784	05392422–6906117	16.19	0.02	16.10	0.03	16.02	0.06	111
785	05392447–6859586	13.34	0.01	12.54	0.01	12.26	0.02	111
786	05392472–6912396	15.54	0.01	15.30	0.02	15.03	0.02	111
787	05392479–6905515	16.12	0.02	16.06	0.03	16.07	0.06	111
788	05392511–6901307	16.18	0.10	15.81	0.02	15.77	0.05	111
789	05392568–6912454	16.42	0.02	16.26	0.02	16.12	0.05	111
790	05392596–6906290	14.76	0.02	14.38	0.01	14.23	0.02	111
791	05392636–6905235	13.63	0.02	12.85	0.01	12.68	0.01	111
792	05392805–6856588	15.97	0.03	15.88	0.03	15.81	0.07	111
793	05392818–6905054	11.43	0.02	10.77	0.02	—	—	153
794	05392915–6858050	15.40	0.01	15.28	0.02	15.01	0.03	111
795	05392946–6909228	15.40	0.02	15.26	0.02	15.17	0.02	111
796	05393009–6858577	16.60	0.02	16.48	0.03	16.27	0.07	111
797	05393064–6909262	14.51	0.02	14.47	0.01	14.48	0.02	111
798	05393089–6913177	15.81	0.02	15.68	0.02	15.67	0.03	111
799	05393114–6904367	16.83	0.02	16.77	0.03	16.82	0.10	111
800	05393146–6912114	15.47	0.02	15.22	0.02	14.89	0.02	111
801	05393165–6859474	16.09	0.01	16.08	0.02	16.06	0.07	111
802	05393258–6900025	14.49	0.01	14.56	0.01	14.59	0.03	111
803	05393363–6908549	13.48	0.02	12.69	0.01	12.45	0.01	111

*continued on next page*

**Table 6.** *continued*

Star [VFTS]	IRSF identification	<i>J</i>	$\sigma J$	<i>H</i>	$\sigma H$	<i>K<sub>s</sub></i>	$\sigma K_s$	qflag
804	05393377–6901019	16.81	0.02	16.73	0.04	16.68	0.10	111
805	05393443–6900193	13.63	0.01	12.82	0.01	12.61	0.02	111
806	05393487–6859486	14.35	0.01	14.40	0.01	14.44	0.03	111
807	05393514–6910306	15.46	0.02	15.38	0.02	15.32	0.03	111
808	05393523–6904004	14.26	0.02	13.54	0.01	13.40	0.01	111
809	05393579–6903067	14.14	0.02	13.43	0.01	13.23	0.03	511
810	05393580–6907080	16.24	0.02	16.17	0.02	16.26	0.07	111
811	05393585–6859027	16.74	0.02	16.72	0.04	16.69	0.10	111
812	05393612–6904590	14.46	0.02	14.40	0.01	14.36	0.02	111
813	05393621–6857296	16.68	0.02	16.73	0.04	16.81	0.10	111
814	05393640–6901078	16.67	0.02	16.60	0.04	16.63	0.10	111
815	05393649–6912003	15.79	0.02	15.56	0.02	15.30	0.03	111
816	05393654–6908488	13.56	0.02	12.78	0.01	12.62	0.01	111
817	05393722–6904043	15.00	0.02	14.90	0.02	14.87	0.02	111
818	05393781–6905008	12.39	0.02	11.39	0.01	11.06	0.02	115
819	05393784–6913330	15.75	0.02	15.55	0.02	15.45	0.03	111
820	05393794–6911462	10.95	0.02	10.19	0.02	10.19	0.04	555
821	05393844–6858360	16.30	0.02	16.38	0.02	16.38	0.07	111
822	05393849–6909004	14.36	0.02	13.63	0.01	12.46	0.01	111
824	05393915–6911552	15.56	0.04	15.61	0.12	—	—	110
825	05393922–6911417	15.39	0.02	15.13	0.03	14.96	0.03	111
826	05393925–6911460	14.31	0.05	—	—	—	—	100
827	05393928–6911442	14.71	0.02	—	—	—	—	100
829	05393964–6912014	14.31	0.02	14.17	0.01	14.09	0.02	111
830	05393976–6904303	15.29	0.01	15.31	0.02	15.34	0.03	111
831	05393987–6912043	12.36	0.02	12.24	0.01	12.16	0.02	111
832	05393997–6911556	15.78	0.03	15.64	0.04	—	—	110
833	05394015–6909022	16.45	0.02	16.36	0.03	16.34	0.07	111
834	05394032–6911439	14.46	0.02	14.32	0.03	14.24	0.04	155
835	05394085–6911524	15.71	0.03	15.49	0.04	15.33	0.05	111
836	05394095–6911536	14.65	0.01	14.36	0.02	13.99	0.02	111
837	05394126–6859379	16.29	0.02	16.36	0.03	16.38	0.07	111
838	05394176–6909324	15.25	0.01	15.17	0.02	15.16	0.02	111
839	05394179–6911309	—	—	9.13	0.03	—	—	353
840	05394219–6911488	15.95	0.02	15.69	0.03	15.49	0.03	111
841	05394225–6913284	13.63	0.01	13.28	0.02	13.06	0.02	111
842	05394270–6911514	15.08	0.01	14.85	0.01	14.53	0.02	111
843	05394338–6901223	15.93	0.02	15.95	0.02	16.06	0.05	111
844	05394365–6910396	13.36	0.02	12.54	0.01	12.33	0.02	111
845	05394381–6905497	14.73	0.01	14.63	0.01	14.62	0.02	111
846	05394463–6914194	16.55	0.02	16.51	0.03	16.49	0.06	111
847	05394559–6904263	15.34	0.01	15.27	0.02	15.20	0.03	111
848	05394567–6912082	14.53	0.01	14.28	0.01	13.99	0.02	111
849	05394737–6859220	15.30	0.01	15.35	0.01	15.39	0.03	111
850	05395117–6911536	15.59	0.02	15.52	0.02	15.51	0.03	111
851	05395154–6902226	16.01	0.02	16.04	0.02	16.08	0.05	111
852	05395240–6909412	10.65	0.01	—	—	9.61	0.03	535
853	05395251–6907387	15.73	0.01	15.51	0.02	15.27	0.03	111
854	05395265–6900198	15.55	0.01	15.36	0.01	15.05	0.03	111
855	05395355–6911310	14.74	0.02	14.67	0.01	14.63	0.02	111
856	05395368–6910346	14.75	0.02	14.50	0.01	14.31	0.02	111
857	05395373–6911022	15.94	0.02	15.92	0.02	15.95	0.04	111
858	05395381–6903018	13.55	0.02	13.37	0.01	13.25	0.02	511
859	05395460–6906402	15.58	0.01	15.58	0.02	15.62	0.03	111
860	05395513–6911221	16.41	0.02	16.39	0.03	16.42	0.06	111
861	05395543–6902266	13.54	0.02	12.88	0.01	12.69	0.01	111
862	05395609–6912050	14.98	0.02	14.54	0.02	14.45	0.02	111
863	05395663–6907429	13.63	0.01	13.16	0.01	13.02	0.01	111
864	05395683–6901231	16.68	0.02	16.70	0.03	16.66	0.09	111
865	05395820–6900207	15.24	0.01	14.85	0.01	14.73	0.02	111
866	05400041–6901163	16.53	0.02	16.61	0.02	16.66	0.08	111
867	05400133–6907596	14.34	0.01	14.27	0.01	14.26	0.02	111
868	05400428–6911030	16.03	0.02	15.91	0.02	15.85	0.03	111
869	05400555–6902449	16.38	0.02	16.23	0.02	16.13	0.05	111
870	05400633–6900011	13.94	0.01	13.65	0.01	13.50	0.02	111
871	05400733–6910427	14.08	0.01	13.79	0.01	13.61	0.01	111
872	05400764–6903240	16.18	0.01	16.19	0.03	16.25	0.05	111
873	05400767–6906440	14.41	0.01	14.29	0.01	14.25	0.01	111
874	05401034–6903049	14.56	0.02	14.35	0.01	14.04	0.02	511
875	05401176–6900379	16.41	0.02	16.40	0.03	16.36	0.07	111
876	05401249–6903582	16.11	0.01	15.99	0.03	15.98	0.05	111
877	05401281–6909103	15.56	0.01	15.38	0.02	15.15	0.02	111
878	05401285–6908135	13.55	0.01	12.83	0.01	12.63	0.01	111

*continued on next page*

**Table 6.** *continued*

Star [VFTS]	IRSF identification	<i>J</i>	$\sigma J$	<i>H</i>	$\sigma H$	<i>K<sub>s</sub></i>	$\sigma K_s$	qflag
879	05401370–6905098	16.42	0.02	16.33	0.03	16.35	0.06	111
880	05401479–6901044	16.48	0.09	16.29	0.10	16.48	0.09	221
881	05401725–6906272	15.78	0.02	15.86	0.03	15.91	0.05	111
882	05401796–6904171	16.14	0.01	16.16	0.03	16.25	0.05	111
883	05401803–6908361	16.21	0.01	16.19	0.03	16.19	0.06	111
884	05401997–6901239	12.45	0.02	11.51	0.01	11.03	0.02	555
885	05402029–6903119	15.90	0.02	15.91	0.02	15.91	0.04	111
886	05402120–6903296	15.88	0.01	15.73	0.02	15.61	0.04	111
887	05402154–6904237	15.09	0.01	15.08	0.01	15.15	0.02	111
888	05402263–6904061	16.28	0.01	16.25	0.03	16.35	0.07	111
889	05402366–6905144	15.59	0.01	15.39	0.02	15.19	0.03	111
890	05402486–6909441	16.17	0.02	16.19	0.02	16.20	0.03	111
891	05402573–6906308	16.35	0.02	16.32	0.03	16.37	0.07	111
892	05402599–6907582	15.58	0.01	15.54	0.02	15.58	0.03	111
893	05403331–6905375	14.38	0.03	14.04	0.01	13.94	0.01	111
1001	05384055–6905572	11.65	0.02	11.35	0.02	11.31	0.05	551
1002	05384067–6906058	15.80	0.09	15.82	0.09	15.65	0.12	222
1003	05384078–6906035	13.86	0.08	13.32	0.05	12.45	0.02	255
1004	05384089–6906046	14.79	0.12	14.62	0.12	14.49	0.12	222
1005	05384100–6906081	16.38	0.08	15.66	0.07	15.91	0.13	511
1006	05384104–6906151	15.16	0.02	14.99	0.03	14.93	0.03	111
1007	05384109–6906019	13.77	0.06	13.66	0.06	13.65	0.05	225
1008	05384107–6905582	—	—	14.51	0.12	—	—	020
1009	05384119–6906030	—	—	—	—	14.29	0.14	002
1010	05384126–6906170	14.79	0.02	14.63	0.02	14.57	0.02	111
1011	05384134–6906140	14.53	0.03	14.32	0.02	14.18	0.02	111
1013	05384142–6906093	15.98	0.06	15.72	0.08	15.54	0.11	222
1016	05384174–6906190	14.70	0.02	14.20	0.04	14.28	0.04	151
1017	05384185–6906144	13.50	0.03	13.26	0.03	13.15	0.02	511
1018	05384188–6906125	13.61	0.03	13.47	0.02	13.40	0.03	551
1020	05384202–6906168	14.99	0.03	14.88	0.03	14.94	0.04	111
1021	05384208–6906144	12.55	0.03	12.46	0.02	12.34	0.02	511
1022	05384238–6906151	12.67	0.03	12.54	0.03	12.36	0.02	551
1023	05384261–6906111	14.39	0.07	14.54	0.05	—	—	210
1026	05384306–6906113	13.59	0.04	13.60	0.03	13.52	0.03	555
1027	05384320–6905426	14.65	0.02	14.59	0.03	—	—	110
1028	05384327–6906166	13.47	0.03	13.42	0.04	13.51	0.02	551
1029	05384335–6905475	14.51	0.02	—	—	—	—	100
1030	05384342–6905422	16.02	0.08	15.95	0.09	—	—	110
1031	05384368–6905479	13.84	0.03	13.70	0.02	13.85	0.03	511
1032	05384406–6905448	14.41	0.02	14.46	0.02	14.30	0.04	111
1033	05384416–6905422	14.39	0.02	14.35	0.02	14.26	0.03	111
1034	05384421–6905471	12.81	0.02	12.72	0.01	12.64	0.02	511
1035	05384434–6905451	15.31	0.09	15.42	0.05	15.05	0.12	112
1036	05384483–6905438	16.11	0.04	16.41	0.07	15.84	0.09	111
1037	05384508–6905429	16.32	0.03	16.47	0.07	15.94	0.07	111

## Appendix A: Observational epochs

**Table A.1.** Epochs of the Medusa observations of Fields A to D. Exposure times for LR02 and LR03 observations are all 1815 s (except the LR02-05 exposures for Field D, with an executed exposure time of 2000s), with longer exposures at HR15N of 2265 s.

Field	$\lambda$ -setting	Epoch	MJD
A	LR02	01 [a+b]	54794.187
	LR02	02 [a+b]	54794.231
	LR02	03 [a+b]	54794.328
	LR02	04 [a+b]	54798.303
		04 [c+d]	54836.146
	LR02	05 [a+b]	54836.191
		05 [c+d]	54867.058
	LR02	06 [a+b]	55108.281
	LR03	01 [a+b]	54794.279
	LR03	02 [a+b]	54795.182
	LR03	03 [a+b]	54795.228
	HR15N	01 [a+b]	54795.281
	HR15N	02 [a+b]	54796.207
B	LR02	01 [a+b]	54804.105
	LR02	02 [a+b]	54804.148
	LR02	03 [a+b]	54804.191
	LR02	04 [a+b]	54836.239
	LR02	05 [a+b]	54836.287
		05 [c+d]	54867.109
	LR02	06 [a+b]	55114.320
		06 [c]	55108.318
	LR03	01 [a+b]	54808.143
	LR03	02 [a+b]	54808.187
	LR03	03 [a+b]	54808.230
	HR15N	01 [a+b]	54804.247
	HR15N	02 [a+b]	54804.300
C	LR02	01 [a+b]	54774.286
	LR02	02 [a+b]	54809.098
	LR02	03 [a+b]	54809.141
	LR02	04 [a+b]	54837.182
	LR02	05 [a+b]	54867.159
	LR02	06 [a+b]	55112.264
	LR02	07 [a+b]	55459.292
	LR03	01 [a+b]	54809.191
	LR03	02 [a+b]	54809.235
	LR03	03 [a+b]	54809.290
	HR15N	01 [a+b]	54808.285
	HR15N	02 [a+b]	54819.262
D	LR02	01 [a+b]	54824.242
	LR02	02 [a+b]	54824.285
	LR02	03 [a+b]	54822.156
	LR02	04 [a+b]	54858.171
	LR02	05 [a+b]	54879.052
	LR02	06 [a+b]	55111.336
	LR03	01 [a+b]	54820.252
	LR03	02 [a+b]	54821.328
	LR03	03 [a+b]	54822.107
	HR15N	01 [a+b]	54818.189
	HR15N	02 [a+b]	54819.062

**Table A.2.** Epochs of the Medusa observations of Fields E to I. Exposure times for LR02 and LR03 observations are all 1815 s, with longer exposures at HR15N of 2265 s.

Field	$\lambda$ -setting	Epoch	MJD
E	LR02	01 [a+b]	54822.254
	LR02	02 [a+b]	54822.298
	LR02	03 [a+b]	54822.341
		03 [c+d]	54824.333
	LR02	04 [a+b]	54858.220
	LR02	05 [a+b]	54889.052
	LR02	06 [a+b]	55114.272
	LR03	01 [a+b]	54825.240
	LR03	02 [a+b]	54825.284
	LR03	03 [a+b]	54825.327
	HR15N	01 [a+b]	54819.120
	HR15N	02 [a+b]	54819.174
F	LR02	01 [a+b]	54748.277
	LR02	02 [a+b]	54748.323
	LR02	03 [a+b]	54749.223
	LR02	04 [a+b]	54837.133
	LR02	05 [a+b]	54868.057
	LR02	06 [a+b]	55112.313
	LR03	01 [a+b]	54810.238
	LR03	01 [c]	54755.188
	LR03	02 [a+b]	54810.281
	LR03	03 [a+b]	54810.336
	HR15N	01 [a+b]	54749.273
	HR15N	02 [a+b]	54810.170
G	LR02	01 [a+b]	54817.223
	LR02	02 [a+b]	54817.267
	LR02	03 [a+b]	54822.058
	LR02	04 [a+b]	54860.105
	LR02	05 [a+b]	54890.041
	LR02	06 [a+b]	55112.361
	LR03	01 [a+b]	54818.243
	LR03	02 [a+b]	54818.287
	LR03	03 [a+b]	54818.330
	HR15N	01 [a+b]	54818.076
	HR15N	02 [a+b]	54818.129
H	LR02	01 [a+b]	54815.276
	LR02	02 [a+b]	54815.328
	LR02	03 [a+b]	54822.206
	LR02	04 [a+b]	54859.231
	LR02	05 [a+b]	54891.084
	LR02	06 [a+b]	55113.329
	LR03	01 [a+b]	54813.240
	LR03	02 [a+b]	54813.285
	LR03	03 [a+b]	54813.336
	HR15N	01 [a+b]	54776.268
	HR15N	02 [a+b]	54776.322
I	LR02	01 [a+b]	54767.334
		01 [c+d]	54827.283
	LR02	02 [a+b]	54828.240
	LR02	03 [a+b]	54828.284
	LR02	04 [a+b]	54860.154
	LR02	05 [a+b]	54886.127
	LR02	06 [a+b]	55114.370
	LR03	01 [a+b]	54828.332
	LR03	02 [a+b]	54836.052
	LR03	03 [a+b]	54836.096
	HR15N	01 [a+b]	54819.323
	HR15N	02 [a+b]	54827.338

**Table A.3.** Epochs of the ARGUS fields (A1-A5). Exposure times for Field A1 were 525 s, with six exposures per OB (except for epoch #05, in which exposure times were  $2 \times 1815$  s per OB). Exposure times for the four other fields are all 1815 s.

Field	$\lambda$ -setting	Epoch	MJD
A1	LR02	01 [a-f]	54761.237
		02 [a-f]	54761.287
		03 [a-f]	54845.177
		03 [g-l]	54767.283
		04 [a-f]	54876.131
		05 [a+b]	55178.167
		05 [c+d]	55173.310
A2	LR02	05 [e+f]	55172.292
		01 [a+b]	54790.290
		02 [a+b]	54791.140
		03 [a+b]	54846.095
		04 [a+b]	54889.102
A3	LR02	05 [a+b]	55173.232
		01 [a+b]	54791.200
		02 [a+b]	54791.247
		03 [a+b]	54846.256
		04 [a+b]	54890.094
A4	LR02	05 [a+b]	55202.149
		01 [a+b]	54791.317
		02 [a+b]	54792.176
		03 [a+b]	54847.161
		04 [a+b]	54898.057
		04 [c+d]	54892.102
		04 [e+f]	54894.039
		04 [g+h]	54896.040
		04 [i]	54987.020
		05 [a+b]	55201.187
A5	LR02	01 [a+b]	54803.172
		02 [a+b]	54803.216
		03 [a+b]	54851.099
		04 [a+b]	54907.085
		04 [c+d]	54893.045
		04 [e+f+g]	54906.014
		05 [a+b]	55204.144